

Goethe Universität Frankfurt

Institute for Theoretical Physics



Effective heavy quark theory
of strong coupling lattice QCD
in 1+1 dimensions

Master Thesis

Alena Schön

August 2018

Supervisor and 1st examiner Prof. Dr. Owe Philipsen

2nd examiner

Dr. Wolfgang Unger

Abstract

In this work, we will derive an effective theory of lattice QCD in 1+1 dimensions in the strong coupling and heavy quark regime. The lattice action will be expanded around heavy quarks so that the integrals over the gauge links can be carried out. This effective action that we calculated is then resummed to an exponential. The resummation produces a correction term which can be inserted in two different ways. We further will obtain some gauge corrections to the effective theory. The effective theory is then mapped to the linked cluster expansion, where we need to take care of the correction terms arising from the resummation of the effective theory. In the last step, we will calculate some thermodynamic quantities and discuss our results.

Contents

1	Introduction	4
2	The Effective Theory	7
2.1	The Character Expansion	7
2.2	The Hopping Parameter Expansion	8
2.2.1	The Static Quark Determinant	9
2.2.2	The Static Quark Propagator	11
2.2.3	The Kinetic Quark Determinant to Leading Order	13
2.2.4	The Kinetic Quark Determinant to Next to Leading Order	15
2.2.5	Multiple Flavours	17
2.3	Resummation	17
2.4	Gauge corrections	18
2.4.1	Corrections to the h_1 Coupling	18
2.4.2	Corrections to the h_2 Couplings	19
3	Analytic Treatment of the Effective Theory	23
3.1	Linked Cluster Expansion	23
3.1.1	Classical Linked Cluster Expansion	23
3.1.2	Graphical Definition of the Linked Cluster Expansion	25
3.1.3	Generalisation of the Linked Cluster Expansion to Polymer Interactions	26
3.2	Linked Cluster Expansion of the Effective Theory	28
3.2.1	Application to the Effective Theory	28
3.2.2	Calculation of the n -Point Functions	29
3.2.3	Calculation of the Correction Term	29
3.3	Observables	30
3.4	Results	32
4	Conclusion and Outlook	38
A	Additional Calculations	39
A.1	Static determinant	39
A.2	Generating Function for W_{nm} Terms	40
A.3	Integration over Polyakov Loops	41
A.4	Moments and Cumulants	41
A.5	Calculation of Spatial Detours	43
A.6	Calculation of Hadron masses	46

B Analytic Results	49
B.1 Effective Action to Order κ^4	49
B.2 Two- and Three-Point Interactions	50
B.3 Integrated LCE z -Functions	51
B.3.1 $N_f = 1$	51
B.3.2 $N_f = 2$	52
B.4 List of Integrals over Polyakov Loops	57
Bibliography	59

Chapter 1

Introduction

Three of the four fundamental forces, electromagnetism, the weak interaction, and the strong interaction, are described by the standard model; only gravity is excluded. These three forces are formulated as quantum field theories which are categorised in gauge groups by their symmetry.

Quantum Chromodynamics (QCD) is the theory of strong interactions, the interactions between quarks and gluons. Six quark flavours are known, the up, down, strange, charm, top, and bottom quark.

Since quarks are fermions, in addition to the electric charge and the flavour charge, a third charge is needed to fulfil the Pauli exclusion principle. Particles like the Δ^{++} , which contains three up-quarks with parallel spins, need an additional quantum number so that the wave function can be symmetric. This quantum number is known as colour and takes the values red, green, and blue.

Free particles always appear as colour singlets that can be built from three (anti-) quarks or a quark-antiquark pair; this is called colour confinement. Another phenomenon is the asymptotic freedom. It describes the behaviour of quarks at small distances or, equivalently, at high momentum transfer. This leads to a weaker coupling at higher energies.

These phenomena indicate a rich phase structure of QCD. The phase diagram in the temperature-chemical potential plane, of which one version is sketched in figure

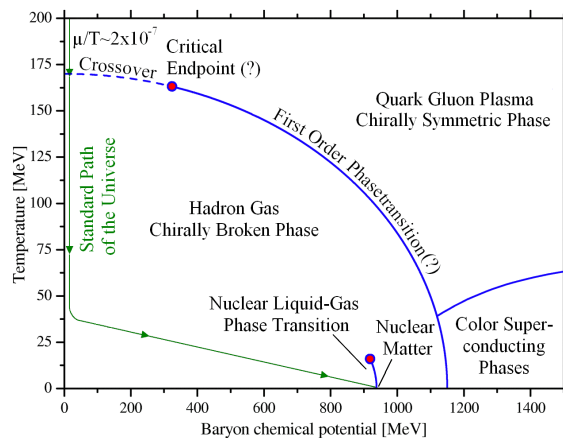


Figure 1.1: Sketch of the QCD phase diagram, taken from [1]

1.1, is of specific interest. At low temperatures and chemical potentials, the quarks are confined to hadronic states. The quark-gluon plasma can be reached moving to higher temperatures. After the crossover transition [2], the energies are high enough for the quarks and gluons to deconfine. This means that the quarks and gluons can move freely, only weakly interacting with each other. It is possible that the crossover turns into a first order phase transition at an unknown critical endpoint at higher chemical potentials.

At zero temperature and a baryon chemical potential around the proton mass, a first order liquid-gas transition is found. At higher temperatures, this transition ends in a critical endpoint. It is predicted that at much higher chemical potentials a colour superconducting phases exist, as a result of quarks on the Fermi surface forming Cooper pairs.

Here, we are going to use the approach of lattice QCD [3, 4] in order to examine the behaviour of the strong interaction. As we are replacing the continuous space-time with a lattice, space-time has to be discretised. This means that the Lagrangian of continuum QCD

$$\mathcal{L} = -\frac{1}{4}F_{\mu\nu}^a(x)F^{\mu\nu a}(x) + \bar{\psi}(i\not{D} - m)\psi \quad (1.0.1)$$

has to be discretised as well.

The gauge part of the Lagrangian has to be rewritten in terms of the so-called gauge links $U_\mu(x)$. They represent the gauge fields, connecting neighbouring lattice sites. Because of the behaviour of the gauge link under a local $SU(3)$ rotation

$$U_\mu(x) \rightarrow W_x U_\mu(x) W_{x+\mu}^\dagger, \quad W_x \in SU(3), \quad (1.0.2)$$

only closed loops are gauge invariant. The smallest closed loop is called plaquette and is build from four link variables:

$$U_{\mu,\nu}(x) = U_\mu(x)U_\nu(x+\mu)U_\mu^\dagger(x+\mu+\nu)U_\nu^\dagger(x). \quad (1.0.3)$$

With the plaquette at hand, we can build the Wilson gauge action [3]

$$\mathcal{S}_g[U] = \frac{\beta}{N_c} \sum_x \sum_{\mu < \nu} \text{Re tr}(\mathbb{1} - U_{\mu,\nu}(x)) = \frac{\beta}{2N_c} \sum_P (\text{tr } U_P + \text{tr } U_P^\dagger), \quad \beta = \frac{2N_c}{g^2}. \quad (1.0.4)$$

Deriving the fermionic action is more complicated since the problem of fermion doubling arises when using a naive approach of discretising the fermion action.

There are different methods of dealing with this issue; we are going to use the approach of Wilson fermions. In this approach, an additional term that breaks chiral symmetry is added to the Lagrangian. This leads to the fermion action

$$\mathcal{S}_f = \bar{\psi}(x)Q[U]\psi(x) \quad (1.0.5)$$

with the Wilson-Dirac-operator

$$Q[U] = \mathbb{1} - \kappa_f \sum_{\nu=0}^3 \left[e^{a\mu\delta_{\nu 0}}(\mathbb{1} + \gamma_\nu)U_\nu(x)\delta_{y,x+\hat{\nu}} + e^{-a\mu\delta_{\nu 0}}(\mathbb{1} - \gamma_\nu)U_\nu^\dagger(y)\delta_{y,x-\hat{\nu}} \right]. \quad (1.0.6)$$

This thesis starts with chapter 2, which contains the derivation of an effective theory of LQCD in 1+1 dimensions. In order to derive the effective theory, the action of lattice QCD is expanded around heavy quarks and $\beta \rightarrow 0$, afterwards the gauge links are integrated out.

The effective action will further be resummed to an exponential, and we will introduce two ways on how to take care of some correction terms of subleading order. Finally, some gauge corrections will be calculated.

In chapter 3, the effective theory is analytically evaluated. The linked cluster expansion is introduced and used to calculate some thermodynamic quantities of the effective theory. These results will be analysed and discussed.

Chapter 4 will finally give a conclusion of the results, as well as a short outlook.

Chapter 2

The Effective Theory

This chapter is based on [5–7], where this derivation is performed in 3+1 dimensions.

We will perform the calculations in 1+1 dimensions, so the index μ runs only from 0 to 1. For this reason, we need to use a two-dimensional formulation of the gamma matrices in our calculations. The euclidean formulation of the two gamma matrices in two dimensions is similar to the first two Pauli matrices:

$$\gamma_0 = \sigma_1 = \begin{pmatrix} 0 & 1 \\ 1 & 0 \end{pmatrix}, \quad \gamma_1 = \sigma_2 = \begin{pmatrix} 0 & -i \\ i & 0 \end{pmatrix} \quad (2.0.1)$$

Furthermore, we will have to pay attention when traces occur, since the trace over the identity matrix equals 2 instead of 4.

The derivation of the effective theory in 1+1 dimensions starts with the LQCD partition function with the Wilson gauge action and the Wilson fermion action

$$\mathcal{Z} = \int \prod_{x,\mu} dU_\mu(x) \det Q[U_\mu] e^{-\mathcal{S}_g[U_\mu]} \quad (2.0.2)$$

with

$$\mathcal{S}_g = \frac{\beta}{2N_c} \sum_P (\text{tr} U_P + \text{tr} U_P^\dagger), \quad \beta = \frac{2N}{g^2}. \quad (2.0.3)$$

Performing an integration over the spatial gauge link variables will yield the effective action

$$\mathcal{Z}_{eff} = \int \prod_x dU_0(x) e^{-\mathcal{S}_{eff}[U_0]}, \quad \mathcal{S}_{eff} = -\log \int \prod_x dU_1(x) \det Q[U_\mu] e^{-\mathcal{S}_g[U_\mu]}. \quad (2.0.4)$$

Now, we will perform an expansion around the gauge action and afterwards an expansion around the fermion determinant, in order to obtain the effective theory.

2.1 The Character Expansion

The gauge action is expanded around $\beta \rightarrow 0$ using the character expansion [8]

$$-\mathcal{S}_{eff} = \log \int [dU_1] \prod_p \left[1 + \sum_{r \neq 0} d_r a_r(\beta) \chi_r(U_p) \right]. \quad (2.1.1)$$

The sum extends over all irreducible representations r , with the dimension d_r , the expansion coefficients $a_r(\beta)$, and the characters $\chi_r(U_p) = \text{tr } U_p^r$.

Terms that do not wind through the temporal boundary of the lattice can be neglected because they become constant contributions independent of the link variables after the integration over the spatial links and therefore cancel out in the expectation values.

In order to obtain the leading contribution, the plaquettes without temporal links are neglected, only chains of plaquettes looping through the temporal boundary remain.

Now, to perform the spatial link integration, the following group integrals are necessary:

$$\int dU \chi_r(XU) \chi_s(U^{-1}Y) = \frac{\delta_{rs}}{d_r} \chi_r(XY) \quad (2.1.2)$$

$$\int dU \chi_r(U) = \delta_{r,0}. \quad (2.1.3)$$

This integration process is the reason why all the plaquettes of a graph belong to the same representation.

From this, we get:

$$- \mathcal{S}_{eff} = \log \prod_{\langle ij \rangle} \left[1 + \sum_{r \neq 0} [a_r(\beta)]^{N_r} \chi_r(W_i) \chi_r(W_j) \right]. \quad (2.1.4)$$

Using the fundamental representation leads to the leading order contribution of this nearest neighbour interaction of Polyakov loops

$$- \mathcal{S}_{eff} = \sum_{\langle \vec{x}\vec{y} \rangle} \log [1 + \lambda_1 (L_{\vec{x}}^* L_{\vec{y}} + L_{\vec{x}} L_{\vec{y}}^*)], \quad \lambda_1 = u^{N_t} + \mathcal{O}(u^{N_t+4}), \quad (2.1.5)$$

with the Polyakov loops

$$L(\vec{x}) = \text{tr } W(\vec{x}) = \text{tr} \prod_{t=0}^{N_t-1} U_0(\vec{x}, t). \quad (2.1.6)$$

The corrections to the coupling λ_1 , known up to order u^{N_t+10} [8], can be obtained by including spatial plaquettes.

We will now proceed to perform the hopping parameter expansion and leave the expansion of the gauge action behind since it is not of further relevance for this thesis. Due to the fact that the calculations are performed in the cold regime, the pure gauge contribution is exponentially suppressed and thus can be neglected.

2.2 The Hopping Parameter Expansion

In the next step, we will expand the quark determinant around heavy quarks, i.e., $\kappa = 0$, with κ as the hopping parameter. We perform this expansion in the strong coupling limit, which we discussed in the previous chapter. The results from this section and the pure gauge contribution can be included independently from each other.

The Wilson Dirac operator, eq. 1.0.6, can be rewritten as

$$Q_f[U] = \mathbb{1} - \kappa_f M[U], \quad \kappa_f = \frac{1}{2(1 + d + am)} \quad (2.2.1)$$

with the hopping matrix $M[U]$ and the hopping parameter κ_f [9]. We can now expand the quark determinant

$$\det Q = \exp(\text{tr log}[\mathbb{1} - \kappa_f M]) = \exp\left(-\sum_{n=1}^{\infty} \frac{\kappa_f^n}{n} \text{tr } M^n\right). \quad (2.2.2)$$

Every factor of M carries a Kronecker delta $\delta_{y,x\pm\hat{\mu}}$, which can be interpreted as a single hop on the lattice. Every hop also carries a spin factor $(1 \pm \gamma_\mu)$. When looking at this and the identity $(1 - \gamma_\mu)(1 + \gamma_\mu) = 0$, it gets apparent that only closed fermion loops without backtracking will give non-vanishing contributions. Therefore, we receive all closed quark lines free of backtracking of length n from this expansion.

2.2.1 The Static Quark Determinant

The first step in the derivation of the effective action is the calculation of the static quark determinant. We will perform this derivation in the case of $N_f = 1$, so the flavour index can be dropped. However, in chapter 2.2.5, the calculation will be extended to two flavours. The hopping matrix $M[U]$ can be split into temporal and spatial hoppings, where *hopping* refers to quark lines connecting neighbouring lattice sites. These temporal and spatial hoppings are then split into positive and negative components. It is now possible to split up the hopping matrix

$$\det_{c,s,x} Q_{x,y} = \det[\mathbb{1} - T_{x,y}^+ - T_{x,y}^- - S_{x,y}^+ - S_{x,y}^-] \quad (2.2.3)$$

using the temporal hoppings $T_{x,y}$ and the spatial hoppings $S_{x,y}$

$$\begin{aligned} T_{x,y}^+ &= \kappa e^{a\mu}(\mathbb{1} + \gamma_0)U_0(x)\delta_{y,x+\hat{0}}, \\ T_{x,y}^- &= \kappa e^{a\mu}(\mathbb{1} - \gamma_0)U_0^\dagger(y)\delta_{y,x-\hat{0}}, \\ S_{x,y}^+ &= \kappa(\mathbb{1} + \gamma_1)U_1(x)\delta_{y,x+\hat{1}}, \\ S_{x,y}^- &= \kappa(\mathbb{1} - \gamma_1)U_1^\dagger(y)\delta_{y,x-\hat{1}}. \end{aligned} \quad (2.2.4)$$

The indices c, s and x of the determinant show that the determinant has to be calculated in the colour, spin, and coordinate space.

As a next step, we split the quark determinant itself into a static and a kinetic part

$$\det_{c,s,x} Q_{x,y} = \det(\mathbb{1} - T - S) = \det(\mathbb{1} - T_{x,y}) \det\left(\mathbb{1} - \frac{S_{x,y}}{\mathbb{1} - T_{x,y}}\right). \quad (2.2.5)$$

We will examine the kinetic quark determinant in the following section.

The static quark determinant contains a positive and a negative part and can be rewritten with the trace-log identity

$$\det Q_{stat} = \det(\mathbb{1} - T) = \exp\left(-\sum_{n=1}^{\infty} \frac{1}{n} \text{tr}(T^+ + T^-)^n\right). \quad (2.2.6)$$

Because backtracking is prohibited, it is not possible to have terms that mix T^+ and T^- . This means that the static determinant can be separated into two parts.

$$\det Q_{stat} = \det(\mathbb{1} - T^+) \det(\mathbb{1} - T^-). \quad (2.2.7)$$

These combinations will reduce to temporal Wilson lines $W(\vec{x}) = \prod_{t=0}^{N_t-1} U_0(\vec{x}, t)$, loops through the temporal boundary of the lattice, because only closed quark lines contribute and we can only move in the temporal direction while in the static limit.

Inserting the temporal hoppings and using the relation $(\mathbb{1} + \gamma_0)^2 = 2(\mathbb{1} + \gamma_0)$ as well as the trace-log identity, the coordinate space determinant can be calculated:

$$\det_{c,s,x} Q_{stat} = \prod_{\vec{x}} \det_{c,s} \left[\mathbb{1} + \frac{1}{2} (2\kappa)^{N_t} e^{N_t a \mu} (\mathbb{1} + \gamma_0) W_{\vec{x}} \right] \det_{c,s} \left[\mathbb{1} + \frac{1}{2} (2\kappa)^{N_t} e^{-N_t a \mu} (\mathbb{1} - \gamma_0) W_{\vec{x}}^\dagger \right] \quad (2.2.8)$$

The additional minus sign in equation 2.2.7 stems from the antiperiodic boundary conditions. The spin determinant can be evaluated with the relation $\det_s [\mathbb{1} + \alpha(1 \pm \gamma_\mu)] = [\mathbb{1} + 2\alpha]^2$:

$$\det_{c,s,x} Q_{stat} = \prod_{\vec{x}} \det_c \left[\mathbb{1} + (2\kappa)^{N_t} e^{N_t a \mu} W_{\vec{x}} \right]^2 \det_c \left[\mathbb{1} + (2\kappa)^{N_t} e^{-N_t a \mu} W_{\vec{x}}^\dagger \right]^2 \quad (2.2.9)$$

We further introduce the effective couplings for the quarks and antiquarks

$$\begin{aligned} h_1(\mu, N_t) &= (2\kappa)^{N_t} e^{N_t a \mu} \\ \bar{h}_1(\mu, N_t) &= (2\kappa)^{N_t} e^{-N_t a \mu}. \end{aligned} \quad (2.2.10)$$

With the couplings, the static determinant simplifies to

$$\det_{c,s,x} Q_{stat} = \prod_{\vec{x}} \det_c \left[\mathbb{1} + h_1(\mu, N_t) W_{\vec{x}} \right]^2 \det_c \left[\mathbb{1} + \bar{h}_1(\mu, N_t) W_{\vec{x}}^\dagger \right]^2. \quad (2.2.11)$$

We use the relation for $SU(3)$ matrices calculated in Appendix A.1

$$\det[\mathbb{1} + \alpha U] = 1 + \alpha \text{tr} U + \alpha^2 \text{tr} U^\dagger + \alpha^3 \quad (2.2.12)$$

in order to calculate the remaining colour determinant.

This leads to the final expression for the static determinant:

$$\det_{c,s,x} Q_{stat} = \prod_{\vec{x}} (1 + h_1 L_{\vec{x}} + h_1^2 L_{\vec{x}}^\dagger + h_1^3)^2 (1 + \bar{h}_1 L_{\vec{x}}^\dagger + \bar{h}_1^2 L_{\vec{x}} + \bar{h}_1^3)^2. \quad (2.2.13)$$

Now, we proceed to calculate the kinetic quark determinant. We rewrite it to

$$\det Q_{kin} = \det \left(\mathbb{1} - \frac{S_{x,y}^+ + S_{x,y}^-}{\mathbb{1} - T} \right) = \det(\mathbb{1} - P - M) \quad (2.2.14)$$

with

$$\begin{aligned} P &= P_x = (\mathbb{1} - T_{x,y})^{-1}(S_{x,y}^+) \\ M &= M_x = (\mathbb{1} - T_{x,y})^{-1}(S_{x,y}^-). \end{aligned} \quad (2.2.15)$$

We see that it is necessary to calculate the static propagator $(\mathbb{1} - T_{x,y})^{-1}$ in order to expand the kinetic quark determinant.

2.2.2 The Static Quark Propagator

In order to start the calculation of the static quark propagator¹, we rewrite T^+ and T^- in a form that is more convenient for this approach:

$$T^\pm(x, y) = z_\pm P_\pm U_{\pm 0}(t_x, \vec{x}) \delta_{t_x, t_y - 1} \delta_{\vec{x}, \vec{y}} b_{t_y}^\mp \quad (2.2.16)$$

with

$$\begin{aligned} z_\pm &= 2\kappa e^{\pm a\mu}, \quad P_\pm = \frac{1}{2}(\mathbb{1} \pm \gamma_0), \quad U_{+0}(t_x, \vec{x}) = U_0(x), \quad U_{-0}(t_x, \vec{x}) = U_0^\dagger(y) \\ b_t^- &= \begin{cases} -1, & t = 0 \\ 1, & t \neq 0 \end{cases}, \quad b_t^+ = \begin{cases} -1, & t = N_t - 1 \\ 1, & t \neq N_t - 1 \end{cases} \end{aligned} \quad (2.2.17)$$

We can see that $z_+ = h_1^{\frac{1}{N_t}}$ and the antiperiodic boundary conditions are taken care of by the factors b^- and b^+ . Because we want to expand the static quark propagator, we need to make sure that the convergence radius $\rho(T)$ is smaller than 1, which is easily fulfilled for $z < 1$ as

$$\rho(T) = z \rho\left(\frac{1}{2}(\mathbb{1} \pm \gamma_0)\right) \rho(U_0(x)) \rho(\delta_{x, y - \hat{0}}) = z. \quad (2.2.18)$$

We can now proceed to expand the static quark propagator using the requirement that backtracking is forbidden, so $T^+ T^- = 0$:

$$(Q_{stat})^{-1} = (\mathbb{1} - T)^{-1} = \sum_{j=0}^{\infty} T^j = \mathbb{1} + \sum_{j=0}^{\infty} [(T^+)^j + (T^-)^j]. \quad (2.2.19)$$

Because the calculation of the sums over T^+ and T^- are analogous to each other, we will discuss only the calculation for T^+ in more detail.

First, we are going to plug in the expression for T^+ :

$$\begin{aligned} (T^+)^j(x, y) &= \delta_{\vec{x}, \vec{y}} \delta_{t_x, t_y - j} z_+^j P_+^j \left[\prod_{i=0}^{j-1} U_0(t_x + i, \vec{x}) \right] \left[\prod_{i=0}^{j-1} b_{t_y - i}^- \right] \\ &= \delta_{\vec{x}, \vec{y}} \delta_{t_x, t_y - j} z_+^j P_+ \prod_{i=0}^{j-1} U_0(t_x + i, \vec{x}) b_{t_y - i}^- \end{aligned} \quad (2.2.20)$$

¹Based on private notes from Jonas Scheunert

Because of the relation $(\mathbb{1} + \gamma_0)^2 = 2(\mathbb{1} + \gamma_0)$, we can use the identity $(P_+)^j = P_+$. As we are in the static case, we can always assume that $\vec{x} = \vec{y}$.

We will proceed to look at two separate cases, one where $t_x = t_y$ and one where $t_x \neq t_y$. We will start with the first case, where we change the exponent from j to jN_t to fulfil the constraint $t_x = t_y$:

$$(T^+)^{jN_t}(x, y) = P_+ h_1^j W^j(t_x, \vec{x}) (-1)^j \quad (2.2.21)$$

with

$$h_1 = z_+^{N_t}, \quad W(t_x, \vec{x}) = \prod_{i=0}^{N_t-1} U_0(t_x + i, \vec{x}). \quad (2.2.22)$$

In the second case, the constraint $t_y - t_x + jN_t > 0$ has to be fulfilled. This leads to

$$(T^+)^{t_y - t_x + jN_t}(x, y) = P_+ z_+^{t_y - t_x} h_1^j \begin{cases} W(t_x, t_y, \vec{x}) W^j(t_y, \vec{x}) (-1)^j, & t_x < t_y \\ W(t_x, t_y, \vec{x}) W^{j-1}(t_y, \vec{x}) (-1)^j, & t_x > t_y \end{cases} \quad (2.2.23)$$

with

$$W(t_x, t_y, \vec{x}) = \begin{cases} \prod_{i=0}^{t_y - t_x - 1} U_0(t_x + i, \vec{x}) & \text{if } t_x < t_y \\ \prod_{i=0}^{N_t - t_x + t_y - 1} U_0(t_x + i, \vec{x}) & \text{if } t_x \geq t_y \end{cases}. \quad (2.2.24)$$

When defining the step function with $\theta(0) = 0$, the results can be summarised and rewritten to the final expression:

$$\sum_{j=1}^{\infty} (T^+)^j(x, y) = \delta_{\vec{x}, \vec{y}} P_+ \left[-\delta_{t_x, t_y} h_1 W(t_x, \vec{x}) (\mathbb{1} + h_1 W(t_x, \vec{x}))^{-1} + z^{t_y - t_x} W(t_x, t_y, \vec{x}) (\mathbb{1} + h_1 W(t_y, \vec{x}))^{-1} (\theta(t_y - t_x) - h_1 \theta(t_x - t_y)) \right]. \quad (2.2.25)$$

In a similar way we calculate the contribution for $\sum_{j=1}^{\infty} (T^-)^j(x, y)$, only z_+ is replaced by z_- and W with W^\dagger . This leads to the full static quark propagator:

$$Q_{stat}^{-1}(x, y) = \delta_{\vec{x}, \vec{y}} \left\{ \delta_{t_x, t_y} \left[\mathbb{1} - P_+ \frac{h_1 W(t_x, \vec{x})}{\mathbb{1} + h_1 W(t_x, \vec{x})} - P_- \frac{\bar{h}_1 W^\dagger(t_x, \vec{x})}{\mathbb{1} + \bar{h}_1 W^\dagger(t_x, \vec{x})} \right] + \theta(t_y - t_x) \left[P_+ z_+^{t_y - t_x} \frac{W(t_x, t_y, \vec{x})}{\mathbb{1} + h_1 W(t_y, \vec{x})} - P_- z_-^{t_x - t_y} \bar{h}_1 \frac{W^\dagger(t_x, t_y, \vec{x})}{\mathbb{1} + \bar{h}_1 W^\dagger(t_y, \vec{x})} \right] + \theta(t_x - t_y) \left[-P_+ z_+^{t_y - t_x} h_1 \frac{W(t_x, t_y, \vec{x})}{\mathbb{1} + h_1 W(t_y, \vec{x})} + P_- z_-^{t_x - t_y} \frac{W^\dagger(t_x, t_y, \vec{x})}{\mathbb{1} + \bar{h}_1 W^\dagger(t_y, \vec{x})} \right] \right\} \quad (2.2.26)$$

For convenience, the static propagator can be split up again:

$$Q_{stat}^{-1}(x, y) = A^+(x, y) + A^-(x, y) + \gamma_0 (B^+(x, y) - B^-(x, y)) \quad (2.2.27)$$

with

$$A^+(x, y) = \frac{1}{2} \delta_{x, y} \left[\mathbb{1} - \frac{h_1 W}{\mathbb{1} + h_1 W} \right] + \frac{1}{2} \delta_{\vec{x}, \vec{y}} h_1^{\frac{t_y - t_x}{N_t}} \frac{W(t_x, t_y)}{\mathbb{1} + h_1 W} \left[\theta(t_y - t_x) - h_1 \theta(t_x - t_y) \right]$$

$$A^-(x, y) = \frac{1}{2} \delta_{x, y} \left[\mathbb{1} - \frac{\bar{h}_1 W^\dagger}{\mathbb{1} + \bar{h}_1 W^\dagger} \right] + \frac{1}{2} \delta_{\vec{x}, \vec{y}} \bar{h}_1^{\frac{t_y - t_x}{N_t}} \frac{W^\dagger(t_x, t_y)}{\mathbb{1} + \bar{h}_1 W^\dagger} \left[\theta(t_x - t_y) - \bar{h}_1 \theta(t_y - t_x) \right]$$

$$\begin{aligned}
B^+(x, y) &= -\frac{1}{2}\delta_{x,y}\frac{h_1W}{\mathbb{1} + h_1W} + \frac{1}{2}\delta_{\bar{x},\bar{y}}h_1\frac{t_y-t_x}{Nt}W(t_x, t_y)\left[\theta(t_y - t_x) - h_1\theta(t_x - t_y)\right] \\
B^-(x, y) &= -\frac{1}{2}\delta_{x,y}\frac{\bar{h}_1W^\dagger}{\mathbb{1} + \bar{h}_1W^\dagger} + \frac{1}{2}\delta_{\bar{x},\bar{y}}\bar{h}_1\frac{t_y-t_x}{Nt}W^\dagger(t_x, t_y)\left[\theta(t_x - t_y) - \bar{h}_1\theta(t_y - t_x)\right].
\end{aligned} \tag{2.2.28}$$

We will further use the shorter notation

$$Q_{stat}^{-1}(x, y) = A_{x,y} + \gamma_0 B_{x,y} \tag{2.2.29}$$

with $A_{x,y} = A^+(x, y) + A^-(x, y)$ and $B_{x,y} = B^+(x, y) - B^-(x, y)$.

As we completed the derivation of the static quark propagator, we can start calculating the kinetic quark determinant.

2.2.3 The Kinetic Quark Determinant to Leading Order

In this work, we will perform the expansion of the kinetic quark determinant

$$\det[\mathbb{1} - P - M] = \exp\left(\text{tr}\sum_{n=1}^{\infty}\left[-\frac{1}{n}(P + M)^n\right]\right) \tag{2.2.30}$$

to order κ^4 . It is again based on [5, 7].

In the first step, we will perform the expansion to leading order. As only closed loops contribute, only terms with an equal number of P and M terms have to be considered, so the leading order is

$$\det Q_{kin} = \exp\left(-\sum_i \text{tr} P_i M_i + \mathcal{O}(\kappa^4)\right). \tag{2.2.31}$$

Because every P and every M comes with a factor of κ , the leading order contribution is of order κ^2 .

We dropped the indices here and in the following chapter because we have only one spatial dimension:

$$\det Q_{kin} = \exp\left(-\text{tr} PM + \mathcal{O}(\kappa^4)\right). \tag{2.2.32}$$

Now, we plug in the static quark propagator:

$$\det Q_{kin} = \exp\left(-\sum_{x,y} \text{tr} [(Q_{stat})_{x,y}^{-1} S_{y,y+\hat{1}}^+ (Q_{stat})_{y+\hat{1},x+\hat{1}}^{-1} S_{x+\hat{1},x}^-] + \mathcal{O}(\kappa^4)\right) \tag{2.2.33}$$

This is analogous to an arbitrary propagation in the temporal direction, one spatial hop forward, again an arbitrary temporal propagation, and another spatial hop backwards.

Furthermore, we can insert the definitions of the static quark propagator and the spatial hoppings:

$$\det Q_{kin} = \exp \left(-\kappa^2 \sum_{x,y} \text{tr} [(A_{x,y} + \gamma_0 B_{x,y})(\mathbb{1} + \gamma_1)U_1(y) \right. \\ \left. (A_{y+\hat{1},x+\hat{1}} + \gamma_0 B_{y+\hat{1},x+\hat{1}})(\mathbb{1} - \gamma_1)U_1^\dagger(x)] + \mathcal{O}(\kappa^4) \right) \quad (2.2.34)$$

After evaluating the gamma matrices, all terms, except for one, drop out:

$$\det Q_{kin} = \exp \left(-4\kappa^2 \sum_{x,y} \text{tr} [B_{x,y}U_1(y)B_{y+\hat{1},x+\hat{1}}U_1^\dagger(x)] + \mathcal{O}(\kappa^4) \right) \quad (2.2.35)$$

In order to perform the integration over the spatial gauge links, we need the following group integrals [10]:

$$\int dU U_{ij} = 0 \\ \int dU U_{ij}^\dagger = 0 \\ \int dU U_{ij} U_{kl}^\dagger = \frac{1}{N_c} \delta_{il} \delta_{jk} \\ \int dU U_{ij} U_{ab} U_{kl}^\dagger U_{cd}^\dagger = \frac{1}{N_c^2 - 1} \left[\delta_{il} \delta_{ad} \delta_{jk} \delta_{bc} + \delta_{id} \delta_{al} \delta_{jc} \delta_{bk} \right] \\ - \frac{1}{N_c(N_c^2 - 1)} \left[\delta_{id} \delta_{al} \delta_{jk} \delta_{bc} + \delta_{il} \delta_{ad} \delta_{jc} \delta_{bk} \right] \quad (2.2.36)$$

The last integral is only relevant for some terms of the $\mathcal{O}(\kappa^4)$ action.

Because single occupied links vanish, we can assume that $x = y$.

In order to actually perform the integration, we have to expand the exponential first. This leads to

$$\int [dU_1] \exp(-\text{tr} PM) = 1 + \int [dU_1] \text{tr} PM + \mathcal{O}(\kappa^4). \quad (2.2.37)$$

The integration over the expanded term gives

$$\int [dU_1] \sum_x \text{tr} [B_{x,x} U_1(x) B_{x+\hat{1},x+\hat{1}} U_1^\dagger(x)] \\ = \frac{4\kappa^2}{N_c} \sum_x \text{tr} [B_{x,x}^+ - B_{x,x}^-] \text{tr} [B_{x+\hat{1},x+\hat{1}}^+ - B_{x+\hat{1},x+\hat{1}}^-] \quad (2.2.38)$$

In the last step, we plug in the expressions for B^+ and B^-

$$\int [dU_1] \det Q_{kin} = 1 - \frac{\kappa^2 N_\tau}{N_c} \sum_{\vec{x}} \left(\text{tr} \left(\frac{h_1 W_{\vec{x}}}{\mathbb{1} + h_1 W_{\vec{x}}} \right) - \text{tr} \left(\frac{\bar{h}_1 W_{\vec{x}}^\dagger}{\mathbb{1} + \bar{h}_1 W_{\vec{x}}^\dagger} \right) \right) \\ \left(\text{tr} \left(\frac{h_1 W_{\vec{x}+\hat{1}}}{\mathbb{1} + h_1 W_{\vec{x}+\hat{1}}} \right) - \text{tr} \left(\frac{\bar{h}_1 W_{\vec{x}+\hat{1}}^\dagger}{\mathbb{1} + \bar{h}_1 W_{\vec{x}+\hat{1}}^\dagger} \right) \right) + \mathcal{O}(\kappa^4). \quad (2.2.39)$$

As those terms are quite lengthy, we also introduce a shorter notation where

$$W_{n_1 m_1 n_2 m_2}(\vec{x}) = \text{tr} \left(\frac{(h_1 W_{\vec{x}})^{m_1}}{(\mathbb{1} + h_1 W_{\vec{x}})^{n_1}} \frac{(\bar{h}_1 W_{\vec{x}}^\dagger)^{m_2}}{(\mathbb{1} + \bar{h}_1 W_{\vec{x}}^\dagger)^{n_2}} \right) \quad (2.2.40)$$

and for even more brevity, because we will need those terms a lot

$$\begin{aligned} W_{n_1 m_1 n_2 m_2}^-(\vec{x}) &= W_{n_1 m_1 00} - W_{00 n_2 m_2} \\ W_{n_1 m_1 n_2 m_2}^+(\vec{x}) &= W_{n_1 m_1 00} + W_{00 n_2 m_2}. \end{aligned} \quad (2.2.41)$$

Also, we introduce the nearest neighbour coupling constant

$$h_2(\kappa, N_\tau) = \frac{\kappa^2 N_\tau}{N_c} \quad (2.2.42)$$

Plugging in this coupling constant, the expression above takes its final form

$$\int [dU_1] \det Q_{kin} = 1 - h_2 \sum_x W_{1111}^-(\vec{x}) W_{1111}^-(\vec{x} + \hat{1}) + \mathcal{O}(\kappa^4). \quad (2.2.43)$$

2.2.4 The Kinetic Quark Determinant to Next to Leading Order

In this chapter, we will perform the calculation of the kinetic quark determinant to order $\mathcal{O}(\kappa^4)$.

Expanding the sum to this order leads to

$$\det Q_{kin} = \exp(-\text{tr} PM - \text{tr} PPMM - \text{tr} PMPM + \mathcal{O}(\kappa^6)) \quad (2.2.44)$$

The exponential has to be expanded again because of the integration, which leads to an additional term:

$$\det Q_{kin} = 1 - \text{tr} PM - \text{tr} PPMM - \text{tr} PMPM - \text{tr} PM \text{tr} PM + \mathcal{O}(\kappa^6). \quad (2.2.45)$$

We will only show the calculation regarding the term $\text{tr} PPMM$, the full action for an arbitrary number of degenerate flavours can then be found in the appendix B.1.

Again, we need to plug in the static quark propagator and the spatial hoppings

$$\begin{aligned} \text{tr} PPMM &= \sum_{x,y} \text{tr} [(Q_{stat})_{x,x}^{-1} S_{x,x+\hat{1}}^+ (Q_{stat})_{x+\hat{1},y+\hat{1}}^{-1} S_{y+\hat{1},y+\hat{1}+\hat{1}}^+ \\ &\quad (Q_{stat})_{y+\hat{1}+\hat{1},y+\hat{1}+\hat{1}}^{-1} S_{y+\hat{1}+\hat{1},y+\hat{1}}^- (Q_{stat})_{y+\hat{1},x+\hat{1}}^{-1} S_{x+\hat{1},x}^-] \\ &= \kappa^4 \sum_{x,y} \text{tr} [(A_{x,x} + \gamma_0 B_{x,x})(\mathbb{1} + \gamma_1) U_1(x) \\ &\quad (A_{x+\hat{1},y+\hat{1}} + \gamma_0 B_{x+\hat{1},y+\hat{1}})(\mathbb{1} + \gamma_1) U_1(y + \hat{1}) \\ &\quad A_{y+\hat{1}+\hat{1},y+\hat{1}+\hat{1}} + \gamma_0 B_{y+\hat{1}+\hat{1},y+\hat{1}+\hat{1}})(\mathbb{1} + \gamma_1) U_1^\dagger(y + \hat{1}) \\ &\quad A_{y+\hat{1},x+\hat{1}} + \gamma_0 B_{y+\hat{1},x+\hat{1}})(\mathbb{1} + \gamma_1) U_1^\dagger(x)]. \end{aligned} \quad (2.2.46)$$

As before, most of the terms vanish after the evaluation of the gamma matrices:

$$\begin{aligned} \text{tr } PPMM = 16\kappa^4 \sum_{x,y} \text{tr} [B_{x,x} U_1(x) A_{x+1,y+1} U_1(y+1) \\ B_{y+1+1,y+1+1} U_1^\dagger(y+1) A_{y+1,x+1} U_1^\dagger(x)]. \end{aligned} \quad (2.2.47)$$

Since we have doubly occupied spatial links, the integration is the same as in chapter 2.2.3:

$$\int [dU_1] \text{tr } PPMM = 16 \frac{\kappa^4}{N_c^2} \sum_{x,y} \text{tr} [B_{x,x}] \text{tr} [A_{x+\hat{1},y+\hat{1}} A_{y+\hat{1},x+\hat{1}}] \text{tr} [B_{y+\hat{1}+\hat{1},y+\hat{1}+\hat{1}}]. \quad (2.2.48)$$

We can set $\vec{x} = \vec{y}$ because $A_{x,y}$ describes a purely temporal propagation. When plugging in the definitions of A and B , we get two different contributions, one where $x_0 = y_0$ and one where $x_0 \neq y_0$.

First, we calculate the term for $x_0 = y_0$. This contribution is evaluated in the same way as in the previous chapter 2.2.3. It results in the first term of equation 2.2.51.

The second term stems from the contribution where $x_0 \neq y_0$. In this case, $A_{x+\hat{1},y+\hat{1}}$ and $A_{y+\hat{1},x+\hat{1}}$ describe fractional Wilson lines which will form one loop around the lattice when multiplied. They can be followed by an arbitrary number of closed loops. Also, forward and backward propagations can mix, because the spatial hoppings are already integrated out, so the backtracking restriction is not violated. These propagations lead to the term proportional to the sum, 2.2.49.

Writing down both contributions in the form of 2.2.40 and 2.2.41 leads to:

$$\begin{aligned} \int [dU_1] \text{tr } PPMM = -h_{3_1} \sum_{\vec{x}} W_{1111}^-(\vec{x} - \hat{1}) \left(2 \cdot \mathbb{1} - W_{1111}^-(\vec{x}) \right)^2 W_{1111}^-(\vec{x} + \hat{1}) \\ - h_{3_2} \sum_x W_{1111}^-(\vec{x} - \hat{1}) \left(W_{2121}^-(\vec{x}) - 2 \frac{1}{N_\tau - 1} \sum_{t=1}^{N_\tau - 1} (2\kappa)^{2t} W_{1010}(\vec{x}) \right) W_{1111}^-(\vec{x} + \hat{1}) \end{aligned} \quad (2.2.49)$$

with

$$h_{3_1} = \frac{\kappa^4 N_\tau}{N_c^2} = \frac{h_2^2}{N_\tau}, \quad h_{3_2} = \frac{\kappa^4 N_\tau (N_\tau - 1)}{N_c^2} = \frac{h_2^2 N_\tau (N_\tau - 1)}{N_\tau}. \quad (2.2.50)$$

Furthermore, we can evaluate the sum and rewrite the other terms, which leads to the result:

$$\begin{aligned} \int [dU_1] \text{tr } PPMM = -h_{3_1} \sum_{\vec{x}} \left[W_{1111}^-(\vec{x} - \hat{1}) W_{2222}^+(\vec{x}) W_{1111}^-(\vec{x} + \hat{1}) \right. \\ \left. + 2 W_{1111}^-(\vec{x} - \hat{1}) W_{1111}(\vec{x}) W_{1111}^-(\vec{x} + \hat{1}) \right. \\ \left. - 4 W_{1111}^-(\vec{x} - \hat{1}) W_{1111}^+(\vec{x}) W_{1111}^-(\vec{x} + \hat{1}) \right] \\ - h_{3_2} \sum_x \left[W_{1111}^-(\vec{x} - \hat{1}) W_{2121}^+(\vec{x}) W_{1111}^-(\vec{x} + \hat{1}) \right. \\ \left. \frac{2[(2\kappa)^{2N_\tau} - (2\kappa)^2]}{(2\kappa^2 - 1)(N_\tau - 1)} W_{1111}^-(\vec{x} - \hat{1}) W_{1010}(\vec{x}) W_{1111}^-(\vec{x} + \hat{1}) \right]. \end{aligned} \quad (2.2.51)$$

The remaining terms, 2.2.44, are calculated similarly, and the final result can be found in appendix B.1.

2.2.5 Multiple Flavours

The previous calculation was done for one flavour, $N_f = 1$. It is also possible to expand this to multiple flavours. Every new flavour adds a second quark determinant and new hopping parameters

$$\mathcal{Z} = \int [dU_\mu] \sum_{f=1}^{N_f} \det Q_{stat,f} \exp \left(- \sum_{f=1}^{N_f} \sum_{n=1}^{\infty} \frac{1}{n} \text{tr}(P_f + M_f)^n \right). \quad (2.2.52)$$

We will perform our calculation with the assumption of degenerate flavours. This is a great simplification, as the additional flavours enter as the number N_f :

$$\mathcal{Z} = \int [dU_\mu] \det Q_{stat}^{N_f} \exp \left(- N_f \sum_{n=1}^{\infty} \frac{1}{n} \text{tr}(P + M)^n \right) \quad (2.2.53)$$

2.3 Resummation

In chapter 2.2.3 and 2.2.4 it was necessary to expand the exponential of the kinetic quark determinant. Hence, we can resum the effective theory to an exponential again. This resummation will improve the convergence of the effective action as it includes an infinite number of graphs.

The effective action is available to order $\mathcal{O}(\kappa^4)$, so the term proportional to κ^2 and the last term of B.1.1 can be resummed.

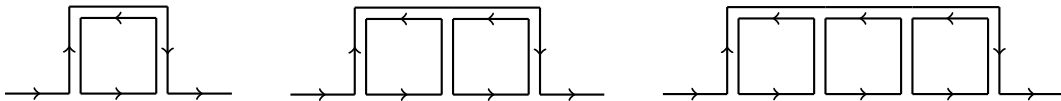
Here, we wrote down the relevant terms, omitting the rest of the $\mathcal{O}(\kappa^4)$ effective action, as this would compromise readability:

$$\begin{aligned} & 1 - N_f \frac{h_2}{2} \sum_{\vec{x}} \sum_{i=\pm 1} W_{1111}^-(\vec{x}) W_{1111}^-(\vec{x} + \hat{i}) \\ & + N_f^2 \frac{h_2^2 (N_\tau - 1)}{4N_\tau} \sum_{\vec{x}} \sum_{i=\pm 1} [W_{1111}^-(\vec{x})]^2 [W_{1111}^-(\vec{x} + \hat{i})]^2 \end{aligned} \quad (2.3.1)$$

The $\mathcal{O}(\kappa^4)$ -term is proportional to $N_\tau(N_\tau - 1)$, which makes the resummation a bit more complicated, as we would need a term proportional to N_τ^2 for a perfect resummation. When we split this term, the leading order term resums perfectly, as expected, but the subleading order term is still present:

$$\begin{aligned} & = 1 - N_f \frac{h_2}{2} \sum_{\vec{x}} \sum_{i=\pm 1} W_{1111}^-(\vec{x}) W_{1111}^-(\vec{x} + \hat{i}) + N_f^2 \frac{h_2^2}{4} \sum_{\vec{x}} \sum_{i=\pm 1} W_{1111}^-(\vec{x}) W_{1111}^-(\vec{x} + \hat{i}) \\ & + N_f^2 \frac{h_2^2}{4N_\tau} \sum_{\vec{x}} \sum_{i=\pm 1} [W_{1111}^-(\vec{x})]^2 [W_{1111}^-(\vec{x} + \hat{i})]^2. \end{aligned} \quad (2.3.2)$$

In order to take care of this subleading order term, we perform the resummation with the leading order term and implement the subleading order term as a correction term.

Figure 2.1: The first three detours of $\mathcal{O}(\kappa^2 u^n)$

We will implement the correction term in two different ways. As the first possibility, further called the first correction, we will add the correction term after the exponential:

$$\begin{aligned}
 &= \exp \left(- N_f \sum_{\vec{x}} \sum_{i=\pm 1} \frac{h_2}{2} W_{1111}^-(\vec{x}) W_{1111}^-(\vec{x} + \hat{i}) \right) \\
 &\quad - \sum_{\vec{x}} \sum_{i=\pm 1} \frac{N_f^2}{4} \frac{h_2^2}{N_\tau} [W_{1111}^-(\vec{x})]^2 [W_{1111}^-(\vec{x} + \hat{i})]^2 + \mathcal{O} \left(\frac{\kappa^6 N_\tau}{N_c^3} \right) \quad (2.3.3)
 \end{aligned}$$

This process does not change when going to higher orders, we would just add all the correction terms after the exponential.

As the second option, further called the second or alternative correction, we put the correction term in the exponential:

$$\begin{aligned}
 &\exp \left(- N_f \sum_{\vec{x}} \sum_{i=\pm 1} \frac{h_2}{2} W_{1111}^-(\vec{x}) W_{1111}^-(\vec{x} + \hat{i}) \right. \\
 &\quad \left. - \sum_{\vec{x}} \sum_{i=\pm 1} \frac{N_f^2}{4} \frac{h_2^2}{N_\tau} [W_{1111}^-(\vec{x})]^2 [W_{1111}^-(\vec{x} + \hat{i})]^2 \right) + \mathcal{O} \left(\frac{\kappa^6 N_\tau}{N_c^3} \right) \quad (2.3.4)
 \end{aligned}$$

To order κ^4 this is trivial, but at higher orders, it is important to calculate counter-correction terms. This is necessary because after expanding the newly obtained exponential again to the order it was expanded to previously, it should be identical to the unresummed effective action.

This makes the calculation of the second correction term a little bit more complicated, but, as we see later, the evaluation of the effective theory is easier.

The terms we neglected in this chapter will appear in the exponential in their normal form.

2.4 Gauge corrections

Until now, we only considered pure gluonic and pure fermionic contributions. In this section, we will discuss how the expansion in κ is affected when mixed with the expansion in β . These corrections can be absorbed into the coupling constants, for example $h_1(\kappa) = h_1(\beta, \kappa)$.

2.4.1 Corrections to the h_1 Coupling

The gauge corrections for h_1 had been calculated for the three dimensional case in [9, 11], the corrections for the anti-quark coupling \bar{h}_1 are identical to these.

We receive the corrections by adding detours to the winding graphs. The resulting diagrams reduce to Polyakov loops after the integration. In order to obtain these diagrams, additional detours of the quark lines are formed and filled with plaquettes as we see, for example, in figure 2.1.

Diagrams of this type also build the leading order corrections at $\mathcal{O}(\kappa^2)$. All diagrams can be placed at N_τ locations and can point in the positive or negative spatial direction, resulting in a factor of 2. We also receive a factor of κ^2 from the two additional links and the factor u^n from the plaquettes filling the detours. Adding up all detours of this type leads to the contribution:

$$\sum_{n=1}^{N_\tau-1} 2N_\tau \kappa^2 u^n = 2N_\tau \kappa^2 \frac{u - u^{N_\tau}}{1 - u}. \quad (2.4.1)$$

In the following, we will include all corrections up to $\mathcal{O}(\kappa^n u^m)$, with $n + m \leq 7$. The calculation of these detours is explained in appendix A.5.

We can resum the term of the detour A.5.4, which is proportional to N_τ^2 , to an exponential. We also include the other terms we calculated, which leads to the total contribution:

$$h_1(\kappa, N_\tau, u) = h_1(\kappa, N_\tau) \exp \left(2N_\tau \kappa^2 \frac{u - u^{N_\tau}}{1 - u} + \kappa^4 N_\tau \left[-8u + 6u^2 + 4u^3 N_\tau \right] \right). \quad (2.4.2)$$

2.4.2 Corrections to the h_2 Couplings

The corrections for h_2 were discussed in [12], and the corrections for h_2^2 , h_{3_1} , and h_{3_2} were evaluated in [5].

The corrections to h_2 are depicted in figure 2.2. Because we are in the one-dimensional case, there is only one type of corrections. These corrections stem from graphs where the spatial quark hoppings take place at different locations. As the links have to be at least doubly occupied, the space between them is filled with plaquettes. Similar to the leading order correction of h_1 , up to $N_\tau - 1$ plaquettes can fill the space between the spatial links and those contributions can be summed

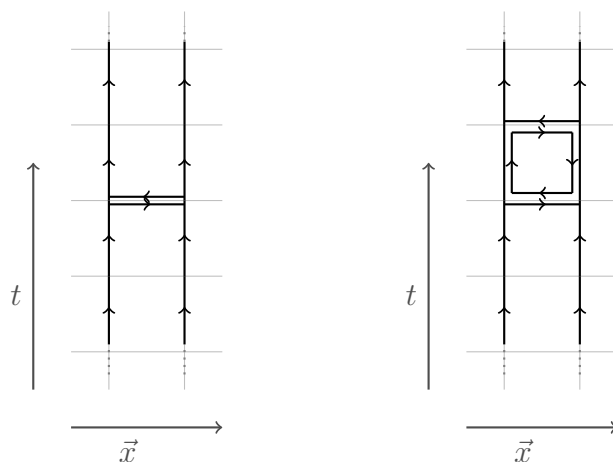


Figure 2.2: Diagrams of the corrections for h_2 , on the left $\mathcal{O}(1)$, on the right $\mathcal{O}(u)$

up. A factor of 2 is added since, in contrary to h_1 , the orientation of the plaquettes is not specified. This leads to the sum

$$\sum_{n=1}^{N_\tau-1} 2u^n = 2 \frac{u - u^{N_\tau}}{1 - u} \quad (2.4.3)$$

and then to the entire correction of h_2

$$h_2(\kappa, N_\tau, u) = \frac{\kappa^2 N_\tau}{N_c} \left(1 + 2 \frac{u - u^{N_\tau}}{1 - u} \right). \quad (2.4.4)$$

Next, we are going to calculate the corrections for h_2^2 . Again, we only get corrections from inserting plaquettes between the spatial quark hoppings. The three Polyakov loops, depicted in figure 2.3, lead to two sums and, if we split up both pairs, a factor of 4 because there are two possibilities for the orientations of the plaquettes. If we split up one pair, we receive a factor of 2 for the orientation and a factor of 2 because it is not fixed at what pair the plaquette is inserted. The sums take the form

$$4 \left(\sum_{n=1}^{N_\tau-1} u^n \right) \left(\sum_{n=0}^{N_\tau-1} u^n \right) = 4 \frac{(1 - u^{N_\tau})(u - u^{N_\tau})}{(1 - u)^2} \quad (2.4.5)$$

which leads to the correction

$$h_2^2(\kappa, N_\tau, u) = \frac{\kappa^4 N_\tau}{N_c^2} \left(1 + 4 \frac{(1 - u^{N_\tau})(u - u^{N_\tau})}{(1 - u)^2} \right). \quad (2.4.6)$$

We can also obtain this correction by squaring the corrections for h_2 , but the method above is a more instructional way of calculating the correction.

There are two other couplings, both taking place between two Polyakov loops. With the first coupling, $h_{3_1} = \frac{\kappa^4 N_\tau}{N_c^2}$, all four spatial links share the same position and with the second one, $h_{3_2} = \frac{\kappa^4 N_\tau (N_\tau - 1)}{N_c^2}$, the spatial links are only doubly occupied.

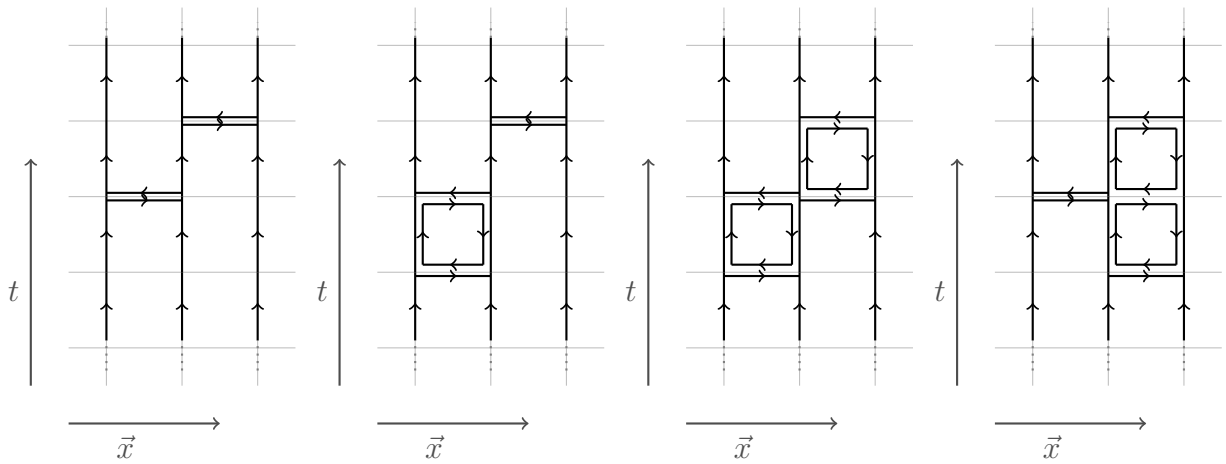


Figure 2.3: Diagrams of the corrections for h_2^2 , on the left $\mathcal{O}(1)$, in the middle one version of $\mathcal{O}(u)$ and on the right two versions of $\mathcal{O}(u^2)$

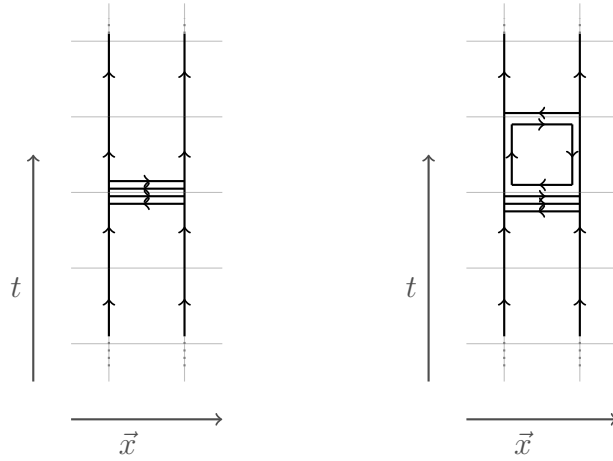


Figure 2.4: Diagrams of the corrections for h_{3_1} , on the left $\mathcal{O}(1)$ and on the right $\mathcal{O}(u)$

Figure 2.4 shows the contributions to h_{3_1} . Again, only one type of the contributions exists in one dimension. The prefactor 4 of the sum stems from the orientation of the plaquettes and the possibility to choose which pair will be split up:

$$2 \cdot 2 \sum_{n=1}^{N_\tau-1} u^n = 4 \frac{u - u^{N_\tau}}{1 - u}. \quad (2.4.7)$$

This leads to the correction

$$h_{3_1}(\kappa, N_\tau, u) = \frac{\kappa^4 N_\tau}{N_c^2} \left(1 + 4 \frac{u - u^{N_\tau}}{1 - u} \right). \quad (2.4.8)$$

The last coupling h_{3_2} has the more complicated form

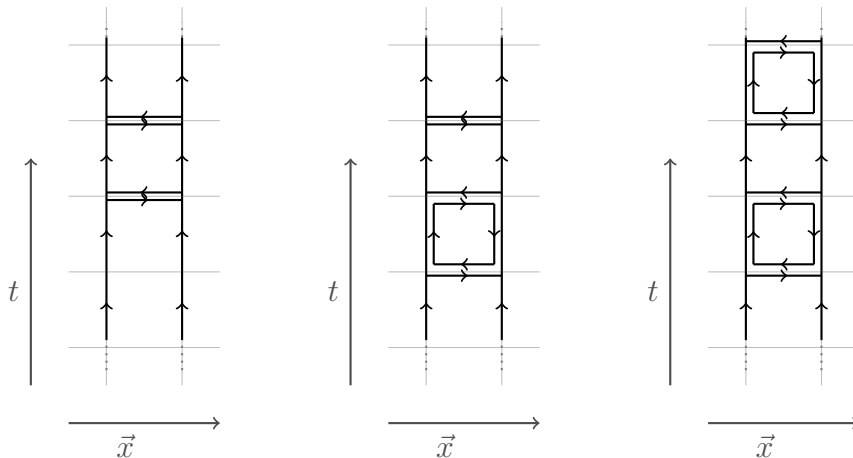


Figure 2.5: Diagrams of the corrections for h_{3_2} , on the left $\mathcal{O}(1)$, in the middle $\mathcal{O}(u^2)$, $N_\tau = 4$ with one split up pair and on the right $\mathcal{O}(u^2)$, $N_\tau = 4$ with two split up pairs

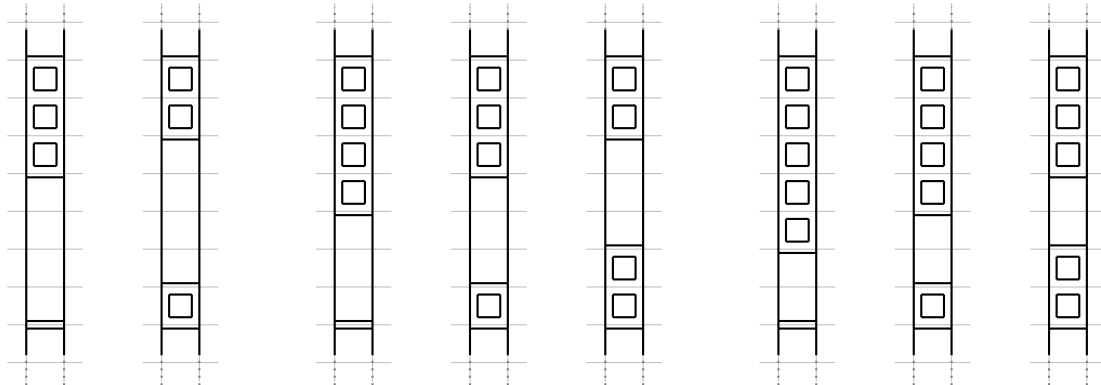


Figure 2.6: All diagrams of the corrections for h_{3_2} at order $\mathcal{O}(u^3)$, $\mathcal{O}(u^4)$, and $\mathcal{O}(u^5)$

$$h_{3_2}(\kappa, N_\tau, u) = \frac{\kappa^4 N_\tau (N_\tau - 1)}{N_c^2} \left(1 + \sum_{n=1}^{N_\tau-2} 4nu^n \frac{N_\tau - (n+1)}{N_\tau - 1} \right), \quad (2.4.9)$$

with n as the number of plaquettes.

As we can see in figure 2.5, the term $N_\tau - (n+1)$ arises, because we can't have spatial links from the different pairs at the same spatial position since these are the contributions from h_{3_1} . We divide by $N_\tau - 1$ to take care of the fact that both links are actually at a fixed position, in contrast to the assumption above that we can choose their position freely.

In order to obtain the prefactor of $\sum_{n=1}^{N_\tau-2} 4nu^n$, we need to add up all the prefactors of the diagrams for every order. In figure 2.6 we see all diagrams for the orders $\mathcal{O}(u^3)$, $\mathcal{O}(u^4)$, and $\mathcal{O}(u^5)$. For each diagram, we have to determine the possible placement and orientation of the plaquettes.

The first diagram for order $\mathcal{O}(u^3)$ receives a prefactor of 4 for the two possible orientations for the plaquette and the distinguishable link pairs, both giving a contribution of 2. The second diagram gives a prefactor of 8 since the link distinguishable pairs lead to a factor of 2, and we receive a factor of 4 from the orientation of the plaquettes. Adding up those prefactors leads to an overall factor of 12, which is equivalent to $4n$ at $n = 3$.

The prefactors of the first two diagrams of order $\mathcal{O}(u^4)$ are identical to the ones from order $\mathcal{O}(u^3)$. The third one has a prefactor of 4, because we have two possible orientations for the plaquettes between the otherwise indistinguishable link pairs. This leads to an overall prefactor of 16, which is again equivalent to $4n$ at $n = 4$.

For the first two diagrams of order $\mathcal{O}(u^5)$, we receive again the prefactors 4 and 8. The third diagram also gives a prefactor of 8 because, in contrast to the third diagram of order $\mathcal{O}(u^4)$, the two link pairs are distinguishable. This leads to the prefactor of 20, or $4n$ at $n = 5$.

This process is repeated at every order, so we always receive an additional factor of 4 with every step. This leads to the conclusion that the universal prefactor of order $\mathcal{O}(u^n)$ is $4n$.

Now that the derivation of the effective theory is complete, we will evaluate it with the linked cluster expansion in the next chapter.

Chapter 3

Analytic Treatment of the Effective Theory

In this chapter, we will evaluate the effective theory with the linked cluster expansion.

3.1 Linked Cluster Expansion

In this part, we will introduce the linked cluster expansion. We will discuss the foundations at the example of a scalar field with nearest neighbour coupling. This introduction is based on the work of [7, 13–16].

3.1.1 Classical Linked Cluster Expansion

The partition function of the scalar field with a two-point coupling has the form:

$$\mathcal{Z} = \int [d\phi_i] e^{-\mathcal{S}_0[\phi_i] + \frac{1}{2} \sum_{x,y} \phi_i(x) v_{ij}(x,y) \phi_j(y)} \quad (3.1.1)$$

with the fields $\phi_i(x)$ and the coupling $v_{ij}(x, y)$, which we assume is small, so that we can perform an expansion around the free theory.

We rewrite the partition function in terms of the source fields $J_i(x)$:

$$\mathcal{Z}[J] = \int [d\phi] e^{-\mathcal{S}[\phi] + \sum_x \sum_i J_i(x) \phi_i(x)} \quad (3.1.2)$$

For the calculation of thermodynamic quantities, we define the grand canonical potential, or generating functional of connected correlation functions, \mathcal{W} :

$$\mathcal{W}[J, v] = \log \mathcal{Z}[J, v] \quad (3.1.3)$$

The linked cluster expansion is equivalent to a Taylor expansion of the generating functional with respect to the coupling $v_{ij}(x, y)$ around the free theory:

$$\mathcal{W}[J, v] = \left(\exp \left(\sum_{x,y} v_{ij}(x, y) \frac{\delta}{\delta v_{ij}(x, y)} \right) \right) \mathcal{W}[J, \hat{v}] \Big|_{\hat{v}=0}. \quad (3.1.4)$$

We rewrite the derivatives with respect to the couplings as derivatives with respect to the sources:

$$\frac{\delta \mathcal{W}}{\delta v_{ij}(x, y)} = \frac{1}{2} \left(\frac{\delta^2 \mathcal{W}}{\delta J_i(x) \delta J_j(y)} + \frac{\delta \mathcal{W}}{\delta J_i(x)} \frac{\delta \mathcal{W}}{\delta J_j(y)} \right). \quad (3.1.5)$$

$\mathcal{W}[J]$ is also the generating functional of the connected n-point functions:

$$\left. \frac{\delta \mathcal{W}}{\delta J_i(x)} \right|_{J=0} = \frac{1}{\mathcal{Z}} \int [d\phi_i] \phi_i(x) e^{-S[\phi_i]} \equiv \langle \phi_i(x) \rangle. \quad (3.1.6)$$

For higher order derivatives, it also produces the cumulants:

$$\left. \frac{\delta^2 \mathcal{W}}{\delta J_i(x) \delta J_j(y)} \right|_{J=0} = \langle \phi_i(x) \phi_j(y) \rangle - \langle \phi_i(x) \rangle \langle \phi_j(y) \rangle. \quad (3.1.7)$$

The methods of moments and cumulants are explained in appendix A.4.

The linked cluster expansion performed to second order gives:

$$\begin{aligned} \mathcal{W}[J, v] = & \mathcal{W}[J, 0] + \sum_{x, y} \sum_{i, j} v_{ij}(x, y) \left. \frac{\delta \mathcal{W}[J, \hat{v}]}{\delta \hat{v}_{ij}(x, y)} \right|_{\hat{v}=0} \\ & + \frac{1}{2} \sum_{x, y} \sum_{z, w} \sum_{i, j} \sum_{k, l} v_{ij}(x, y) v_{kl}(z, w) \left. \frac{\delta^2 \mathcal{W}[J, \hat{v}]}{\delta \hat{v}_{ij}(x, y) \delta \hat{v}_{kl}(z, w)} \right|_{\hat{v}=0} + \dots \end{aligned} \quad (3.1.8)$$

We can also define the coupled n-point functions:

$$\mathcal{M}_n(x_1, x_2, \dots, x_n) = \frac{\delta^n \mathcal{W}[J, v]}{\delta J(x_1) \delta J(x_2) \dots \delta J(x_n)}. \quad (3.1.9)$$

These then define the free n-point functions:

$$\mathcal{M}_n(x_1, x_2, \dots, x_n)|_{v=0} \equiv M_n(x_1) \delta(x_1, x_2, \dots, x_n). \quad (3.1.10)$$

The Kronecker deltas arise from the free theory because of:

$$x \neq y \Rightarrow \langle \phi_i(x) \phi_j(y) \rangle|_{v=0} = \langle \phi_i(x) \rangle \langle \phi_j(y) \rangle \quad (3.1.11)$$

The Kronecker deltas lead to the disappearance of any disconnected graphs, which makes the linked cluster expansion an expansion in connected graphs.

We rewrite the derivatives with respect to the couplings from equation 3.1.8 to derivatives with respect to the sources, so they are expressed as free n-point functions:

$$\begin{aligned} \mathcal{W}[v] = & \mathcal{W}[0] + \frac{1}{2} \sum_{x, y} \sum_{i, j} M_i(x) v_{ij}(x, y) M_j(y) \\ & + \frac{1}{4} \sum_{x, y} \sum_{i, j, k, l} M_{ik}(x) v_{ij}(x, y) v_{kl}(x, y) M_{jl}(y) \\ & + \frac{1}{2} \sum_{x, y, z} \sum_{i, j, k, l} M_i(x) v_{ij}(x, y) M_{jk}(y) v_{kl}(y, z) M_l(z) + \dots \end{aligned} \quad (3.1.12)$$

As this process gets quite lengthy at higher orders, the graphical approach discussed in the next section will be very useful in further calculations.

3.1.2 Graphical Definition of the Linked Cluster Expansion

In order to understand the graphical linked cluster expansion, we have to establish some definitions from graph theory and also a rule for their implementation, analogous to [7, 13].

A graph is defined as a set of vertices and bonds with every bond connecting two distinct vertices. An n -rooted graph has n fixed, distinguishable, external vertices, all remaining internal vertices are free.

The number of edges incident at a vertex is called the valence of that vertex. An n -valent vertex has a valence n .

A graph where any pair of vertices is joined by a continuous sequence of bonds is called connected otherwise it is disconnected.

If it is possible to find a labelling of the bonds and vertices of two n -rooted graphs so that the bonds and vertices of those two graphs can be made identical, those graphs are isomorphic. The symmetry factor is the number of distinct isomorphic labellings of a graph.

For the calculation of \mathcal{W} , we need the set of all topologically distinct 0-rooted connected graphs. The number of bonds determines the order of the graph, so for order $\mathcal{O}(v^2)$ we need all 0-rooted graphs with one or two bonds. We will also need a rule that describes how to switch between the mathematical expression and the graphical representation of \mathcal{W} .

1. Assign a symbol x_1, x_2, \dots, x_n to every vertex
2. Add a factor $v(x_i, x_j)$ to every bond connecting the vertices x_i and x_j
3. Add a factor $M_p(x_i)$ for every vertex x_i with valence p
4. For every vertex symbol x_i add a sum over the entire lattice
5. Divide by the symmetry factor of the graph

This leads to the graphical expression of the grand canonical potential, which is equivalent to 3.1.12

$$\mathcal{W}[v] = \bullet + \frac{1}{2} \begin{array}{c} \bullet \\ | \\ \bullet \end{array} + \frac{1}{2} \begin{array}{c} \bullet \\ \diagup \quad \diagdown \\ \bullet \end{array} + \frac{1}{4} \begin{array}{c} \bullet \\ \circlearrowleft \\ \bullet \end{array} + \dots \quad (3.1.13)$$

The equality between this graphical rule and the linked cluster expansion of the grand canonical potential is proven in [17, 18].

Until now, we did not specify the type of the interaction. When we choose the interaction to be a nearest neighbour coupling

$$v(x, y) = \begin{cases} v & \text{for } x \text{ and } y \text{ nearest neighbours} \\ 0 & \text{else} \end{cases}, \quad (3.1.14)$$

the mathematical expression of the grand canonical potential simplifies to:

$$\mathcal{W}[v] = NM_0 + \frac{q}{2}vNM_1^2 + \frac{q}{4}v^2NM_2^2 + \frac{q^2}{2}v^2NM_1^2M_2 + \dots \quad (3.1.15)$$

N is the number of lattice sites and stems from the sum over the whole lattice. q is called the embedding number and differs depending on the lattice that is used, in our case it is equivalent to $2d$, with d the dimension of the lattice. It describes how many possibilities we have to put the graph on a given lattice without violating the restriction of the nearest-neighbour coupling.

3.1.3 Generalisation of the Linked Cluster Expansion to Polymer Interactions

Later, we will need a possibility to perform the linked cluster expansion on a three-point coupling. Therefore, we are going to introduce a generalisation established in [15].

First, we need to expand the scalar field by a three-point coupling:

$$\begin{aligned} \mathcal{Z} = \int [d\phi_i] \exp \left(-\mathcal{S}_0[\phi_i] + \frac{1}{2!} \sum_{x,y} \sum_{i,j} v_{ij}(x,y) \phi_i(x) \phi_j(y) + \right. \\ \left. \frac{1}{3!} \sum_{x,y,z} \sum_{i,j,k} u_{ijk}(x,y,z) \phi_i(x) \phi_j(y) \phi_k(z) \right). \end{aligned} \quad (3.1.16)$$

By following the steps of chapter 3.1.1, we obtain the linked cluster expansion for the grand canonical potential

$$\begin{aligned} \mathcal{W}[v, u] = \left[\exp \left(\frac{1}{2!} \sum_{x,y} \sum_{i,j} v_{ij}(x,y) \frac{\delta}{\delta \hat{v}_{ij}(x,y)} \right) \right. \\ \left. \exp \left(\frac{1}{3!} \sum_{x,y,z} \sum_{i,j,k} u_{ijk}(x,y,z) \frac{\delta}{\delta \hat{u}_{ijk}(x,y,z)} \right) \right] \mathcal{W}[\hat{v}, \hat{u}] \Big|_{\hat{v}=\hat{u}=0}. \end{aligned} \quad (3.1.17)$$

Furthermore, we have to express the derivative with respect to the three-point coupling as a derivative with respect to the sources:

$$\begin{aligned} \frac{\delta \mathcal{W}}{\delta u_{ijk}(x,y,z)} = \frac{\delta^3 \mathcal{W}}{\delta J_i(x) \delta J_j(y) \delta J_k(z)} + \frac{\delta \mathcal{W}}{\delta J_i(x)} \frac{\delta^2 \mathcal{W}}{\delta J_j(y) \delta J_k(z)} \frac{\delta \mathcal{W}}{\delta J_j(y)} \frac{\delta^2 \mathcal{W}}{\delta J_i(x) \delta J_k(z)} \\ + \frac{\delta \mathcal{W}}{\delta J_k(z)} \frac{\delta^2 \mathcal{W}}{\delta J_i(x) \delta J_j(y)} + \frac{\delta \mathcal{W}}{\delta J_i(x)} \frac{\delta \mathcal{W}}{\delta J_j(y)} \frac{\delta \mathcal{W}}{\delta J_k(z)}. \end{aligned} \quad (3.1.18)$$

When we go up to order $\mathcal{O}(v^2, u)$, which means the graphs can have up to two bonds, and assume a cyclic three-point coupling, we get:

$$\begin{aligned}
 \mathcal{W}[v] = & \mathcal{W}[0] + \frac{1}{2} \sum_{x,y} \sum_{i,j} M_i(x) v_{ij}(x,y) M_j(y) \\
 & + \frac{1}{4} \sum_{x,y} \sum_{i,j,k,l} M_{ik}(x) v_{ij}(x,y) v_{kl}(x,y) M_{jl}(y) \\
 & + \frac{1}{2} \sum_{x,y,z} \sum_{i,j,k,l} M_i(x) v_{ij}(x,y) M_{jk}(y) v_{kl}(y,z) M_l(z) \\
 & + \frac{1}{3!} \sum_{x,y,z} \sum_{i,j,k} u_{ijk}(x,y,z) M_i(x) M_j(y) M_k(z) \\
 & + \frac{1}{2} \sum_{x,y} \sum_{i,j,k} u_{ijk}(x,y,y) M_i(x) M_{jk}(y) + \dots
 \end{aligned} \tag{3.1.19}$$

We specify the three-point interaction as a set of two nearest neighbour interactions:

$$u(x,y,z) = \begin{cases} u & \text{for } \langle x,y \rangle \text{ and } \langle y,z \rangle \text{ nearest neighbours,} \\ u & \text{for } \langle x,y \rangle \text{ and } \langle x,z \rangle \text{ nearest neighbours,} \\ u & \text{for } \langle x,z \rangle \text{ and } \langle y,z \rangle \text{ nearest neighbours,} \\ 0 & \text{else} \end{cases} \tag{3.1.20}$$

This shortens the expression of \mathcal{W} :

$$\begin{aligned}
 \mathcal{W}[v,u] = & NM_0 + \frac{q}{2} v N M_1^2 + \frac{q^2}{2} v^2 N M_1^2 M_2 + \frac{q}{4} v^2 N M_2^2 \\
 & + \frac{q^2}{2} u N M_1^3 + \frac{q}{2} u N M_1 M_2 + \dots
 \end{aligned} \tag{3.1.21}$$

As we won't go to higher orders, the two- and three-point interactions don't mix, which makes the rules for the graphical representation a lot simpler.

The graphical representation will look like this:

$$\mathcal{W}[v] = \bullet + \frac{1}{2} \text{---} + \frac{1}{2} \text{---} + \frac{1}{4} \text{---} + \frac{1}{2} \text{---} + \frac{1}{2} \text{---} + \dots \tag{3.1.22}$$

The purple coloured bonds belong to the two-point coupling and the blue coloured bonds to the three-point coupling. Some graphs have circles around their vertices, one for every base interaction, in order to make the two vertices of the last graph distinguishable. Therefore, the triangular graph with the two-point coupling has a circle around its middle vertex because the two couplings meet there, whereas the graph with the three-point coupling hasn't because only one interaction takes place.

Because those are the only graphs we will consider, our rules stay simple. Now, we determine M_n by counting the number of the circles, including the dot, at each vertex. The vertex without a circle leads to $n = 1$, a vertex with one circle to $n = 2$ etc. We also have to take into account that the symmetry factor depends on the type of the interaction because more vertices are now distinguishable. We can see this with the last graph, which does not have the same symmetry factor as its two-point coupling counterpart.

When going to higher orders, this gets more complicated because the different couplings start mixing. Since we don't need to consider this case, we will now apply the linked cluster expansion to the effective theory.

3.2 Linked Cluster Expansion of the Effective Theory

As we derived the necessary parts of the formalism, we can now map the effective theory to it, according to [7]. At first, we will disregard the correction term of the resummation, but we will discuss its implementation in the last part of this chapter.

3.2.1 Application to the Effective Theory

Here, we will apply the linked cluster expansion to the resummed effective action to order $\mathcal{O}(\kappa^2)$ and at $N_f = 1$,

$$\mathcal{Z} = \int [dU_0] \det Q_{stat} \exp \left(-\frac{h_2}{2} \sum_{\langle x,y \rangle} W_{1111}^-(x) W_{1111}^-(y) \right), \quad (3.2.1)$$

where $\langle x, y \rangle$ describes pairs of nearest neighbours. We can rewrite the sum as $\sum_x \sum_{i \pm 1}$, which leads to the additional factor of $\frac{1}{2}$ in order to avoid overcounting.

Comparing this to the partition function for the two-point coupling

$$\mathcal{Z} = \int [d\phi_i] \exp \left(\mathcal{S}_0[\phi_i] + \frac{1}{2} \sum_{x,y} \phi_i(x) v_{ij}(x, y) \phi_j(y) \right) \quad (3.2.2)$$

shows how it is possible to connect both equations:

$$\phi_i \Leftrightarrow W_{1111}^-, \quad v \Leftrightarrow h_2, \quad e^{-\mathcal{S}_0[\phi_i]} \Leftrightarrow \mathcal{J}(U_0, W_{1111}^-) \det Q_{stat} \quad (3.2.3)$$

with $\mathcal{J}(U_0, W_{1111}^-)$ as the Jacobian determinant. We do not have to calculate it explicitly since the free energy depends solely on the expectation values of the free theory.

At order $\mathcal{O}(\kappa^4)$, we have more than one field, which leads to the correspondence:

$$\begin{aligned} \phi_i &\leftrightarrow (W_{1111}^-, W_{2222}^+, W_{1111}, [W_{1111}^-]^2, W_{2121}^+, W_{1010}, W_{1111}^+, W_{0000}) \\ e^{-\mathcal{S}_0[\phi_i]} &\Leftrightarrow \mathcal{J}(U_0, W_{1111}^-, W_{2222}^+, W_{1111}, [W_{1111}^-]^2, W_{2121}^+, W_{1010}, W_{1111}^+, W_{0000}) \det Q_{stat}. \end{aligned} \quad (3.2.4)$$

The two- and three-point interactions are written down in appendix B.2, as these expressions are quite lengthy.

After we established this relation between the linked cluster expansion and the effective theory, we can solve the remaining integrals over U_0 .

3.2.2 Calculation of the n -Point Functions

To calculate the integrals, we have to express the n -point functions in terms of cumulants. For brevity, we introduce the following naming scheme for the integrals:

$$z_{[(n_1 m_1 n_2 m_2)^x]^k} = \int dW \det Q_{stat}^{N_f} (W_{n_1 m_1 n_2 m_2}^x)^k \quad (3.2.5)$$

with x either $+$, $-$, or blank.

The only exception from the naming scheme is z_0 , which stands for

$$z_0 = \int dW \det Q_{stat}^{N_f}. \quad (3.2.6)$$

The n -point functions relevant for our calculations are of the form:

$$\begin{aligned} M_0 &= \log z_0, & M_1 &= \frac{z_{(1111)^-}}{z_0}, & M_2 &= \frac{z_{(2222)^+}}{z_0}, & M_3 &= \frac{z_{(1111)}}{z_0}, \\ M_4 &= \frac{z_{[(1111)^-]^2}}{z_0}, & M_5 &= \frac{z_{(2121)^+}}{z_0}, & M_6 &= \frac{z_{(1010)}}{z_0}, & M_7 &= \frac{z_{(1111)^+}}{z_0}, \\ M_8 &= 1, & M_{11} &= \frac{z_{[(1111)^-]^2}}{z_0} - \frac{z_{(1111)^-}^2}{z_0^2}. \end{aligned} \quad (3.2.7)$$

We also have to rewrite the $W_{n_1 m_1 n_2 m_2}$ terms in terms of Polyakov loops. This calculation is described in appendix A.2. The integrals will then be solved with the techniques presented in appendix A.3.

We wrote down the results for $N_f = 1$ and $N_f = 2$ in appendix B.3, as they are quite lengthy.

3.2.3 Calculation of the Correction Term

Now, we still need to implement the correction term 2.3 into the framework of the linked cluster expansion.

Considering the first correction term, the effective action looks like

$$\mathcal{Z} = \int [dU_0] \det Q_{stat} \exp(\mathcal{S}_o) - \int [dU_0] \det Q_{stat} \mathcal{S}_{corr}, \quad (3.2.8)$$

with \mathcal{S}_o denoting the effective action without the correction term and

$$\mathcal{S}_{corr} = \sum_{\vec{x}} \frac{N_f^2}{2} \frac{h_2^2}{N_\tau} [W_{1111}^-(\vec{x})]^2 [W_{1111}^-(\vec{x} - \hat{1})]^2 \quad (3.2.9)$$

the correction term.

We will expand the generating functional at $\mathcal{S}_{corr} = 0$, as we can not apply the linked cluster expansion directly to this action

$$\begin{aligned}
\mathcal{W} &= \log \mathcal{Z} \\
&= \log \left(\int [dU_0] \det Q_{stat} \exp(\mathcal{S}_o) \right) \\
&\quad - \frac{1}{\int [dU_0] \det Q_{stat} \exp(\mathcal{S}_o)} \cdot \int [dU_0] \det Q_{stat} \mathcal{S}_{corr} \\
&= \log \left(\int [dU_0] \det Q_{stat} \exp(\mathcal{S}_o) \right) \\
&\quad - \exp \left(- \log \left(\int [dU_0] \det Q_{stat} \exp(\mathcal{S}_o) \right) \right) \int [dU_0] \det Q_{stat} \mathcal{S}_{corr}. \quad (3.2.10)
\end{aligned}$$

The first term and the term inside the exponential had been calculated previously in chapter 3.2.1.

The correction term itself evaluates to:

$$\int [dU_0] \det Q_{stat} \mathcal{S}_{corr} = V \frac{N_f^2}{2} \frac{h_2^2}{N_\tau} z_{((1111)^-)^2} z_0^{V-2} \quad (3.2.11)$$

with V the spatial volume of the lattice.

At higher orders, this integration gets more complicated because one has to take care of the embedding of the correction terms.

The second correction is unproblematic to this order because we can evaluate it with the normal linked cluster expansion.

It is not entirely clear how to take care of this correction when going to higher orders because it is only possible to investigate this problem when all the terms to order $\mathcal{O}(\kappa^8)$ are known fully, without the abbreviations of the dense limit. The correction terms can either be evaluated only to first order in the linked cluster expansion or to the highest order that was used for the other terms. Because of the counter correction terms, it is probably necessary to perform the evaluation to the highest order, but it was not possible to investigate this problem further in this thesis.

3.3 Observables

In this chapter, we will calculate the pressure p , the baryon number density n_B , the baryon mass m_B , and the binding energy ϵ , analogous to [6, 7, 15].

The pressure is defined as proportional to the generating functional:

$$p = T \left(\frac{\partial}{\partial V} \log \mathcal{Z} \right)_{T,z} = \frac{T}{V} \mathcal{W}. \quad (3.3.1)$$

The quark number is defined as the derivative of the generating functional with respect to the fugacity:

$$n_q = z \left(\frac{\partial}{\partial z} \log \mathcal{Z} \right)_{\beta,V}. \quad (3.3.2)$$

Using a simple relation between the fugacity and h_1

$$z \frac{\partial}{\partial z} \Big|_{T,V} = h_1 \frac{\partial}{\partial h_1} \Big|_{T,V} \quad (3.3.3)$$

we can rewrite the quark number in terms of h_1 :

$$n_q = h_1 \left(\frac{\partial}{\partial h_1} \frac{\mathcal{W}}{V} \right)_{T,V} \quad (3.3.4)$$

The antiquark density is calculated similarly, only replacing h_1 with \bar{h}_1 . Combining both the quark and the antiquark density leads to the baryon number density:

$$n_B = \frac{1}{3} \left(h_1 \frac{\partial}{\partial h_1} \frac{\mathcal{W}}{V} - \bar{h}_1 \frac{\partial}{\partial \bar{h}_1} \frac{\mathcal{W}}{V} \right)_{T,V}. \quad (3.3.5)$$

In our plots, the baryon chemical potential will be normalised with the baryon mass [19]

$$\begin{aligned} am_{M,\beta=0} &= -2 \log(2\kappa) \\ am_{B,\beta=0} &= -3 \log(2\kappa). \end{aligned} \quad (3.3.6)$$

The lowest order gauge corrections for the masses in three dimensions are known from [6]. For our one dimensional result, we calculated them up to order $\mathcal{O}(\kappa^n u^m)$ with $n + m \leq 7$:

$$\begin{aligned} am_M &= m_{M,\beta=0} - 8\kappa^2 \frac{u}{1-u} + 32\kappa^4 u - 64\kappa^4 u^2 - 80\kappa^4 u^3 \\ am_B &= m_{B,\beta=0} - 6\kappa^2 \frac{u}{1-u} + 24\kappa^4 u - 54\kappa^4 u^2 - 60\kappa^4 u^3. \end{aligned} \quad (3.3.7)$$

An outline of the calculation of the masses and their corrections can also be found in A.6.

The binding energy is calculated as a dimensionless ratio, which contains the energy density e and the baryon mass:

$$\epsilon = \frac{e - m_B n_B}{m_B n_B} \quad (3.3.8)$$

The energy density is defined as the derivative of the generating functional with respect to the lattice spacing a :

$$e = -\frac{1}{N_\tau} \left(\frac{\partial}{\partial a} \frac{\mathcal{W}}{V} \right)_z. \quad (3.3.9)$$

We can replace the derivative with respect to a with derivatives with respect to the couplings:

$$\begin{aligned} e &= -\frac{1}{N_\tau} \frac{\partial \kappa}{\partial a} \frac{\partial h_1}{\partial \kappa} \frac{\partial}{\partial h_1} \frac{\mathcal{W}}{V} \Big|_z - \frac{1}{N_\tau} \frac{\partial \kappa}{\partial a} \frac{\partial \bar{h}_1}{\partial \kappa} \frac{\partial}{\partial \bar{h}_1} \frac{\mathcal{W}}{V} \Big|_z - \frac{1}{N_\tau} \frac{\partial \kappa}{\partial a} \frac{\partial h_2}{\partial \kappa} \frac{\partial}{\partial h_2} \frac{\mathcal{W}}{V} \Big|_z \\ &\quad - \frac{1}{N_\tau} \frac{\partial \kappa}{\partial a} \frac{\partial h_{3_1}}{\partial \kappa} \frac{\partial}{\partial h_{3_1}} \frac{\mathcal{W}}{V} \Big|_z - \frac{1}{N_\tau} \frac{\partial \kappa}{\partial a} \frac{\partial h_{3_2}}{\partial \kappa} \frac{\partial}{\partial h_{3_2}} \frac{\mathcal{W}}{V} \Big|_z \end{aligned} \quad (3.3.10)$$

Making use of the equation

$$\frac{\partial \kappa}{\partial a} = -\kappa \frac{m_B}{3}, \quad (3.3.11)$$

the energy density simplifies to:

$$e = \frac{\kappa m_B}{3N_\tau} \left(\frac{\partial h_1}{\partial \kappa} \frac{\partial}{\partial h_1} \frac{\mathcal{W}}{V} + \frac{\partial \bar{h}_1}{\partial \kappa} \frac{\partial}{\partial \bar{h}_1} \frac{\mathcal{W}}{V} + \frac{\partial h_2}{\partial \kappa} \frac{\partial}{\partial h_2} \frac{\mathcal{W}}{V} + \frac{\partial h_{3_1}}{\partial \kappa} \frac{\partial}{\partial h_{3_1}} \frac{\mathcal{W}}{V} + \frac{\partial h_{3_2}}{\partial \kappa} \frac{\partial}{\partial h_{3_2}} \frac{\mathcal{W}}{V} \right). \quad (3.3.12)$$

3.4 Results

We present every observable for the generating functional to order κ^2 , identified with W_2 , and to order κ^4 without the correction term, depicted as W_4 . Further, we present the observables for the κ^4 action including the correction term. W_{corr} corresponds to the first correction term, where we added it after the exponential, and W_{calt} corresponds to the second, or alternative, correction term, where we inserted the correction into the exponential. Most of the times, the single terms will overlap, it is mostly the first correction term that differs visibly from the rest.

Figure 3.1 shows the baryon number density at different values of κ , N_τ , V , u , and N_f . Every plot shows the silver blaze property, which means that the baryon number density stays at zero until the chemical potential reaches the constituent quark mass. Slightly before this point, the baryon number density starts to rise and eventually, we will reach the saturation with the value $2N_f$. The saturation is a lattice artefact, so even before it is reached, the results are mainly dependent on these artefacts and can be ignored.

The first correction term dips between $\mu = 1$ and the saturation. Due to the connection of h_2 with κ and N_τ , decreasing one of them decreases the difference between the different terms, especially the dip for W_{corr} . Also, the change in the volume V has this effect on the first correction term. Including the gauge corrections, so that $u \neq 0$, increases the difference between the terms. When switching to $N_f = 2$, the corrections differ more from the uncorrected terms, so we keep the volume smaller as the first correction term would start to diverge badly at $V = 75$.

Figure 3.2 shows the behaviour of the pressure. It generally increases with increasing baryon chemical potential, just as we expected. Here we have the same effects as with the baryon number density, when lowering κ , N_τ and V , considering $u \neq 0$ and changing to $N_f = 2$. We can also observe that the overall value of the pressure increases with smaller κ , N_τ , and higher N_f , but stays mostly the same when changing the volume or turning on u .

In figure 3.3, the plots for the binding energy can be found. The binding energy drops below 0, which indicates that the quarks are bound. Overall, the behaviour stays the same as for the pressure and the baryon number density. For the terms of order κ^4 , the contribution gets bigger at lower N_τ and higher κ but seems mostly unchanged by a change in the volume or by turning on the gauge corrections. When going to higher N_f , the contribution gets smaller. The first correction term W_{corr} is actually saturating in the first plot and the last two plots, but at much lower values

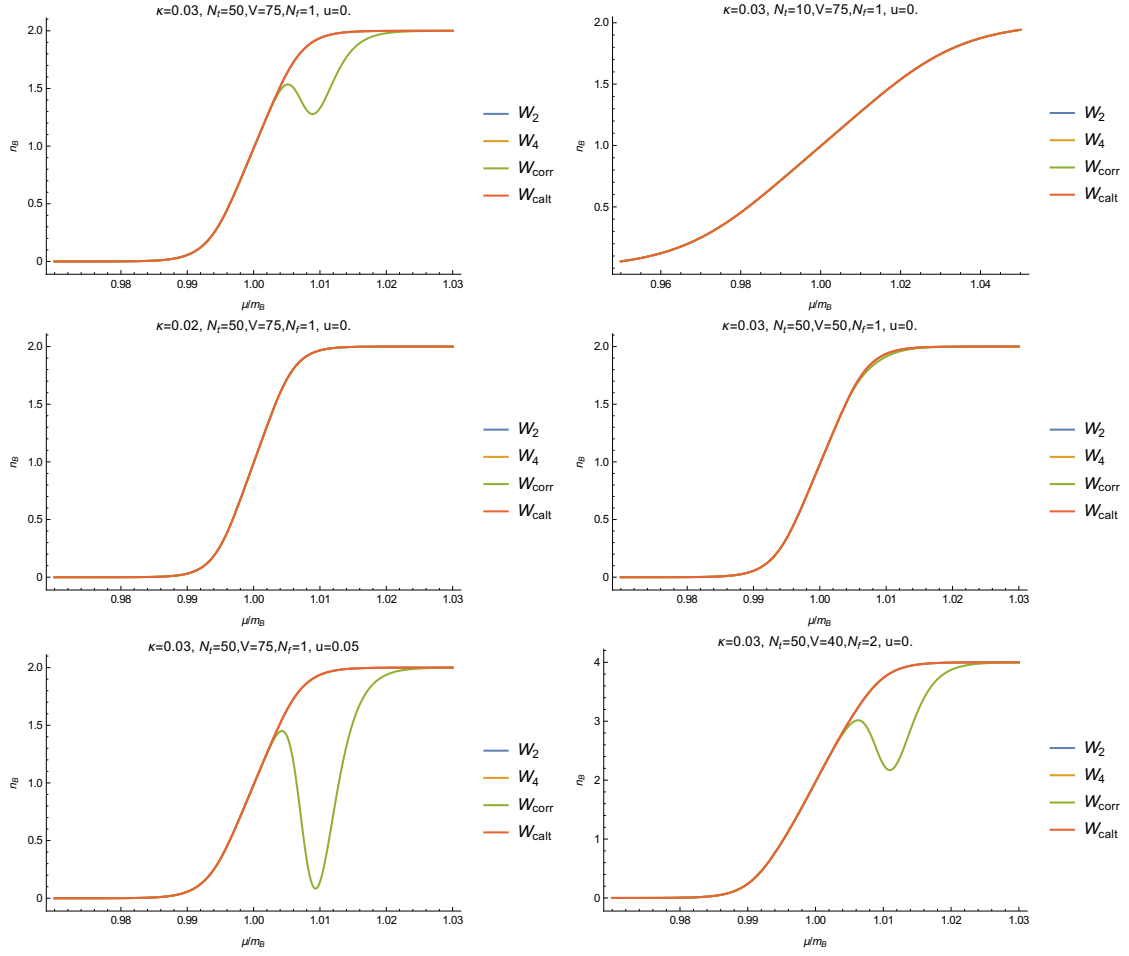


Figure 3.1: The baryon number density for $N_f = 1$ at different values of κ, N_τ, V, m and u and at $N_f = 2$

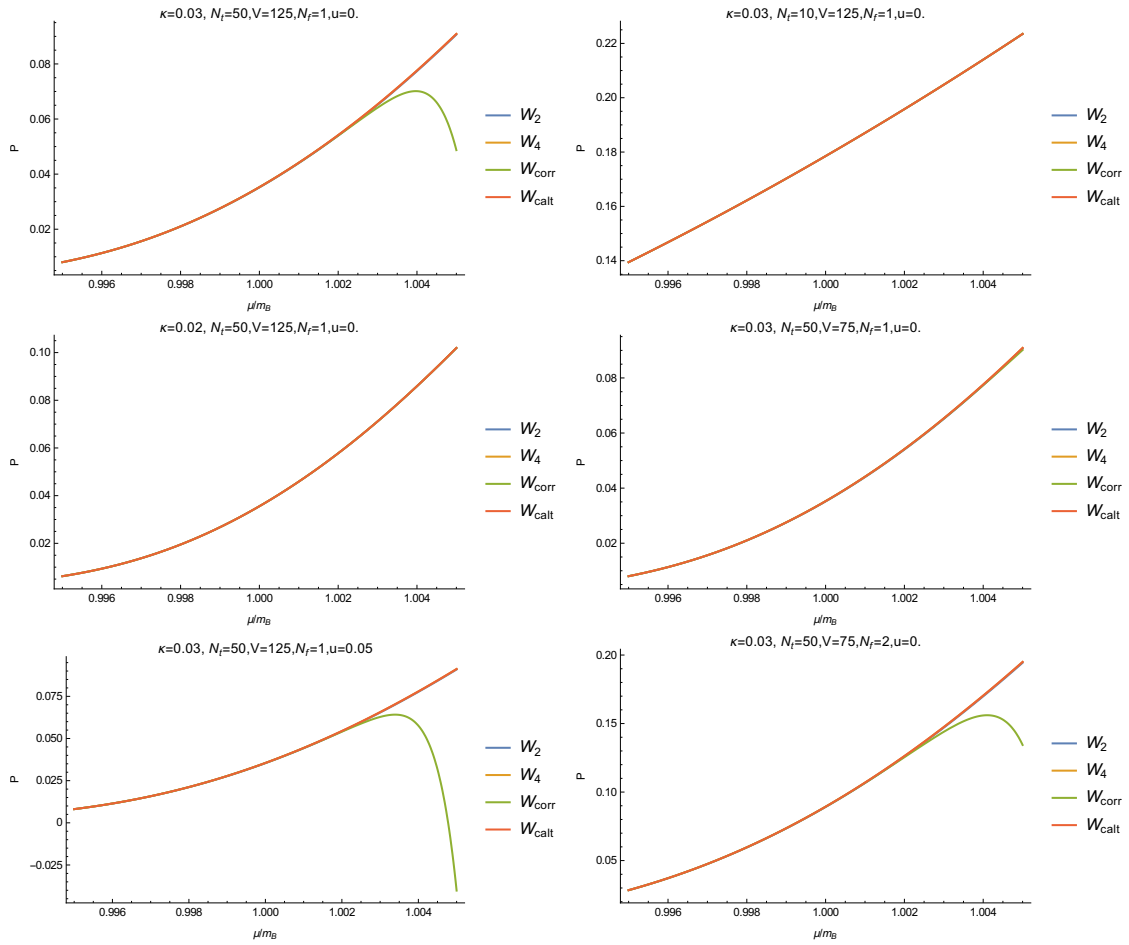


Figure 3.2: The pressure for $N_f = 1$ at different values of κ , N_τ , V and u and at $N_f = 2$

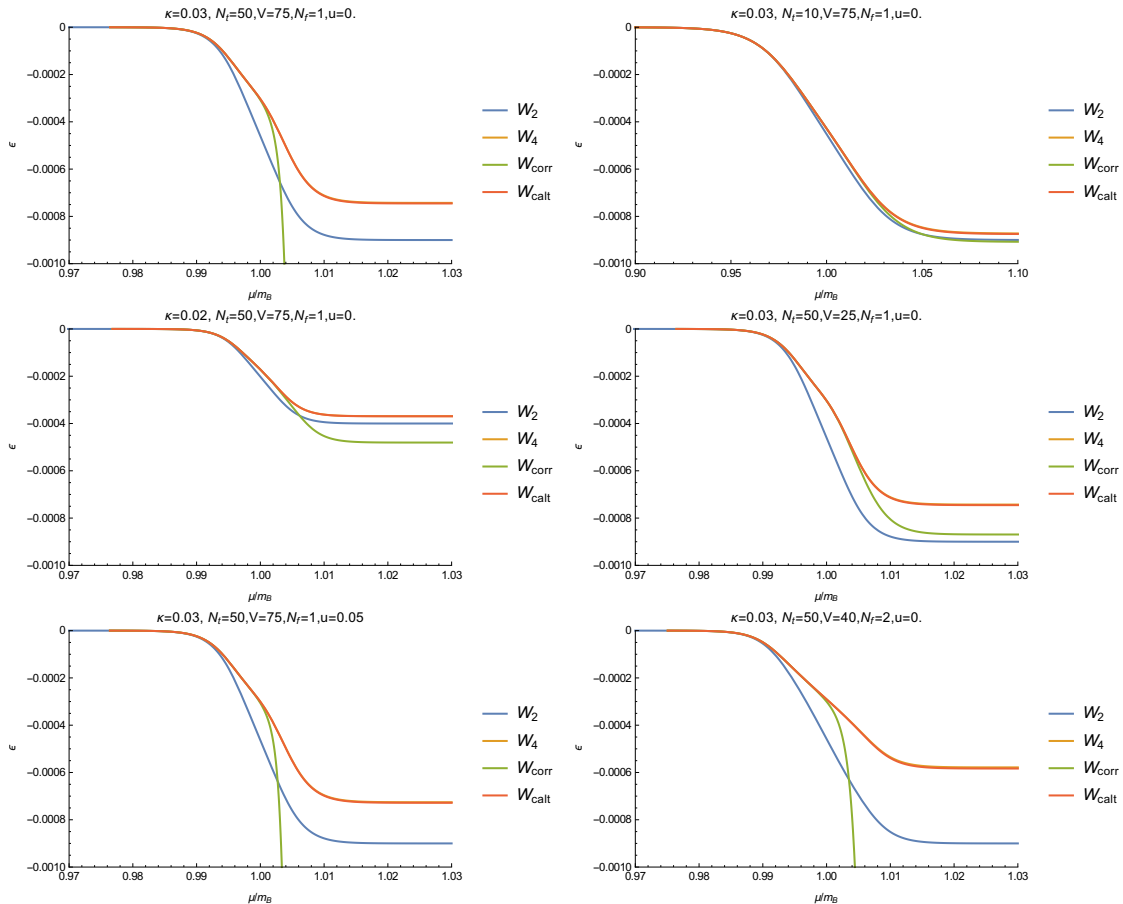


Figure 3.3: The binding energy for $N_f = 1$ at different values of κ , N_τ , V and u and at $N_f = 2$.

of the binding energy, so that the other graphs would not be distinguishable when scaling the plot according to it.

Figure 3.4 shows the baryon number density at varying u . For the first correction term, mainly the depth of the dip changes, it gets bigger for higher u . The second correction term changes less with u . The transition moves further to the left for higher u and at very high u its shift to the left as well as the shape indicate that the expansion breaks down.

In figure 3.5, we see two different plots. In the left plot, the correction terms themselves are plotted for two different values of N_τ . We can see that the contribution of the first correction term is much bigger as the contribution of the second correction term. Also, they grow with increasing N_τ , which is a behaviour we don't want because those terms should be neglected when going to the high- N_τ -limit.

In the right, we see all the terms of subleading order of N_τ at different values of N_τ . Here, the terms get again bigger with increasing N_τ .

Luckily, the contribution of all those terms is quite small compared to the overall contribution. But as the error of the high- N_τ -limit increases when going to bigger κ , which is necessary to reach the continuum limit [7], [5], it is of great use to have an estimate of the influence of these terms.

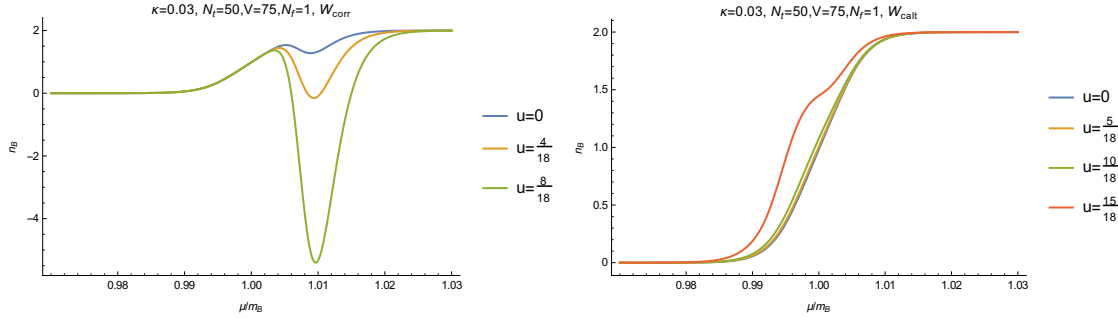


Figure 3.4: The first and second correction term at $\kappa = 0.03$ and $N_\tau = 50$ at different values of u

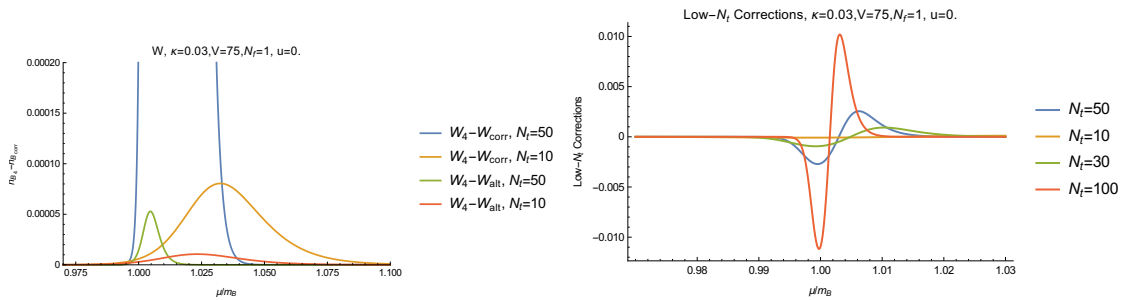


Figure 3.5: The correction terms for $N_f = 1$ at different N_τ . In the left we see the correction terms and in the right we see the Low- N_τ -corrections.

In figure 3.6, we see six of these curves. We have the first correction term and the second correction term at an error of 20% and 10%, as well as $N_f = 1$ and $N_f = 2$. We chose the first value of N_τ in a way that convergence is given. The shape of the curve correlates with our expectations, and only the first correction term looks different. As the calculations get really expensive for $N_f = 2$, we had to choose quite big steps for κ and what we see here is the first value of κ we were looking at. Therefore, the parameters we can choose are very restricted, so it might not be advisable anyway to use the first correction at $N_f = 2$. At lower N_τ we can choose κ bigger as at higher N_τ .

Looking at all the results, we can observe that the first correction term behaves in a more problematic way than the second correction term. As we can see in figure 3.5, those differences only start at $\mu \simeq 1$ where we have to be careful anyway, because the baryon number density gets more and more influenced by lattice artefacts and h_1 reaches $h_1 = 1$ which leads to problems with our expansions. Also, the second correction term is calculated in a simpler way, so it might be preferable to use it instead of the first correction term, but this definitely needs to be checked at higher orders of κ .

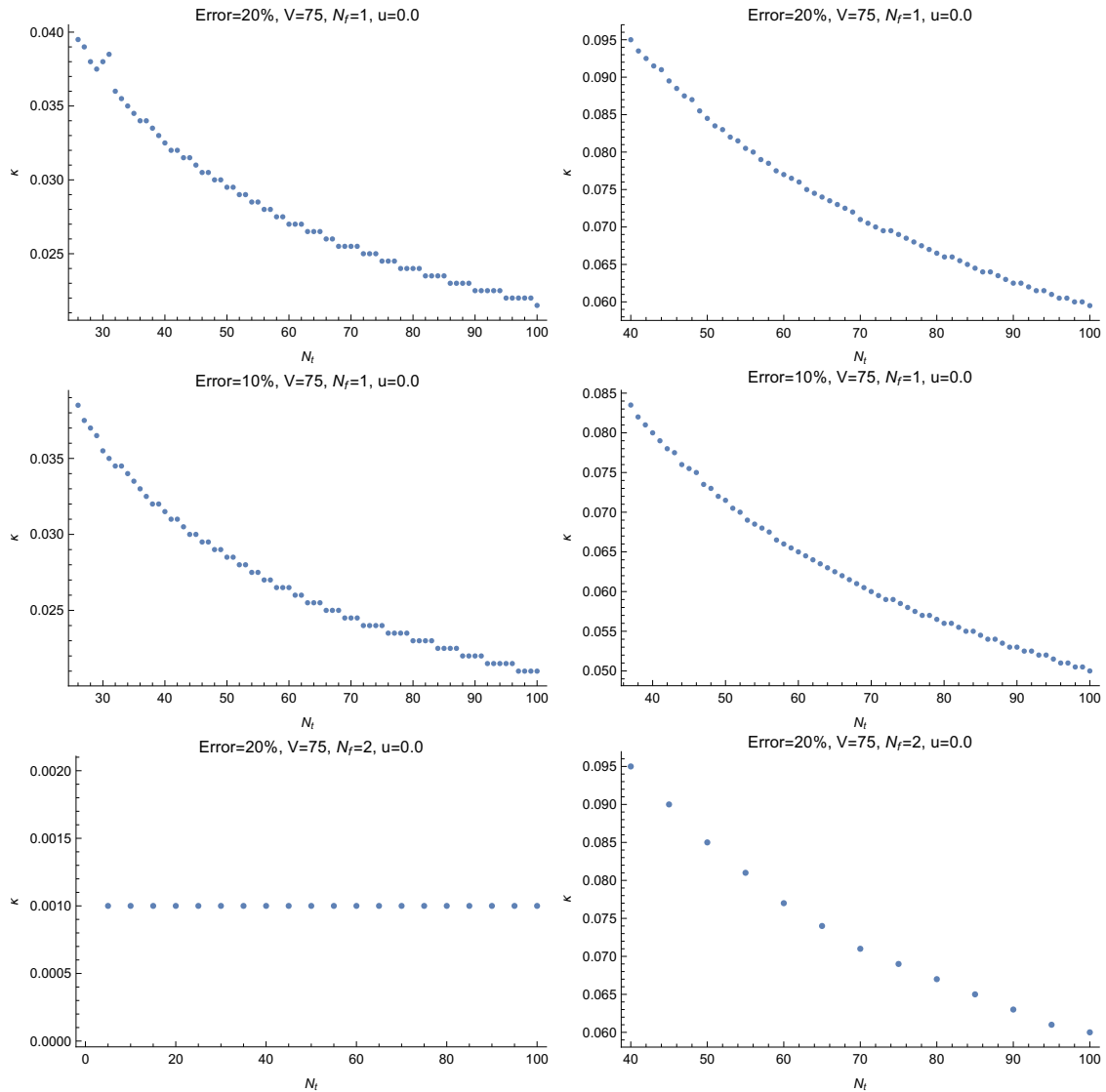


Figure 3.6: κ as a function of N_τ shown at $V = 75$. The left contribution is the error for the low- N_τ -corrections with the first correction term in relation to the high- N_τ baryon number density, the right contribution for the second correction term. From top to bottom, we have for $N_f = 1$ an error of 20%, an error of 10%, and for $N_f = 2$ an error of 20%.

Chapter 4

Conclusion and Outlook

In this thesis, we derived the effective theory of lattice QCD in 1+1 dimensions and treated it analytically with the linked cluster expansion. While doing this, we had to take care of a newly arising correction term, as we did not neglect the terms of subleading order in N_τ , as it was done in previous three dimensional calculations. Furthermore, we investigated the behaviour of this correction term. We used two different methods to calculate the correction term and compared them to each other.

This led to the finding that the contribution of these terms increases with increasing N_τ . This behaviour is not desirable, as we leave out those terms when going to the high- N_τ -limit. Therefore, we gave an estimate of the contribution of these terms depending on κ and N_τ , so that it is possible to choose these parameters in a way that the high- N_τ -limit does not break down.

This gets important when thinking about the continuum limit, as we need to change κ and N_τ , our error increases when we go to smaller lattice spacings. As our calculation took place in 1+1 dimensions, we could not test this hypothesis because we could not obtain the continuum limit, since the established methods are designed for 3+1 dimensional calculations. Therefore, it would be of great interest to repeat the calculations of the subleading order terms in 3+1 dimensions in order to take a look at the continuum limit.

Appendix A

Additional Calculations

In this appendix, we will derive the colour determinant from chapter 2.2.1 in more detail, as it was done in [7], and furthermore calculate the generating functional for the $W_{n_1 m_1 n_2 m_2}$ terms as in [5]. Also, we will give a short introduction to the integration over Polyakov loops [7] and in the methods of moments and cumulants [20], [21]. Lastly, we will show the calculations of the gauge corrections and the masses.

A.1 Static determinant

In order to calculate the quark determinant, we need to prove equation 2.2.12. This equation can be expressed as:

$$\det[\mathbb{1} + h_1 W] \quad (\text{A.1.1})$$

with $W \in \text{SU}(N)$.

We rewrite the determinant with the trace log identity and expand the arising logarithm:

$$\det(\mathbb{1} + h_1 W) = \sum_{n=0}^N \sum_{\{k_i\}_n} \prod_{l=1}^N \frac{(-1)^{(l+1)k_l}}{l^{k_l} k_l!} h_1^{l k_l} \text{tr}(W^l)^{k_l}. \quad (\text{A.1.2})$$

with N the degree of $\text{SU}(N)$. The indices $\{k_i\}_n$ are bound by the two equations:

$$\sum_{i=1}^N k_i = n, \quad \text{and} \quad \sum_{i=1}^N i k_i \leq N. \quad (\text{A.1.3})$$

We will use the Cayley-Hamilton equation

$$A^n + c_{n-1} A^{n-1} + \dots + c_1 A + (-1)^n \det(A) I_n = 0, \quad (\text{A.1.4})$$

here depicted for $\text{SU}(N)$.

The determinant corresponds to the coefficient c_0 . Also, the coefficients are given in terms of complete exponential Bell polynomials which can be rewritten in terms of traces of powers of A .

For $\text{SU}(3)$, the Cayley-Hamilton equation, expressed in terms of powers of traces, reads

$$\det(A) = \frac{1}{6} \left((\text{tr } A)^3 - 3 \text{tr}(A^2) (\text{tr } A) + 2 \text{tr}(A^3) \right). \quad (\text{A.1.5})$$

This fixes the highest power term of the logarithm because of the fact that $\det(W) = 1$.

Therefore, we can rewrite the determinant as:

$$\det(\mathbb{1} + h_1 W) = 1 + h_1^3 + h_1 \operatorname{tr}(W) + \frac{1}{2} h_1^2 \left(\operatorname{tr}(W)^2 - \operatorname{tr}(W^2) \right). \quad (\text{A.1.6})$$

We make use of the relation $\operatorname{tr}(W^2) = \operatorname{tr}(W)^2 - 2 \operatorname{tr}(W^\dagger)$ to reach the final result:

$$\det(\mathbb{1} + h_1 W) = 1 + h_1 \operatorname{tr} W + h_1^2 \operatorname{tr} W^\dagger + h_1^3. \quad (\text{A.1.7})$$

A.2 Generating Function for W_{nm} Terms

To solve the integrals in 3.2.2, we have to rewrite the $W_{n_1 m_1 n_2 m_2}$ -terms

$$W_{n_1 m_1 n_2 m_2} = \operatorname{tr} \left(\frac{(h_1 W_{\vec{x}})^{m_1}}{(\mathbb{1} + h_1 W_{\vec{x}})^{n_1}} \frac{(\bar{h}_1 W_{\vec{x}}^\dagger)^{m_2}}{(\mathbb{1} + \bar{h}_1 W_{\vec{x}}^\dagger)^{n_2}} \right) \quad (\text{A.2.1})$$

into Polyakov loops, as it is not possible to integrate directly over the fraction and the trace.

We will make use of a generating function that gives, depending on our evaluation process, the usual formulation or the expression in terms of Polyakov loops. We need three different generating functions, depending on the form of $W_{n_1 m_1 n_2 m_2}$.

The first one, for the terms of the form W_{nm00} , stems from [5]:

$$G(\alpha, \beta) = \log \det[\alpha + \beta h_1 W]. \quad (\text{A.2.2})$$

The one for the quite similar term W_{00nm} looks like:

$$G(\alpha, \beta) = \log \det[\alpha + \beta \bar{h}_1 W^\dagger] \quad (\text{A.2.3})$$

The last case is specifically constructed for W_{1010} :

$$G(\alpha, \beta) = \frac{1}{2(1 - h_1 \bar{h}_1)} \left(\log \left(\det \left((\alpha + \beta h_1 W)(\alpha + \beta \bar{h}_1 W^\dagger) \right) \right) - \log \left(\det \left((\beta + \alpha h_1 W)(\beta + \alpha \bar{h}_1 W^\dagger) \right) \right) \right). \quad (\text{A.2.4})$$

For W_{1111} , we can use the same generating function but multiplied by $-h_1 \bar{h}_1$.

Then, we receive all terms by taking derivatives with respect to α and β and setting $\alpha = \beta = 1$ afterwards:

$$W_{nmnm} = \frac{(-1)^{n-1}}{(n-1)!} \frac{\partial^{n-m}}{\partial \alpha^{n-m}} \frac{\partial^m}{\partial \beta^m} G(\alpha, \beta) \Big|_{\alpha=\beta=1}. \quad (\text{A.2.5})$$

When setting $n_1 = n_2$ and $m_1 = m_2$, we can also use this formula for the last case A.2.4.

It is possible to check if the generating function returns the right $W_{n_1 m_1 n_2 m_2}$ term by using Jacobi's formula when calculating the derivative

$$\frac{d}{dt} \log \det A(t) = \text{tr} \left(A(t)^{-1} \frac{d}{dt} A(t) \right). \quad (\text{A.2.6})$$

In order to obtain the expressions in terms of Polyakov loops, we need to express the generating function in terms of Polyakov loops first. For this task, we can use the method from appendix A.1, which also works for the more complicated generating function A.2.4. For example, the first generating function takes the form

$$G(\alpha, \beta) = \log[\alpha^3 + \alpha^2 \beta h_1 L + \alpha \beta^2 h_1^2 L^\dagger + \beta^3 h_1^3]. \quad (\text{A.2.7})$$

When we take the derivative now, we receive the expression for $W_{n_1 m_1 n_2 m_2}$ in terms of Polyakov loops, which finally enables us to perform the integration.

A.3 Integration over Polyakov Loops

At first, we have to change the measure of our integration from temporal links to Polyakov loops. This process leads to a Jacobian in the form of an effective potential

$$\int [dW] = \int [dL] e^V. \quad (\text{A.3.1})$$

This potential is equivalent to the SU(3) Haar measure, calculated in [7]

$$V = \frac{1}{2} \log(27 - 18|L|^2 + 8\text{Re}(L^3) - |L|^4) \quad (\text{A.3.2})$$

We can parametrise the Polyakov loops in terms of two angles, which brings them into a diagonal form [22]:

$$L(\theta, \phi) = e^{i\theta} + e^{i\phi} + e^{-i(\theta+\phi)}, \quad \theta, \phi \in [-\pi, \pi). \quad (\text{A.3.3})$$

We can rewrite the measure as

$$\int [dW] = \int [dL] e^V = \int [d\theta][d\phi] e^{2V}. \quad (\text{A.3.4})$$

This introduces another Jacobian identical to the previous one A.3.2.

Now, we can easily solve the integrals, as they reduce to integrals over exponential functions.

A.4 Moments and Cumulants

The method of moments and cumulants is an important part of the linked cluster expansion [7] and is also used in other fields [20], [21].

The moment is a collection of symmetric functions that assigns a number $\langle \alpha, \dots, \beta \rangle$ to each combination (α, \dots, β) , with $\langle \phi \rangle = 0$ for the empty combination. The moment product

$$\langle \rangle_1 \otimes \langle \rangle_2 = \langle \rangle_3 \quad (\text{A.4.1})$$

is defined by a sum over all partitions P_2 of (α, \dots, β) in two sets

$$\langle \alpha, \dots, \beta \rangle_3 = \sum_{P_2} \langle \alpha, \dots, \delta \rangle \langle \gamma, \dots, \epsilon \rangle_2. \quad (\text{A.4.2})$$

One example for a set made out of three entries is:

$$\begin{aligned} \langle \alpha, \beta, \gamma \rangle_3 &= \langle \alpha \rangle_1 \langle \beta, \gamma \rangle_2 + \langle \beta \rangle_1 \langle \alpha, \gamma \rangle_2 + \langle \gamma \rangle_1 \langle \alpha, \beta \rangle_2 \\ &\quad + \langle \alpha, \beta \rangle_1 \langle \gamma \rangle_2 + \langle \beta, \gamma \rangle_1 \langle \alpha \rangle_2 + \langle \alpha, \gamma \rangle_1 \langle \beta \rangle_2, \end{aligned} \quad (\text{A.4.3})$$

$$\langle \alpha, \alpha, \alpha \rangle = 3 \langle \alpha \rangle \langle \alpha, \alpha \rangle_2 + 3 \langle \alpha, \alpha \rangle_1 \langle \alpha \rangle_2. \quad (\text{A.4.4})$$

We define the cumulant making use of the exponential of the moment

$$\exp_{\otimes} [] = 1 + \sum_{n=1}^{\infty} \frac{1}{n!} []^{\otimes n} \equiv 1 + \langle \rangle. \quad (\text{A.4.5})$$

This makes it possible to define the moments and cumulants in terms of each other:

$$\langle \alpha_1, \dots, \alpha_n \rangle = \sum_{k=1}^n \sum_{P_k} [\alpha_1, \dots, \alpha_m]_1 \dots [\alpha_i, \dots, \alpha_j]_k \quad (\text{A.4.6})$$

$$[\alpha_1, \dots, \alpha_n] = \sum_{k=1}^n (-1)^{k-1} (k-1)! \sum_{P_k} \langle \alpha_1, \dots, \alpha_m \rangle_1 \dots \langle \alpha_i, \dots, \alpha_j \rangle_k \quad (\text{A.4.7})$$

Here, we can see some examples of these relations:

$$\begin{aligned} \langle \alpha \rangle &= [\alpha], \\ \langle \alpha, \beta \rangle &= [\alpha, \beta] + [\alpha][\beta], \\ \langle \alpha, \beta, \gamma \rangle &= [\alpha, \beta, \gamma] + [\alpha, \beta][\gamma] + [\beta, \gamma][\alpha] + [\alpha, \gamma][\beta] + [\alpha][\beta][\gamma], \end{aligned} \quad (\text{A.4.8})$$

$$\begin{aligned} [\alpha] &= \langle \alpha \rangle, \\ [\alpha, \beta] &= \langle \alpha, \beta \rangle - \langle \alpha \rangle \langle \beta \rangle, \\ [\alpha, \beta, \gamma] &= \langle \alpha, \beta, \gamma \rangle - \langle \alpha, \beta \rangle \langle \gamma \rangle - \langle \alpha, \gamma \rangle \langle \beta \rangle - \langle \beta, \gamma \rangle \langle \alpha \rangle + 2 \langle \alpha \rangle \langle \beta \rangle \langle \gamma \rangle. \end{aligned} \quad (\text{A.4.9})$$

We define the generating functional of the moments as:

$$f_{\langle \rangle}(\{x_{\alpha}\}) = \sum_{n=1}^{\infty} \sum_{\alpha_1, \dots, \alpha_n} \frac{1}{n!} \langle \alpha_1, \dots, \alpha_n \rangle x_{\alpha_1} \dots x_{\alpha_n}. \quad (\text{A.4.10})$$

The generating functional of the cumulants is defined in a similar way.

The main theorem of the methods of moments and cumulants states that

$$\exp f_{\langle \rangle}(\{x_{\alpha}\}) = 1 + f_{\langle \rangle}(\{x_{\alpha}\}). \quad (\text{A.4.11})$$

This can be proved by induction.

Furthermore, we can apply the formalism to a general polymer system. The function $I(X_i)$ describes the value we are left with after the integration over the polymer X_i . We define a cluster moment

$$\langle X_1, \dots, X_n \rangle = \begin{cases} 1, & \text{if every pair } X_i, X_j \text{ is disconnected} \\ 0, & \text{otherwise} \end{cases} \quad (\text{A.4.12})$$

so that the generating functional of the moment is the same as the partition function of the polymer system

$$\mathcal{Z}(\{I(X)\}) = 1 + \sum_{n=1}^{\infty} \sum_{X_1, \dots, X_n} \frac{1}{n!} \langle X_1, \dots, X_n \rangle I(X_1) \dots I(X_n). \quad (\text{A.4.13})$$

Using the main theorem, we obtain the logarithm of the partition function:

$$\log \mathcal{Z}(\{I(X)\}) = \sum_{n=1}^{\infty} \sum_{X_1, \dots, X_n} \frac{1}{n!} [X_1, \dots, X_n] I(X_1) \dots I(X_n). \quad (\text{A.4.14})$$

It can be proved that the cumulants possess the opposite property of the moments:

$$[X_1, \dots, X_n] = 0 \Leftrightarrow X_1 \cup \dots \cup X_n \text{ is connected.} \quad (\text{A.4.15})$$

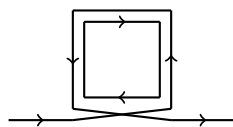
If we define the general polymer system as the effective action

$$e^{-S_{eff}} = \int [dU_1] \exp \left(- \sum_{n=1}^{\infty} \frac{1}{n} \text{tr}(P + M)^n \right) \quad (\text{A.4.16})$$

and choose the variables X_i to represent a combination of $\text{tr}(P + M)^n$ factors, this leads to the conclusion that the effective action can be exponentiated when only connected polymers are considered. This only holds in the infinite volume limit, but corrections could be calculated.

A.5 Calculation of Spatial Detours

This chapter contains a detailed calculation of the corrections to the coupling h_1 , which was discussed in 2.4.1.

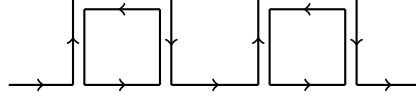


This detour adds 4 links and 1 plaquette, which gives a factor of $\kappa^4 u$. It can be attached in N_τ locations and can point in 2 directions, which means upwards or downwards in the one dimensional case. The trace gets adjusted to

$$\text{tr} [(\mathbb{1} - \gamma_0)^{N_\tau} (\mathbb{1} - \gamma_1) (\mathbb{1} + \gamma_0) (\mathbb{1} + \gamma_1) (\mathbb{1} - \gamma_0)] = -4 \text{tr} [(\mathbb{1} - \gamma_0)^{N_\tau}] \quad (\text{A.5.1})$$

which leads to the overall contribution

$$c_a = -8\kappa^4 u N_\tau. \quad (\text{A.5.2})$$

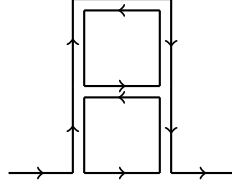


The first of these detours can be placed at N_τ locations in 2 directions, the second detour can be placed in 2 directions as well but only at $N_\tau - 3$ locations. Each detour gives a factor of $\kappa^2 u$, and we have to include a combinatorial factor of $\frac{1}{2!}$ to take care of the double counting. The trace

$$\begin{aligned} & \text{tr} [(\mathbb{1} - \gamma_0)^{N_\tau - 3} (\mathbb{1} - \gamma_1) (\mathbb{1} - \gamma_0) (\mathbb{1} + \gamma_1) (\mathbb{1} - \gamma_0) (\mathbb{1} - \gamma_1) (\mathbb{1} - \gamma_0) (\mathbb{1} + \gamma_1)] \\ &= \text{tr} [(\mathbb{1} - \gamma_0)^{N_\tau}] \end{aligned} \quad (\text{A.5.3})$$

gives no additional factor, so the full contribution is

$$c_b = 2\kappa^4 u^2 N_\tau (N_\tau - 3). \quad (\text{A.5.4})$$

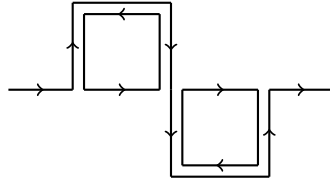


Again, we can place this detour at N_τ locations. The lower part can be placed in 2 directions, and the upper part has to point in the same direction as the lower part. The trace

$$\text{tr} [(\mathbb{1} - \gamma_0)^{N_\tau - 1} (\mathbb{1} - \gamma_1) (\mathbb{1} - \gamma_1) (\mathbb{1} - \gamma_0) (\mathbb{1} + \gamma_1) (\mathbb{1} + \gamma_1)] = 4 \text{tr} [(\mathbb{1} - \gamma_0)^{N_\tau}] \quad (\text{A.5.5})$$

gives a factor of 4, leading to the contribution

$$c_c = 8\kappa^4 u^2 N_\tau. \quad (\text{A.5.6})$$

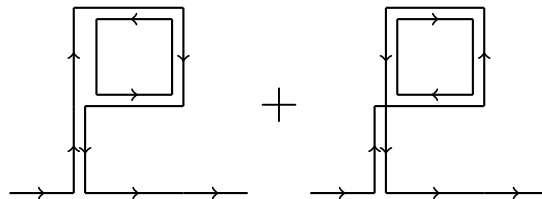


There are N_τ locations to place the detour, 2 directions for the first detour and 1 for the first detour. The trace gives

$$\begin{aligned} & \text{tr} [(\mathbb{1} - \gamma_0)^{N_\tau - 2} (\mathbb{1} - \gamma_1) (\mathbb{1} - \gamma_0) (\mathbb{1} + \gamma_1) (\mathbb{1} + \gamma_1) (\mathbb{1} - \gamma_0) (\mathbb{1} - \gamma_1)] \\ &= 2 \text{tr} [(\mathbb{1} - \gamma_0)^{N_\tau}] \end{aligned} \quad (\text{A.5.7})$$

This leads to the contribution

$$c_d = 4\kappa^4 u^2 N_\tau. \quad (\text{A.5.8})$$



Both detours come with a factor of N_τ for their location, a factor of 2 for the direction and an additional factor of 2 because they can also point to the left. But, the trace for both diagrams cancels, since the trace for the first diagram gives

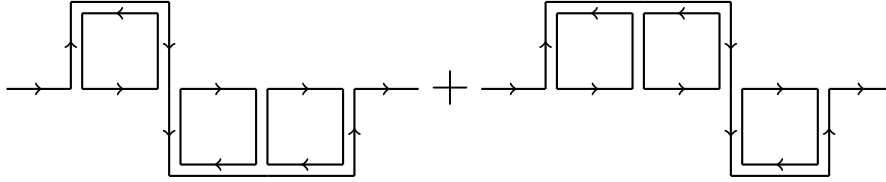
$$\text{tr} [(\mathbb{1} - \gamma_0)^{N_\tau} (\mathbb{1} - \gamma_1) (\mathbb{1} - \gamma_1) (\mathbb{1} - \gamma_0) (\mathbb{1} + \gamma_1) (\mathbb{1} + \gamma_0) (\mathbb{1} + \gamma_1)] = 8 \text{tr} [(\mathbb{1} - \gamma_0)^{N_\tau}] \quad (\text{A.5.9})$$

and the trace for the second diagram gives

$$\begin{aligned} & \text{tr} [(\mathbb{1} - \gamma_0)^{N_\tau} (\mathbb{1} - \gamma_1) (\mathbb{1} - \gamma_0) (\mathbb{1} - \gamma_1) (\mathbb{1} + \gamma_0) (\mathbb{1} + \gamma_1) (\mathbb{1} + \gamma_1)] \\ &= -8 \text{tr} [(\mathbb{1} - \gamma_0)^{N_\tau}]. \end{aligned} \quad (\text{A.5.10})$$

Therefore, we get

$$c_e = 0. \quad (\text{A.5.11})$$



The detours in both diagrams can be placed at N_τ different locations, and they can point in 2 directions. The trace for the first diagram has the value

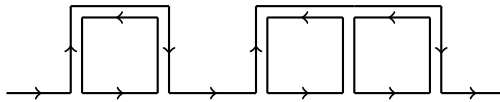
$$\begin{aligned} & \text{tr} [(\mathbb{1} - \gamma_0)^{N_\tau-3} (\mathbb{1} - \gamma_1) (\mathbb{1} - \gamma_0) (\mathbb{1} + \gamma_1) (\mathbb{1} + \gamma_1) (\mathbb{1} - \gamma_0) (\mathbb{1} - \gamma_0) (\mathbb{1} + \gamma_1)] \\ &= 2 \text{tr} [(\mathbb{1} - \gamma_0)^{N_\tau}] \end{aligned} \quad (\text{A.5.12})$$

For the second diagram, the trace gives the same result:

$$\begin{aligned} & \text{tr} [(\mathbb{1} - \gamma_0)^{N_\tau-3} (\mathbb{1} - \gamma_1) (\mathbb{1} - \gamma_0) (\mathbb{1} - \gamma_0) (\mathbb{1} + \gamma_1) (\mathbb{1} + \gamma_1) (\mathbb{1} - \gamma_0) (\mathbb{1} + \gamma_1)] \\ &= 2 \text{tr} [(\mathbb{1} - \gamma_0)^{N_\tau}] \end{aligned} \quad (\text{A.5.13})$$

Adding up both diagrams results in the contribution

$$c_f = 8\kappa^4 u^3 N_\tau. \quad (\text{A.5.14})$$

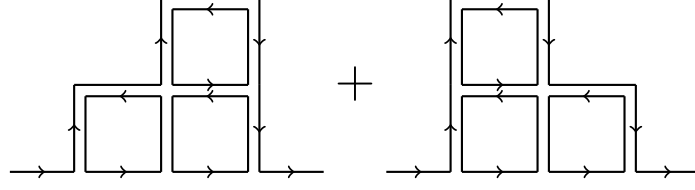


The first detour can be placed at N_τ locations, the second detour at $N_\tau - 4$ locations. Also, both detours can be placed in 2 directions. The trace gives no additional factor:

$$\begin{aligned} & \text{tr} [(\mathbb{1} - \gamma_0)^{N_\tau-4} (\mathbb{1} - \gamma_1) (\mathbb{1} - \gamma_0) (\mathbb{1} + \gamma_1) (\mathbb{1} - \gamma_0) (\mathbb{1} - \gamma_1) (\mathbb{1} - \gamma_0) (\mathbb{1} - \gamma_0) (\mathbb{1} + \gamma_1)] \\ &= \text{tr} [(\mathbb{1} - \gamma_0)^{N_\tau}]. \end{aligned} \quad (\text{A.5.15})$$

This leads to the contribution

$$c_g = 4\kappa^4 u^3 N_\tau (N_\tau - 4). \quad (\text{A.5.16})$$



Again, we have two diagrams that give the same contribution. The detours can be placed at N_τ locations and can point in 2 directions. The trace for the first diagram gives

$$\begin{aligned} & \text{tr} [(\mathbb{1} - \gamma_0)^{N_\tau} (\mathbb{1} - \gamma_1) (\mathbb{1} - \gamma_0) (\mathbb{1} - \gamma_1) (\mathbb{1} - \gamma_0) (\mathbb{1} + \gamma_1) (\mathbb{1} + \gamma_1)] \\ &= 2 \text{tr} [(\mathbb{1} - \gamma_0)^{N_\tau}] \end{aligned} \quad (\text{A.5.17})$$

and the trace for the second diagram gives the same contribution:

$$\begin{aligned} & \text{tr} [(\mathbb{1} - \gamma_0)^{N_\tau} (\mathbb{1} - \gamma_1) (\mathbb{1} - \gamma_1) (\mathbb{1} - \gamma_0) (\mathbb{1} + \gamma_1) (\mathbb{1} - \gamma_0) (\mathbb{1} + \gamma_1)] \\ &= 2 \text{tr} [(\mathbb{1} - \gamma_0)^{N_\tau}]. \end{aligned} \quad (\text{A.5.18})$$

Both diagrams together lead to the contribution

$$c_h = 8\kappa^4 u^3 N_\tau. \quad (\text{A.5.19})$$

A.6 Calculation of Hadron masses

In this section, we will go over the calculation of the Hadron masses, following [19], and their corrections up to $\mathcal{O}(\kappa^n u^m)$ with $n + m \leq 7$.

For the calculation of the mass, it is necessary to specify an operator. The operator for the pions look like:

$$\begin{aligned} \pi_+(x) &\equiv \bar{d}_{ac}(x) (\gamma_5)_{a\beta} u_{\beta c}(x) \\ \pi_-(x) &\equiv \bar{u}_{ac}(x) (\gamma_5)_{a\beta} d_{\beta c}(x). \end{aligned} \quad (\text{A.6.1})$$

For the proton and antiproton, we have the operators

$$\begin{aligned} p_\alpha^+(x) &\equiv \varepsilon_{cde} (C \gamma_5)_{\beta\gamma} u_{ac}(x) [u_{\beta d}(x) d_{\gamma e}(x) - d_{\beta d}(x) u_{\gamma e}(x)] \\ p_\delta^-(y) &\equiv \varepsilon_{fgh} (C \gamma_5)_{\epsilon\varphi} \bar{u}_{\delta f}(y) [\bar{d}_{eg}(y) \bar{u}_{\varphi h}(y) - \bar{u}_{eg}(y) \bar{d}_{\varphi h}(y)] \end{aligned} \quad (\text{A.6.2})$$

with

$$\begin{aligned} C \gamma_\mu C^{-1} &= -\gamma_\mu^T \\ -C &= C^T = C^{-1} = C^\dagger. \end{aligned} \quad (\text{A.6.3})$$

We want to calculate the pion propagator

$$C(t) \equiv \left\langle \pi_+(0, 0) [\pi_+(0, t)]^\dagger \right\rangle_S = \left\langle \text{tr} [\gamma_5 P_d(0, t) \gamma_5 P_u(t, 0)] \right\rangle_{S_{eff}}, \quad (\text{A.6.4})$$

with the quark propagator

$$P_f[U]_{yx} = (1 - \kappa_f M[U])_{yx}^{-1} = \sum_{l=0} \kappa_f^l M[U]_{yx}^-. \quad (\text{A.6.5})$$

Using

$$P_f(y, x) = \gamma_5 P_f^\dagger(x, y) \gamma_5, \quad (\text{A.6.6})$$

we can rewrite the pion correlator to

$$C(t) = \left\langle \text{tr}[P_d^\dagger(t, 0)P_u(t, 0)] \right\rangle_{S_{eff}}. \quad (\text{A.6.7})$$

In general, the computation of such expectation values looks like

$$\langle \mathcal{O} \rangle = \frac{1}{Z} \int [dU d\bar{\psi} d\psi] e^{-S[U, \bar{\psi}, \psi]} \mathcal{O}[U, \bar{\psi}, \psi]. \quad (\text{A.6.8})$$

With the hopping parameter expansion, we have to compute

$$C(t) = \frac{1}{Z} \int [dU] \exp \left[\sum_f \sum_{l=1}^{\infty} \frac{\kappa_f^l}{l} \text{tr} M[U]^l \right] \text{tr} [P_d^\dagger(t, 0)P_u(t, 0)]. \quad (\text{A.6.9})$$

As we are calculating the leading order, we can set Z and the effective action to 1, which leads us to

$$C(t) = \kappa_u^t \kappa_d^t \int [dU] \text{tr} \left[(1 + \gamma_0)^{2t} U_0(t \rightarrow 0) U_0^\dagger(t \rightarrow 0) \right]. \quad (\text{A.6.10})$$

Using the relations

$$\begin{aligned} \gamma_5(1 - \gamma_\mu)\gamma_5 &= (1 + \gamma_\mu) \\ \text{tr}[(1 + \gamma_\mu)^N] &= \text{tr}[2^{N-1}(1 + \gamma_\mu)] = 2^N \end{aligned} \quad (\text{A.6.11})$$

we get the result

$$C(t) = \frac{1}{N_c} (2\kappa_u)^t (2\kappa_d)^t. \quad (\text{A.6.12})$$

We plug this into the following correlation function

$$\begin{aligned} m(A) &= -\lim_{t \rightarrow \infty} \frac{1}{t} \log \langle A(0)A^\dagger(t) \rangle \quad \text{for mesons,} \\ m(B) &= -\lim_{t \rightarrow \infty} \frac{1}{t} \log \langle B(0)\bar{B}(t) \rangle \quad \text{for baryons,} \end{aligned} \quad (\text{A.6.13})$$

which leads to a meson mass of

$$m_M = -\log(2\kappa_u) - \log(2\kappa_d) \quad (\text{A.6.14})$$

or, in our case of degenerated flavours

$$m_M = -2 \log(2\kappa). \quad (\text{A.6.15})$$

When we perform this calculation for baryons, we receive the degenerate baryon mass

$$m_B = -3 \log(2\kappa). \quad (\text{A.6.16})$$

We calculate the gauge corrections of the masses at $N_\tau \rightarrow \infty$. This calculation is along the lines of the calculation of the h_1 corrections, but with an additional factor taking care of the additional quark lines.

Again, we calculate the corrections up to $\mathcal{O}(\kappa^n u^m)$ with $n + m \leq 7$ and we receive graphs similar to the ones in appendix A.5. The only difference is that the plaquettes sit on different quark lines. This leads to the contributions

$$\begin{aligned} c_M &= -8\kappa^2 \frac{u}{1-u} + 32\kappa^4 u - 64\kappa^4 u^2 - 80\kappa^4 u^3 \\ c_B &= -6\kappa^2 \frac{u}{1-u} + 24\kappa^4 u - 54\kappa^4 u^2 - 60\kappa^4 u^3. \end{aligned} \tag{A.6.17}$$

Appendix B

Analytic Results

This appendix collects all expressions too lengthy for the main text.

B.1 Effective Action to Order κ^4

This chapter contains the terms of the kinetic quark determinant to order κ^4 in the $W_{n_1 m_1 n_2 m_2}$ -notation. All sums are already evaluated. We set $k_1 = \frac{2[(2\kappa)^{2N_\tau} - (2\kappa)^2]}{((2\kappa)^2 - 1)(N_\tau - 1)}$, the couplings should be well known from chapter 2.2.3 and chapter 2.2.4. The sum over $i = \pm 1$ includes forward and backward hops, therefore, the prefactors had to be adjusted in regard to chapter 2.2.

$$\begin{aligned}
\mathcal{S}_{eff} = & - \sum_{\vec{x}} \log \det Q_{stat}(\vec{x}) + \sum_{\vec{x}} \sum_{i=\pm 1} \left(N_f \frac{h_2}{2} W_{1111}^-(\vec{x}) W_{1111}^-(\vec{x} + i) \right. \\
& + N_f \frac{h_{31}}{2} \left\{ W_{1111}^-(\vec{x} - i) \text{tr}(4) W_{1111}^-(\vec{x} + i) \right. \\
& \quad + W_{1111}^-(\vec{x} - i) W_{2222}^+(\vec{x}) W_{1111}^-(\vec{x} + i) \\
& \quad + 2 W_{1111}^-(\vec{x} - i) W_{1111}(\vec{x}) W_{1111}^-(\vec{x} + i) \\
& \quad \left. - 4 W_{1111}^-(\vec{x} - i) W_{1111}^+(\vec{x}) W_{1111}^-(\vec{x} + i) \right\} \\
& - N_f \frac{h_{32}}{2} \left\{ W_{1111}^-(\vec{x} - i) W_{2121}^+(\vec{x}) W_{1111}^-(\vec{x} + i) \right. \\
& \quad \left. - k_1 W_{1111}^-(\vec{x} - i) W_{1010}(\vec{x}) W_{1111}^-(\vec{x} + i) \right\} \\
& + N_f \frac{h_{31}}{4} \frac{N_c^2}{N_c^2 - 1} \left\{ \left(W_{2222}^+(\vec{x}) - 2 W_{1111}(\vec{x}) \right) [W_{1111}^-(\vec{x} + i)]^2 \right. \\
& \quad \left. + [W_{1111}^-(\vec{x})]^2 \left(W_{2222}^+(\vec{x} + i) - 2 W_{1111}(\vec{x} + i) \right) \right\} \\
& - N_f \frac{h_{31}}{4} \frac{N_c}{N_c^2 - 1} \left\{ [W_{1111}^-(\vec{x})]^2 [W_{1111}^-(\vec{x} + i)]^2 \right. \\
& \quad \left. + \left(W_{2222}^+(\vec{x}) - 2 W_{1111}(\vec{x}) \right) \left(W_{2222}^+(\vec{x} + i) - 2 W_{1111}(\vec{x} + i) \right) \right\} \\
& - N_f \frac{h_{32}}{4} \left\{ [W_{1111}^-(\vec{x})]^2 \left(W_{2121}^+(\vec{x} + i) + k_1 W_{1010}(\vec{x} + i) \right) \right.
\end{aligned}$$

$$\begin{aligned}
& \left(W_{2121}^+(\vec{x}) + k_1 W_{1010}(\vec{x}) \right) [W_{1111}^-(\vec{x} + i)]^2 \Big\} \\
& - N_f^2 \frac{h_{31}}{4} \frac{N_c^2}{N_c^2 - 1} \left\{ [W_{1111}^-(\vec{x})]^2 [W_{1111}^-(\vec{x} + i)]^2 \right. \\
& \quad \left. + \left(W_{2222}^+(\vec{x}) - 2W_{1111}(\vec{x}) \right) \left(W_{2222}^+(\vec{x} + i) - 2W_{1111}(\vec{x} + i) \right) \right\} \\
& + N_f^2 \frac{h_{31}}{4} \frac{N_c}{N_c^2 - 1} \left\{ \left(W_{2222}^+(\vec{x}) - 2W_{1111}(\vec{x}) \right) [W_{1111}^-(\vec{x} + i)]^2 \right. \\
& \quad \left. + [W_{1111}^-(\vec{x})]^2 \left(W_{2222}^+(\vec{x} + i) - 2W_{1111}(\vec{x} + i) \right) \right\} \\
& - N_f^2 \frac{h_{32}}{4} \left\{ W_{2121}^+(\vec{x}) W_{2121}^+(\vec{x} + i) \right. \\
& \quad + k_1 W_{2121}^+(\vec{x}) W_{1010}(\vec{x} + i) + k_1 W_{1010}(\vec{x}) W_{2121}^+(\vec{x} + i) \\
& \quad + 2 \left[(2\kappa)^{2N_\tau} + \frac{(2\kappa)^{4N_\tau} - (2\kappa)^4}{((2\kappa)^4 - 1)(N_\tau - 1)} \right] W_{1010}(\vec{x}) W_{1010}(\vec{x} + i) \\
& \quad \left. + [W_{1111}^-(\vec{x})]^2 [W_{1111}^-(\vec{x} + i)]^2 \right\} \\
& - \sum_{\vec{x} \neq \vec{y}} \sum_{i=\pm 1} N_f^2 \frac{h_2^2}{4} W_{1111}^-(\vec{x}) W_{1111}^-(\vec{x} + i) W_{1111}^-(\vec{y}) W_{1111}^-(\vec{y} + i) \tag{B.1.1}
\end{aligned}$$

B.2 Two- and Three-Point Interactions

This chapter contains the two- and three-point interactions from chapter 3.2.1.

$$\begin{aligned}
v_{ij}(\vec{x}, \vec{y}) = & \delta(\langle \vec{x}, \vec{y} \rangle) \left[- N_f h_2 \delta_{i1} \delta_{j1} \right. \\
& + N_f \frac{h_{31}}{2} \left(N_f \frac{N_c^2}{N_c^2 - 1} + \frac{N_c^2}{N_c^3 - N_c} \right) \delta_{i2} \delta_{j2} \\
& + N_f 2h_{31} \left(N_f \frac{N_c^2}{N_c^2 - 1} + \frac{N_c^2}{N_c^3 - N_c} \right) \delta_{i3} \delta_{j3} \\
& + N_f \frac{h_{31}}{2} \left(N_f \frac{N_c^2}{N_c^2 - 1} + \frac{N_c^2}{N_c^3 - N_c} \right) \delta_{i4} \delta_{j4} \\
& + N_f^2 \frac{h_{32}}{2} \delta_{i5} \delta_{j5} \\
& + N_f^2 h_{32} \left[(2\kappa)^{2N_\tau} + \frac{(2\kappa)^{4N_\tau} - (2\kappa)^4}{((2\kappa)^4 - 1)(N_\tau - 1)} \right] \delta_{i6} \delta_{j6} \\
& - N_f h_{31} \left(N_f \frac{N_c^2}{N_c^2 - 1} + \frac{N_c^2}{N_c^3 - N_c} \right) (\delta_{i2} \delta_{j3} + \delta_{i3} \delta_{j2}) \\
& - N_f \frac{h_{31}}{2} \left(\frac{N_c^2}{N_c^2 - 1} + N_f \frac{N_c^2}{N_c^3 - N_c} \right) (\delta_{i2} \delta_{j4} + \delta_{i4} \delta_{j2}) \\
& + N_f h_{31} \left(\frac{N_c^2}{N_c^2 - 1} + N_f \frac{N_c^2}{N_c^3 - N_c} \right) (\delta_{i3} \delta_{j4} + \delta_{i4} \delta_{j3}) \\
& \left. + N_f \frac{h_{32}}{2} (\delta_{i4} \delta_{j5} + \delta_{i5} \delta_{j4}) \right]
\end{aligned}$$

$$\begin{aligned}
& + N_f \frac{h_{32}}{2} k_1 (\delta_{i4} \delta_{j6} + \delta_{i6} \delta_{j4}) \\
& + N_f^2 \frac{h_{32}}{2} k_1 (\delta_{i5} \delta_{j6} + \delta_{i6} \delta_{j5}) \Big] \tag{B.2.1}
\end{aligned}$$

$$\begin{aligned}
u_{ijk}(\vec{x}, \vec{y}, \vec{z}) = & \delta(\langle \vec{x}, \vec{y} \rangle) \delta(\langle \vec{y}, \vec{z} \rangle) \Big[- N_f h_{31} \delta_{i1} \delta_{j2} \delta_{k1} - N_f 2 h_{31} \delta_{i1} \delta_{j3} \delta_{k1} \\
& + N_f h_{32} \delta_{i1} \delta_{j5} \delta_{k1} - N_f k_1 h_{32} \delta_{i1} \delta_{j6} \delta_{k1} \\
& + N_f 4 h_{31} \delta_{i1} \delta_{j7} \delta_{k1} - N_f h_{31} \text{tr}(4) \delta_{i1} \delta_{j8} \delta_{k1} \Big] \\
& + \delta(\langle \vec{x}, \vec{z} \rangle) \delta(\langle \vec{y}, \vec{z} \rangle) \Big[- N_f h_{31} \delta_{i1} \delta_{j1} \delta_{k2} - N_f 2 h_{31} \delta_{i1} \delta_{j1} \delta_{k3} \\
& + N_f h_{32} \delta_{i1} \delta_{j1} \delta_{k5} - N_f k_1 h_{32} \delta_{i1} \delta_{j1} \delta_{k6} \\
& + N_f 4 h_{31} \delta_{i1} \delta_{j1} \delta_{k7} - N_f h_{31} \text{tr}(4) \delta_{i1} \delta_{j1} \delta_{k8} \Big] \\
& + \delta(\langle \vec{x}, \vec{y} \rangle) \delta(\langle \vec{x}, \vec{z} \rangle) \Big[- N_f h_{31} \delta_{i2} \delta_{j1} \delta_{k1} - N_f 2 h_{31} \delta_{i3} \delta_{j1} \delta_{k1} \\
& + N_f h_{32} \delta_{i5} \delta_{j1} \delta_{k1} - N_f k_1 h_{32} \delta_{i6} \delta_{j1} \delta_{k1} \\
& + N_f 4 h_{31} \delta_{i7} \delta_{j1} \delta_{k1} - N_f h_{31} \text{tr}(4) \delta_{i8} \delta_{j1} \delta_{k1} \Big] \tag{B.2.2}
\end{aligned}$$

B.3 Integrated LCE z -Functions

B.3.1 $N_f = 1$

Below are all z -functions evaluated with $N_c = 3$ and $N_f = 1$, needed in Chapter 3.2.2.

$$\begin{aligned}
z_0 & = 1 + 4h_1^3 + h_1^6 + 4h_1 \bar{h}_1 + 6h_1^4 \bar{h}_1 + 10h_1^2 \bar{h}_1^2 + 6h_1^5 \bar{h}_1^2 \\
& + 20h_1^3 \bar{h}_1^3 + 4h_1^6 \bar{h}_1^3 + 4\bar{h}_1^3 + 6h_1 \bar{h}_1^4 + 10h_1^4 \bar{h}_1^4 + 6h_1^2 \bar{h}_1^5 \\
& + 4h_1^5 \bar{h}_1^5 + \bar{h}_1^6 + 4h_1^3 \bar{h}_1^6 + h_1^6 \bar{h}_1^6 \tag{B.3.1a}
\end{aligned}$$

$$\begin{aligned}
z_{(1100)} & = 6h_1^3 + 3h_1^6 + 2h_1 \bar{h}_1 + 12h_1^4 \bar{h}_1 + 10h_1^2 \bar{h}_1^2 + 15h_1^5 \bar{h}_1^2 \\
& + 30h_1^3 \bar{h}_1^3 + 12h_1^6 \bar{h}_1^3 + 3h_1 \bar{h}_1^4 + 20h_1^4 \bar{h}_1^4 + 6h_1^2 \bar{h}_1^5 \\
& + 10h_1^5 \bar{h}_1^5 + 6h_1^3 \bar{h}_1^6 + 3h_1^6 \bar{h}_1^6 \tag{B.3.1b}
\end{aligned}$$

$$\begin{aligned}
z_{(0011)} & = 2h_1 \bar{h}_1 + 3h_1^4 \bar{h}_1 + 10h_1^2 \bar{h}_1^2 + 6h_1^5 \bar{h}_1^2 + 6\bar{h}_1^3 + 30h_1^3 \bar{h}_1^3 \\
& + 6h_1^6 \bar{h}_1^3 + 12h_1 \bar{h}_1^4 + 20h_1^4 \bar{h}_1^4 + 15h_1^2 \bar{h}_1^5 + 10h_1^5 \bar{h}_1^5 \\
& + 3\bar{h}_1^6 + 12h_1^3 \bar{h}_1^6 + 3h_1^6 \bar{h}_1^6 \tag{B.3.1c}
\end{aligned}$$

$$\begin{aligned}
z_{(1111)} & = 3h_1 \bar{h}_1 + 6h_1^4 \bar{h}_1 + 11h_1^2 \bar{h}_1^2 + 9h_1^5 \bar{h}_1^2 + 21h_1^3 \bar{h}_1^3 + 6h_1^6 \bar{h}_1^3 \\
& + 6h_1 \bar{h}_1^4 + 21h_1^4 \bar{h}_1^4 + 9h_1^2 \bar{h}_1^5 + 11h_1^5 \bar{h}_1^5 + 6h_1^3 \bar{h}_1^6 + 3h_1^6 \bar{h}_1^6 \tag{B.3.1d}
\end{aligned}$$

$$\begin{aligned}
z_{(2200)} & = -4h_1^3 + 3h_1^6 + 4h_1^4 \bar{h}_1 - 2h_1^2 \bar{h}_1^2 + 12h_1^5 \bar{h}_1^2 - 12h_1^3 \bar{h}_1^3 \\
& + 12h_1^6 \bar{h}_1^3 + 8h_1^4 \bar{h}_1^4 - 2h_1^2 \bar{h}_1^5 + 8h_1^5 \bar{h}_1^5 - 4h_1^3 \bar{h}_1^6 + 3h_1^6 \bar{h}_1^6 \tag{B.3.1e}
\end{aligned}$$

$$z_{(0022)} = -2h_1^2 \bar{h}_1^2 - 2h_1^5 \bar{h}_1^2 - 4\bar{h}_1^3 - 12h_1^3 \bar{h}_1^3 - 4h_1^6 \bar{h}_1^3 + 4h_1 \bar{h}_1^4$$

$$\begin{aligned}
& + 8h_1^4\bar{h}_1^4 + 12h_1^2\bar{h}_1^5 + 8h_1^5\bar{h}_1^5 + 3\bar{h}_1^6 + 12h_1^3\bar{h}_1^6 + 3h_1^6\bar{h}_1^6 & (B.3.1f) \\
z_{(2100)} & = 10h_1^3 + 2h_1\bar{h}_1 + 8h_1^4\bar{h}_1 + 12h_1^2\bar{h}_1^2 + 3h_1^5\bar{h}_1^2 + 42h_1^3\bar{h}_1^3 \\
& + 3h_1\bar{h}_1^4 + 12h_1^4\bar{h}_1^4 + 8h_1^2\bar{h}_1^5 + 2h_1^5\bar{h}_1^5 + 10h_1^3\bar{h}_1^6 & (B.3.1g) \\
z_{(0021)} & = 2h_1\bar{h}_1 + 3h_1^4\bar{h}_1 + 12h_1^2\bar{h}_1^2 + 8h_1^5\bar{h}_1^2 + 10\bar{h}_1^3 + 42h_1^3\bar{h}_1^3 \\
& + 10h_1^6\bar{h}_1^3 + 8h_1\bar{h}_1^4 + 12h_1^4\bar{h}_1^4 + 3h_1^2\bar{h}_1^5 + 2h_1^5\bar{h}_1^5 & (B.3.1h) \\
z_{(1010)} & = 3 + 6h_1^3 + 11h_1\bar{h}_1 + 9h_1^4\bar{h}_1 + 21h_1^2\bar{h}_1^2 + 6h_1^5\bar{h}_1^2 + 6\bar{h}_1^3 \\
& + 21h_1^3\bar{h}_1^3 + 9h_1\bar{h}_1^4 + 11h_1^4\bar{h}_1^4 + 6h_1^2\bar{h}_1^5 + 3h_1^5\bar{h}_1^5 & (B.3.1i) \\
z_{(1100)^2} & = 4h_1^3 + 9h_1^6 + 20h_1^4\bar{h}_1 + 4h_1^2\bar{h}_1^2 + 36h_1^5\bar{h}_1^2 + 24h_1^3\bar{h}_1^3 + 36h_1^6\bar{h}_1^3 \\
& + 34h_1^4\bar{h}_1^4 + 2h_1^2\bar{h}_1^5 + 24h_1^5\bar{h}_1^5 + 4h_1^3\bar{h}_1^6 + 9h_1^6\bar{h}_1^6 & (B.3.1j) \\
z_{(0011)^2} & = 4h_1^2\bar{h}_1^2 + 2h_1^5\bar{h}_1^2 + 4\bar{h}_1^3 + 24h_1^3\bar{h}_1^3 + 4h_1^6\bar{h}_1^3 + 20h_1\bar{h}_1^4 \\
& + 34h_1^4\bar{h}_1^4 + 36h_1^2\bar{h}_1^5 + 24h_1^5\bar{h}_1^5 + 9\bar{h}_1^6 + 36h_1^3\bar{h}_1^6 + 9h_1^6\bar{h}_1^6 & (B.3.1k) \\
z_{(1100)(0011)} & = h_1\bar{h}_1 + 6h_1^4\bar{h}_1 + 10h_1^2\bar{h}_1^2 + 15h_1^5\bar{h}_1^2 + 45h_1^3\bar{h}_1^3 + 18h_1^6\bar{h}_1^3 \\
& + 6h_1\bar{h}_1^4 + 40h_1^4\bar{h}_1^4 + 15h_1^2\bar{h}_1^5 + 25h_1^5\bar{h}_1^5 + 18h_1^3\bar{h}_1^6 + 9h_1^6\bar{h}_1^6 & (B.3.1l) \\
z_{(1111)^-} & = 6h_1^3 + 3h_1^6 + 9h_1^4\bar{h}_1 + 9h_1^5\bar{h}_1^2 - 6\bar{h}_1^3 + 6h_1^6\bar{h}_1^3 - 9h_1\bar{h}_1^4 \\
& - 9h_1^2\bar{h}_1^5 - 3\bar{h}_1^6 - 6h_1^3\bar{h}_1^6 & (B.3.1m) \\
z_{(2222)^+} & = -4h_1^3 + 4h_1^4\bar{h}_1 - 4h_1^2\bar{h}_1^2 + 10h_1^5\bar{h}_1^2 - 4\bar{h}_1^3 - 24h_1^3\bar{h}_1^3 \\
& + 8h_1^6\bar{h}_1^3 + 4h_1\bar{h}_1^4 + 3h_1^6 + 16h_1^4\bar{h}_1^4 + 10h_1^2\bar{h}_1^5 + 16h_1^5\bar{h}_1^5 \\
& + 3\bar{h}_1^6 + 8h_1^3\bar{h}_1^6 + 6h_1^6\bar{h}_1^6 & (B.3.1n) \\
z_{((1111)^-)^2} & = 4h_1^3 + 9h_1^6 - 2h_1\bar{h}_1 + 8h_1^4\bar{h}_1 - 12h_1^2\bar{h}_1^2 + 8h_1^5\bar{h}_1^2 + 4\bar{h}_1^3 \\
& - 42h_1^3\bar{h}_1^3 + 4h_1^6\bar{h}_1^3 + 8h_1\bar{h}_1^4 - 12h_1^4\bar{h}_1^4 + 8h_1^2\bar{h}_1^5 \\
& - 2h_1^5\bar{h}_1^5 + 9\bar{h}_1^6 + 4h_1^3\bar{h}_1^6 & (B.3.1o) \\
z_{(2121)^+} & = 10h_1^3 + 4h_1\bar{h}_1 + 11h_1^4\bar{h}_1 + 24h_1^2\bar{h}_1^2 + 11h_1^5\bar{h}_1^2 + 10\bar{h}_1^3 \\
& + 84h_1^3\bar{h}_1^3 + 10h_1^6\bar{h}_1^3 + 11h_1\bar{h}_1^4 + 24h_1^4\bar{h}_1^4 + 11h_1^2\bar{h}_1^5 \\
& + 4h_1^5\bar{h}_1^5 + 10h_1^3\bar{h}_1^6 & (B.3.1p) \\
z_{(1111)^+} & = 6h_1^3 + 3h_1^6 + 4h_1\bar{h}_1 + 15h_1^4\bar{h}_1 + 20h_1^2\bar{h}_1^2 + 21h_1^5\bar{h}_1^2 \\
& + 6\bar{h}_1^3 + 60h_1^3\bar{h}_1^3 + 18h_1^6\bar{h}_1^3 + 15h_1\bar{h}_1^4 + 40h_1^4\bar{h}_1^4 \\
& + 21h_1^2\bar{h}_1^5 + 20h_1^5\bar{h}_1^5 + 3\bar{h}_1^6 + 18h_1^3\bar{h}_1^6 + 6h_1^6\bar{h}_1^6 & (B.3.1q)
\end{aligned}$$

B.3.2 $N_f = 2$

Below are all z -functions evaluated with $N_c = 3$ and $N_f = 2$, needed in Chapter 3.2.2.

$$\begin{aligned}
z_0 & = 1 + 20h_1^3 + 50h_1^6 + 20h_1^9 + h_1^{12} + 16h_1\bar{h}_1 + 180h_1^4\bar{h}_1 \\
& + 240h_1^7\bar{h}_1 + 40h_1^{10}\bar{h}_1 + 136h_1^2\bar{h}_1^2 + 816h_1^5\bar{h}_1^2 + 570h_1^8\bar{h}_1^2 \\
& + 40h_1^{11}\bar{h}_1^2 + 20\bar{h}_1^3 + 816h_1^3\bar{h}_1^3 + 2320h_1^6\bar{h}_1^3 + 800h_1^9\bar{h}_1^3 \\
& + 20h_1^{12}\bar{h}_1^3 + 180h_1\bar{h}_1^4 + 2651h_1^4\bar{h}_1^4 + 3720h_1^7\bar{h}_1^4 \\
& + 570h_1^{10}\bar{h}_1^4 + 816h_1^2\bar{h}_1^5 + 5312h_1^5\bar{h}_1^5 + 3720h_1^8\bar{h}_1^5 \\
& + 240h_1^{11}\bar{h}_1^5 + 50\bar{h}_1^6 + 2320h_1^3\bar{h}_1^6 + 6832h_1^6\bar{h}_1^6 \\
& + 2320h_1^9\bar{h}_1^6 + 50h_1^{12}\bar{h}_1^6 + 240h_1\bar{h}_1^7 + 3720h_1^4\bar{h}_1^7
\end{aligned}$$

$$\begin{aligned}
& + 5312h_1^7\bar{h}_1^7 + 816h_1^{10}\bar{h}_1^7 + 570h_1^2\bar{h}_1^8 + 3720h_1^5\bar{h}_1^8 \\
& + 2651h_1^8\bar{h}_1^8 + 180h_1^{11}\bar{h}_1^8 + 20\bar{h}_1^9 + 800h_1^3\bar{h}_1^9 + 2320h_1^6\bar{h}_1^9 \\
& + 816h_1^9\bar{h}_1^9 + 20h_1^{12}\bar{h}_1^9 + 40h_1\bar{h}_1^{10} + 570h_1^4\bar{h}_1^{10} + 816h_1^7\bar{h}_1^{10} \\
& + 136h_1^{10}\bar{h}_1^{10} + 40h_1^2\bar{h}_1^{11} + 240h_1^5\bar{h}_1^{11} + 180h_1^8\bar{h}_1^{11} + 16h_1^{11}\bar{h}_1^{11} \\
& + \bar{h}_1^{12} + 20h_1^3\bar{h}_1^{12} + 50h_1^6\bar{h}_1^{12} + 20h_1^9\bar{h}_1^{12} + h_1^{12}\bar{h}_1^{12} \quad (\text{B.3.2a}) \\
z_{(1100)} = & 15h_1^3 + 75h_1^6 + 45h_1^9 + 3h_1^{12} + 4h_1\bar{h}_1 + 180h_1^4\bar{h}_1 + 420h_1^7\bar{h}_1 \\
& + 100h_1^{10}\bar{h}_1 + 68h_1^2\bar{h}_1^2 + 1020h_1^5\bar{h}_1^2 + 1140h_1^8\bar{h}_1^2 + 110h_1^{11}\bar{h}_1^2 \\
& + 612h_1^3\bar{h}_1^3 + 3480h_1^6\bar{h}_1^3 + 1800h_1^9\bar{h}_1^3 + 60h_1^{12}\bar{h}_1^3 + 45h_1\bar{h}_1^4 \\
& + 2651h_1^4\bar{h}_1^4 + 6510h_1^7\bar{h}_1^4 + 1425h_1^{10}\bar{h}_1^4 + 408h_1^2\bar{h}_1^5 \\
& + 6640h_1^5\bar{h}_1^5 + 7440h_1^8\bar{h}_1^5 + 660h_1^{11}\bar{h}_1^5 + 1740h_1^3\bar{h}_1^6 \\
& + 10248h_1^6\bar{h}_1^6 + 5220h_1^9\bar{h}_1^6 + 150h_1^{12}\bar{h}_1^6 + 60h_1\bar{h}_1^7 \\
& + 3720h_1^4\bar{h}_1^7 + 9296h_1^7\bar{h}_1^7 + 2040h_1^{10}\bar{h}_1^7 + 285h_1^2\bar{h}_1^8 \\
& + 4650h_1^5\bar{h}_1^8 + 5302h_1^8\bar{h}_1^8 + 495h_1^{11}\bar{h}_1^8 + 600h_1^3\bar{h}_1^9 \\
& + 3480h_1^6\bar{h}_1^9 + 1836h_1^9\bar{h}_1^9 + 60h_1^{12}\bar{h}_1^9 + 10h_1\bar{h}_1^{10} + 570h_1^4\bar{h}_1^{10} \\
& + 1428h_1^7\bar{h}_1^{10} + 340h_1^{10}\bar{h}_1^{10} + 20h_1^2\bar{h}_1^{11} + 300h_1^5\bar{h}_1^{11} + 360h_1^8\bar{h}_1^{11} \\
& + 44h_1^{11}\bar{h}_1^{11} + 15h_1^3\bar{h}_1^{12} + 75h_1^6\bar{h}_1^{12} + 45h_1^9\bar{h}_1^{12} + 3h_1^{12}\bar{h}_1^{12} \quad (\text{B.3.2b}) \\
z_{(0011)} = & 4h_1\bar{h}_1 + 45h_1^4\bar{h}_1 + 60h_1^7\bar{h}_1 + 10h_1^{10}\bar{h}_1 + 68h_1^2\bar{h}_1^2 + 408h_1^5\bar{h}_1^2 \\
& + 285h_1^8\bar{h}_1^2 + 20h_1^{11}\bar{h}_1^2 + 15\bar{h}_1^3 + 612h_1^3\bar{h}_1^3 + 1740h_1^6\bar{h}_1^3 \\
& + 600h_1^9\bar{h}_1^3 + 15h_1^{12}\bar{h}_1^3 + 180h_1\bar{h}_1^4 + 2651h_1^4\bar{h}_1^4 + 3720h_1^7\bar{h}_1^4 \\
& + 570h_1^{10}\bar{h}_1^4 + 1020h_1^2\bar{h}_1^5 + 6640h_1^5\bar{h}_1^5 + 4650h_1^8\bar{h}_1^5 \\
& + 300h_1^{11}\bar{h}_1^5 + 75\bar{h}_1^6 + 3480h_1^3\bar{h}_1^6 + 10248h_1^6\bar{h}_1^6 + 3480h_1^9\bar{h}_1^6 \\
& + 75h_1^{12}\bar{h}_1^6 + 420h_1\bar{h}_1^7 + 6510h_1^4\bar{h}_1^7 + 9296h_1^7\bar{h}_1^7 \\
& + 1428h_1^{10}\bar{h}_1^7 + 1140h_1^2\bar{h}_1^8 + 7440h_1^5\bar{h}_1^8 + 5302h_1^8\bar{h}_1^8 \\
& + 360h_1^{11}\bar{h}_1^8 + 45\bar{h}_1^9 + 1800h_1^3\bar{h}_1^9 + 5220h_1^6\bar{h}_1^9 + 1836h_1^9\bar{h}_1^9 \\
& + 45h_1^{12}\bar{h}_1^9 + 100h_1\bar{h}_1^{10} + 1425h_1^4\bar{h}_1^{10} + 2040h_1^7\bar{h}_1^{10} \\
& + 340h_1^{10}\bar{h}_1^{10} + 110h_1^2\bar{h}_1^{11} + 660h_1^5\bar{h}_1^{11} + 495h_1^8\bar{h}_1^{11} + 44h_1^{11}\bar{h}_1^{11} \\
& + 3\bar{h}_1^{12} + 60h_1^3\bar{h}_1^{12} + 150h_1^6\bar{h}_1^{12} + 60h_1^9\bar{h}_1^{12} + 3h_1^{12}\bar{h}_1^{12} \quad (\text{B.3.2c}) \\
z_{(1111)} = & 3h_1\bar{h}_1 + 45h_1^4\bar{h}_1 + 75h_1^7\bar{h}_1 + 15h_1^{10}\bar{h}_1 + 43h_1^2\bar{h}_1^2 + 360h_1^5\bar{h}_1^2 \\
& + 315h_1^8\bar{h}_1^2 + 25h_1^{11}\bar{h}_1^2 + 315h_1^3\bar{h}_1^3 + 1380h_1^6\bar{h}_1^3 + 600h_1^9\bar{h}_1^3 \\
& + 15h_1^{12}\bar{h}_1^3 + 45h_1\bar{h}_1^4 + 1539h_1^4\bar{h}_1^4 + 3120h_1^7\bar{h}_1^4 + 600h_1^{10}\bar{h}_1^4 \\
& + 360h_1^2\bar{h}_1^5 + 4190h_1^5\bar{h}_1^5 + 4050h_1^8\bar{h}_1^5 + 315h_1^{11}\bar{h}_1^5 \\
& + 1380h_1^3\bar{h}_1^6 + 6846h_1^6\bar{h}_1^6 + 3120h_1^9\bar{h}_1^6 + 75h_1^{12}\bar{h}_1^6 + 75h_1\bar{h}_1^7 \\
& + 3120h_1^4\bar{h}_1^7 + 6846h_1^7\bar{h}_1^7 + 1380h_1^{10}\bar{h}_1^7 + 315h_1^2\bar{h}_1^8 \\
& + 4050h_1^5\bar{h}_1^8 + 4190h_1^8\bar{h}_1^8 + 360h_1^{11}\bar{h}_1^8 + 600h_1^3\bar{h}_1^9 + 3120h_1^6\bar{h}_1^9 \\
& + 1539h_1^9\bar{h}_1^9 + 45h_1^{12}\bar{h}_1^9 + 15h_1\bar{h}_1^{10} + 600h_1^4\bar{h}_1^{10} + 1380h_1^7\bar{h}_1^{10} \\
& + 315h_1^{10}\bar{h}_1^{10} + 25h_1^2\bar{h}_1^{11} + 315h_1^5\bar{h}_1^{11} + 360h_1^8\bar{h}_1^{11} + 43h_1^{11}\bar{h}_1^{11} \\
& + 15h_1^3\bar{h}_1^{12} + 75h_1^6\bar{h}_1^{12} + 45h_1^9\bar{h}_1^{12} + 3h_1^{12}\bar{h}_1^{12} \quad (\text{B.3.2d}) \\
z_{(2200)} = & -6h_1^3 + 5h_1^6 + 24h_1^9 + 3h_1^{12} - 12h_1^4\bar{h}_1 + 136h_1^7\bar{h}_1 + 76h_1^{10}\bar{h}_1
\end{aligned}$$

$$\begin{aligned}
& -4h_1^2\bar{h}_1^2 + 112h_1^5\bar{h}_1^2 + 564h_1^8\bar{h}_1^2 + 100h_1^{11}\bar{h}_1^2 - 72h_1^3\bar{h}_1^3 \\
& + 776h_1^6\bar{h}_1^3 + 1120h_1^9\bar{h}_1^3 + 60h_1^{12}\bar{h}_1^3 + 51h_1^4\bar{h}_1^4 + 2460h_1^7\bar{h}_1^4 \\
& + 1115h_1^{10}\bar{h}_1^4 - 24h_1^2\bar{h}_1^5 + 928h_1^5\bar{h}_1^5 + 3824h_1^8\bar{h}_1^5 \\
& + 600h_1^{11}\bar{h}_1^5 - 152h_1^3\bar{h}_1^6 + 2520h_1^6\bar{h}_1^6 + 3328h_1^9\bar{h}_1^6 \\
& + 150h_1^{12}\bar{h}_1^6 + 104h_1^4\bar{h}_1^7 + 3584h_1^7\bar{h}_1^7 + 1608h_1^{10}\bar{h}_1^7 - 25h_1^2\bar{h}_1^8 \\
& + 600h_1^5\bar{h}_1^8 + 2702h_1^8\bar{h}_1^8 + 450h_1^{11}\bar{h}_1^8 - 80h_1^3\bar{h}_1^9 + 776h_1^6\bar{h}_1^9 \\
& + 1152h_1^9\bar{h}_1^9 + 60h_1^{12}\bar{h}_1^9 - 6h_1^4\bar{h}_1^{10} + 520h_1^7\bar{h}_1^{10} + 268h_1^{10}\bar{h}_1^{10} \\
& - 4h_1^2\bar{h}_1^{11} + 16h_1^5\bar{h}_1^{11} + 168h_1^8\bar{h}_1^{11} + 40h_1^{11}\bar{h}_1^{11} - 6h_1^3\bar{h}_1^{12} \\
& + 5h_1^6\bar{h}_1^{12} + 24h_1^9\bar{h}_1^{12} + 3h_1^{12}\bar{h}_1^{12}
\end{aligned} \tag{B.3.2e}$$

$$\begin{aligned}
z_{(0022)} & = -4h_1^2\bar{h}_1^2 - 24h_1^5\bar{h}_1^2 - 25h_1^8\bar{h}_1^2 - 4h_1^{11}\bar{h}_1^2 - 6\bar{h}_1^3 - 72h_1^3\bar{h}_1^3 \\
& - 152h_1^6\bar{h}_1^3 - 80h_1^9\bar{h}_1^3 - 6h_1^{12}\bar{h}_1^3 - 12h_1\bar{h}_1^4 + 51h_1^4\bar{h}_1^4 \\
& + 104h_1^7\bar{h}_1^4 - 6h_1^{10}\bar{h}_1^4 + 112h_1^2\bar{h}_1^5 + 928h_1^5\bar{h}_1^5 + 600h_1^8\bar{h}_1^5 \\
& + 16h_1^{11}\bar{h}_1^5 + 5\bar{h}_1^6 + 776h_1^3\bar{h}_1^6 + 2520h_1^6\bar{h}_1^6 + 776h_1^9\bar{h}_1^6 \\
& + 5h_1^{12}\bar{h}_1^6 + 136h_1\bar{h}_1^7 + 2460h_1^4\bar{h}_1^7 + 3584h_1^7\bar{h}_1^7 + 520h_1^{10}\bar{h}_1^7 \\
& + 564h_1^2\bar{h}_1^8 + 3824h_1^5\bar{h}_1^8 + 2702h_1^8\bar{h}_1^8 + 168h_1^{11}\bar{h}_1^8 + 24\bar{h}_1^9 \\
& + 1120h_1^3\bar{h}_1^9 + 3328h_1^6\bar{h}_1^9 + 1152h_1^9\bar{h}_1^9 + 24h_1^{12}\bar{h}_1^9 + 76h_1\bar{h}_1^{10} \\
& + 1115h_1^4\bar{h}_1^{10} + 1608h_1^7\bar{h}_1^{10} + 268h_1^{10}\bar{h}_1^{10} + 100h_1^2\bar{h}_1^{11} \\
& + 600h_1^5\bar{h}_1^{11} + 450h_1^8\bar{h}_1^{11} + 40h_1^{11}\bar{h}_1^{11} + 3\bar{h}_1^{12} + 60h_1^3\bar{h}_1^{12} \\
& + 150h_1^6\bar{h}_1^{12} + 60h_1^9\bar{h}_1^{12} + 3h_1^{12}\bar{h}_1^{12}
\end{aligned} \tag{B.3.2f}$$

$$\begin{aligned}
z_{(2100)} & = 21h_1^3 + 70h_1^6 + 21h_1^9 + 4h_1\bar{h}_1 + 192h_1^4\bar{h}_1 + 284h_1^7\bar{h}_1 \\
& + 24h_1^{10}\bar{h}_1 + 72h_1^2\bar{h}_1^2 + 908h_1^5\bar{h}_1^2 + 576h_1^8\bar{h}_1^2 + 10h_1^{11}\bar{h}_1^2 \\
& + 684h_1^3\bar{h}_1^3 + 2704h_1^6\bar{h}_1^3 + 680h_1^9\bar{h}_1^3 + 45h_1\bar{h}_1^4 + 2600h_1^4\bar{h}_1^4 \\
& + 4050h_1^7\bar{h}_1^4 + 310h_1^{10}\bar{h}_1^4 + 432h_1^2\bar{h}_1^5 + 5712h_1^5\bar{h}_1^5 \\
& + 3616h_1^8\bar{h}_1^5 + 60h_1^{11}\bar{h}_1^5 + 1892h_1^3\bar{h}_1^6 + 7728h_1^6\bar{h}_1^6 \\
& + 1892h_1^9\bar{h}_1^6 + 60h_1\bar{h}_1^7 + 3616h_1^4\bar{h}_1^7 + 5712h_1^7\bar{h}_1^7 + 432h_1^{10}\bar{h}_1^7 \\
& + 310h_1^2\bar{h}_1^8 + 4050h_1^5\bar{h}_1^8 + 2600h_1^8\bar{h}_1^8 + 45h_1^{11}\bar{h}_1^8 + 680h_1^3\bar{h}_1^9 \\
& + 2704h_1^6\bar{h}_1^9 + 684h_1^9\bar{h}_1^9 + 10h_1\bar{h}_1^{10} + 576h_1^4\bar{h}_1^{10} + 908h_1^7\bar{h}_1^{10} \\
& + 72h_1^{10}\bar{h}_1^{10} + 24h_1^2\bar{h}_1^{11} + 284h_1^5\bar{h}_1^{11} + 192h_1^8\bar{h}_1^{11} + 4h_1^{11}\bar{h}_1^{11} \\
& + 21h_1^3\bar{h}_1^{12} + 70h_1^6\bar{h}_1^{12} + 21h_1^9\bar{h}_1^{12}
\end{aligned} \tag{B.3.2g}$$

$$\begin{aligned}
z_{(0021)} & = 4h_1\bar{h}_1 + 45h_1^4\bar{h}_1 + 60h_1^7\bar{h}_1 + 10h_1^{10}\bar{h}_1 + 72h_1^2\bar{h}_1^2 + 432h_1^5\bar{h}_1^2 \\
& + 310h_1^8\bar{h}_1^2 + 24h_1^{11}\bar{h}_1^2 + 21\bar{h}_1^3 + 684h_1^3\bar{h}_1^3 + 1892h_1^6\bar{h}_1^3 \\
& + 680h_1^9\bar{h}_1^3 + 21h_1^{12}\bar{h}_1^3 + 192h_1\bar{h}_1^4 + 2600h_1^4\bar{h}_1^4 \\
& + 3616h_1^7\bar{h}_1^4 + 576h_1^{10}\bar{h}_1^4 + 908h_1^2\bar{h}_1^5 + 5712h_1^5\bar{h}_1^5 \\
& + 4050h_1^8\bar{h}_1^5 + 284h_1^{11}\bar{h}_1^5 + 70\bar{h}_1^6 + 2704h_1^3\bar{h}_1^6 + 7728h_1^6\bar{h}_1^6 \\
& + 2704h_1^9\bar{h}_1^6 + 70h_1^{12}\bar{h}_1^6 + 284h_1\bar{h}_1^7 + 4050h_1^4\bar{h}_1^7 \\
& + 5712h_1^7\bar{h}_1^7 + 908h_1^{10}\bar{h}_1^7 + 576h_1^2\bar{h}_1^8 + 3616h_1^5\bar{h}_1^8 \\
& + 2600h_1^8\bar{h}_1^8 + 192h_1^{11}\bar{h}_1^8 + 21\bar{h}_1^9 + 680h_1^3\bar{h}_1^9 + 1892h_1^6\bar{h}_1^9 \\
& + 684h_1^9\bar{h}_1^9 + 21h_1^{12}\bar{h}_1^9 + 24h_1\bar{h}_1^{10} + 310h_1^4\bar{h}_1^{10} + 432h_1^7\bar{h}_1^{10}
\end{aligned}$$

$$\begin{aligned}
& + 72h_1^{10}\bar{h}_1^{10} + 10h_1^2\bar{h}_1^{11} + 60h_1^5\bar{h}_1^{11} + 45h_1^8\bar{h}_1^{11} + 4h_1^{11}\bar{h}_1^{11} \quad (\text{B.3.2h}) \\
z_{(1010)} & = 3 + 45h_1^3 + 75h_1^6 + 15h_1^9 + 43h_1\bar{h}_1 + 360h_1^4\bar{h}_1 + 315h_1^7\bar{h}_1 \\
& + 25h_1^{10}\bar{h}_1 + 315h_1^2\bar{h}_1^2 + 1380h_1^5\bar{h}_1^2 + 600h_1^8\bar{h}_1^2 + 15h_1^{11}\bar{h}_1^2 \\
& + 45\bar{h}_1^3 + 1539h_1^3\bar{h}_1^3 + 3120h_1^6\bar{h}_1^3 + 600h_1^9\bar{h}_1^3 + 360h_1\bar{h}_1^4 \\
& + 4190h_1^4\bar{h}_1^4 + 4050h_1^7\bar{h}_1^4 + 315h_1^{10}\bar{h}_1^4 + 1380h_1^2\bar{h}_1^5 \\
& + 6846h_1^5\bar{h}_1^5 + 3120h_1^8\bar{h}_1^5 + 75h_1^{11}\bar{h}_1^5 + 75\bar{h}_1^6 + 3120h_1^3\bar{h}_1^6 \\
& + 6846h_1^6\bar{h}_1^6 + 1380h_1^9\bar{h}_1^6 + 315h_1\bar{h}_1^7 + 4050h_1^4\bar{h}_1^7 + 4190h_1^7\bar{h}_1^7 \\
& + 360h_1^{10}\bar{h}_1^7 + 600h_1^2\bar{h}_1^8 + 3120h_1^5\bar{h}_1^8 + 1539h_1^8\bar{h}_1^8 \\
& + 45h_1^{11}\bar{h}_1^8 + 15\bar{h}_1^9 + 600h_1^3\bar{h}_1^9 + 1380h_1^6\bar{h}_1^9 + 315h_1^9\bar{h}_1^9 \\
& + 25h_1\bar{h}_1^{10} + 315h_1^4\bar{h}_1^{10} + 360h_1^7\bar{h}_1^{10} + 43h_1^{10}\bar{h}_1^{10} + 15h_1^2\bar{h}_1^{11} \\
& + 75h_1^5\bar{h}_1^{11} + 45h_1^8\bar{h}_1^{11} + 3h_1^{11}\bar{h}_1^{11} \quad (\text{B.3.2i}) \\
z_{(1100)^2} & = 6h_1^3 + 95h_1^6 + 96h_1^9 + 9h_1^{12} + 132h_1^4\bar{h}_1 + 664h_1^7\bar{h}_1 + 244h_1^{10}\bar{h}_1 \\
& + 16h_1^2\bar{h}_1^2 + 1048h_1^5\bar{h}_1^2 + 2136h_1^8\bar{h}_1^2 + 300h_1^{11}\bar{h}_1^2 + 288h_1^3\bar{h}_1^3 \\
& + 4544h_1^6\bar{h}_1^3 + 3880h_1^9\bar{h}_1^3 + 180h_1^{12}\bar{h}_1^3 + 2001h_1^4\bar{h}_1^4 \\
& + 10380h_1^7\bar{h}_1^4 + 3485h_1^{10}\bar{h}_1^4 + 96h_1^2\bar{h}_1^5 + 6872h_1^5\bar{h}_1^5 \\
& + 13976h_1^8\bar{h}_1^5 + 1800h_1^{11}\bar{h}_1^5 + 832h_1^3\bar{h}_1^6 + 13440h_1^6\bar{h}_1^6 \\
& + 11272h_1^9\bar{h}_1^6 + 450h_1^{12}\bar{h}_1^6 + 2816h_1^4\bar{h}_1^7 + 14840h_1^7\bar{h}_1^7 \\
& + 4992h_1^{10}\bar{h}_1^7 + 65h_1^2\bar{h}_1^8 + 4800h_1^5\bar{h}_1^8 + 9954h_1^8\bar{h}_1^8 \\
& + 1350h_1^{11}\bar{h}_1^8 + 280h_1^3\bar{h}_1^9 + 4544h_1^6\bar{h}_1^9 + 3960h_1^9\bar{h}_1^9 \\
& + 180h_1^{12}\bar{h}_1^9 + 426h_1^4\bar{h}_1^{10} + 2272h_1^7\bar{h}_1^{10} + 832h_1^{10}\bar{h}_1^{10} \\
& + 4h_1^2\bar{h}_1^{11} + 304h_1^5\bar{h}_1^{11} + 672h_1^8\bar{h}_1^{11} + 120h_1^{11}\bar{h}_1^{11} + 6h_1^3\bar{h}_1^{12} \\
& + 95h_1^6\bar{h}_1^{12} + 96h_1^9\bar{h}_1^{12} + 9h_1^{12}\bar{h}_1^{12} \quad (\text{B.3.2j}) \\
z_{(0011)^2} & = 16h_1^2\bar{h}_1^2 + 96h_1^5\bar{h}_1^2 + 65h_1^8\bar{h}_1^2 + 4h_1^{11}\bar{h}_1^2 + 6\bar{h}_1^3 + 288h_1^3\bar{h}_1^3 \\
& + 832h_1^6\bar{h}_1^3 + 280h_1^9\bar{h}_1^3 + 6h_1^{12}\bar{h}_1^3 + 132h_1\bar{h}_1^4 + 2001h_1^4\bar{h}_1^4 \\
& + 2816h_1^7\bar{h}_1^4 + 426h_1^{10}\bar{h}_1^4 + 1048h_1^2\bar{h}_1^5 + 6872h_1^5\bar{h}_1^5 \\
& + 4800h_1^8\bar{h}_1^5 + 304h_1^{11}\bar{h}_1^5 + 95\bar{h}_1^6 + 4544h_1^3\bar{h}_1^6 + 13440h_1^6\bar{h}_1^6 \\
& + 4544h_1^9\bar{h}_1^6 + 95h_1^{12}\bar{h}_1^6 + 664h_1\bar{h}_1^7 + 10380h_1^4\bar{h}_1^7 \\
& + 14840h_1^7\bar{h}_1^7 + 2272h_1^{10}\bar{h}_1^7 + 2136h_1^2\bar{h}_1^8 + 13976h_1^5\bar{h}_1^8 \\
& + 9954h_1^8\bar{h}_1^8 + 672h_1^{11}\bar{h}_1^8 + 96\bar{h}_1^9 + 3880h_1^3\bar{h}_1^9 + 11272h_1^6\bar{h}_1^9 \\
& + 3960h_1^9\bar{h}_1^9 + 96h_1^{12}\bar{h}_1^9 + 244h_1\bar{h}_1^{10} + 3485h_1^4\bar{h}_1^{10} \\
& + 4992h_1^7\bar{h}_1^{10} + 832h_1^{10}\bar{h}_1^{10} + 300h_1^2\bar{h}_1^{11} + 1800h_1^5\bar{h}_1^{11} \\
& + 1350h_1^8\bar{h}_1^{11} + 120h_1^{11}\bar{h}_1^{11} + 9\bar{h}_1^{12} + 180h_1^3\bar{h}_1^{12} \\
& + 450h_1^6\bar{h}_1^{12} + 180h_1^9\bar{h}_1^{12} + 9h_1^{12}\bar{h}_1^{12} \quad (\text{B.3.2k}) \\
z_{(1100)(0011)} & = h_1\bar{h}_1 + 45h_1^4\bar{h}_1 + 105h_1^7\bar{h}_1 + 25h_1^{10}\bar{h}_1 + 34h_1^2\bar{h}_1^2 + 510h_1^5\bar{h}_1^2 \\
& + 570h_1^8\bar{h}_1^2 + 55h_1^{11}\bar{h}_1^2 + 459h_1^3\bar{h}_1^3 + 2610h_1^6\bar{h}_1^3 + 1350h_1^9\bar{h}_1^3 \\
& + 45h_1^{12}\bar{h}_1^3 + 45h_1\bar{h}_1^4 + 2651h_1^4\bar{h}_1^4 + 6510h_1^7\bar{h}_1^4 + 1425h_1^{10}\bar{h}_1^4 \\
& + 510h_1^2\bar{h}_1^5 + 8300h_1^5\bar{h}_1^5 + 9300h_1^8\bar{h}_1^5 + 825h_1^{11}\bar{h}_1^5 \\
& + 2610h_1^3\bar{h}_1^6 + 15372h_1^6\bar{h}_1^6 + 7830h_1^9\bar{h}_1^6 + 225h_1^{12}\bar{h}_1^6
\end{aligned}$$

$$\begin{aligned}
& + 105h_1\bar{h}_1^7 + 6510h_1^4\bar{h}_1^7 + 16268h_1^7\bar{h}_1^7 + 3570h_1^{10}\bar{h}_1^7 \\
& + 570h_1^2\bar{h}_1^8 + 9300h_1^5\bar{h}_1^8 + 10604h_1^8\bar{h}_1^8 + 990h_1^{11}\bar{h}_1^8 \\
& + 1350h_1^3\bar{h}_1^9 + 7830h_1^6\bar{h}_1^9 + 4131h_1^9\bar{h}_1^9 + 135h_1^{12}\bar{h}_1^9 \\
& + 25h_1\bar{h}_1^{10} + 1425h_1^4\bar{h}_1^{10} + 3570h_1^7\bar{h}_1^{10} + 850h_1^{10}\bar{h}_1^{10} \\
& + 55h_1^2\bar{h}_1^{11} + 825h_1^5\bar{h}_1^{11} + 990h_1^8\bar{h}_1^{11} + 121h_1^{11}\bar{h}_1^{11} + 45h_1^3\bar{h}_1^{12} \\
& + 225h_1^6\bar{h}_1^{12} + 135h_1^9\bar{h}_1^{12} + 9h_1^{12}\bar{h}_1^{12} \tag{B.3.2l} \\
z_{(11111)-} & = 15h_1^3 + 75h_1^6 + 45h_1^9 + 3h_1^{12} + 135h_1^4\bar{h}_1 + 360h_1^7\bar{h}_1 + 90h_1^{10}\bar{h}_1 \\
& + 612h_1^5\bar{h}_1^2 + 855h_1^8\bar{h}_1^2 + 90h_1^{11}\bar{h}_1^2 - 15\bar{h}_1^3 + 1740h_1^6\bar{h}_1^3 \\
& + 1200h_1^9\bar{h}_1^3 + 45h_1^{12}\bar{h}_1^3 - 135h_1\bar{h}_1^4 + 2790h_1^7\bar{h}_1^4 + 855h_1^{10}\bar{h}_1^4 \\
& - 612h_1^2\bar{h}_1^5 + 2790h_1^8\bar{h}_1^5 + 360h_1^{11}\bar{h}_1^5 - 75\bar{h}_1^6 - 1740h_1^3\bar{h}_1^6 \\
& + 1740h_1^9\bar{h}_1^6 + 75h_1^{12}\bar{h}_1^6 - 360h_1\bar{h}_1^7 - 2790h_1^4\bar{h}_1^7 + 612h_1^{10}\bar{h}_1^7 \\
& - 855h_1^2\bar{h}_1^8 - 2790h_1^5\bar{h}_1^8 + 135h_1^{11}\bar{h}_1^8 - 45\bar{h}_1^9 - 1200h_1^3\bar{h}_1^9 \\
& - 1740h_1^6\bar{h}_1^9 + 15h_1^{12}\bar{h}_1^9 - 90h_1\bar{h}_1^{10} - 855h_1^4\bar{h}_1^{10} - 612h_1^7\bar{h}_1^{10} \\
& - 90h_1^2\bar{h}_1^{11} - 360h_1^5\bar{h}_1^{11} - 135h_1^8\bar{h}_1^{11} - 3\bar{h}_1^{12} - 45h_1^3\bar{h}_1^{12} \\
& - 75h_1^6\bar{h}_1^{12} - 15h_1^9\bar{h}_1^{12} \tag{B.3.2m} \\
z_{(2222)+} & = -6h_1^3 + 5h_1^6 + 24h_1^9 + 3h_1^{12} - 12h_1^4\bar{h}_1 + 136h_1^7\bar{h}_1 \\
& + 76h_1^{10}\bar{h}_1 - 8h_1^2\bar{h}_1^2 + 88h_1^5\bar{h}_1^2 + 539h_1^8\bar{h}_1^2 + 96h_1^{11}\bar{h}_1^2 - 6\bar{h}_1^3 \\
& - 144h_1^3\bar{h}_1^3 + 624h_1^6\bar{h}_1^3 + 1040h_1^9\bar{h}_1^3 + 54h_1^{12}\bar{h}_1^3 - 12h_1\bar{h}_1^4 \\
& + 102h_1^4\bar{h}_1^4 + 2564h_1^7\bar{h}_1^4 + 1109h_1^{10}\bar{h}_1^4 + 88h_1^2\bar{h}_1^5 + 1856h_1^5\bar{h}_1^5 \\
& + 4424h_1^8\bar{h}_1^5 + 616h_1^{11}\bar{h}_1^5 + 5\bar{h}_1^6 + 624h_1^3\bar{h}_1^6 + 5040h_1^6\bar{h}_1^6 \\
& + 4104h_1^9\bar{h}_1^6 + 155h_1^{12}\bar{h}_1^6 + 136h_1\bar{h}_1^7 + 2564h_1^4\bar{h}_1^7 \\
& + 7168h_1^7\bar{h}_1^7 + 2128h_1^{10}\bar{h}_1^7 + 539h_1^2\bar{h}_1^8 + 4424h_1^5\bar{h}_1^8 \\
& + 5404h_1^8\bar{h}_1^8 + 618h_1^{11}\bar{h}_1^8 + 24\bar{h}_1^9 + 1040h_1^3\bar{h}_1^9 + 4104h_1^6\bar{h}_1^9 \\
& + 2304h_1^9\bar{h}_1^9 + 84h_1^{12}\bar{h}_1^9 + 76h_1\bar{h}_1^{10} + 1109h_1^4\bar{h}_1^{10} \\
& + 2128h_1^7\bar{h}_1^{10} + 536h_1^{10}\bar{h}_1^{10} + 96h_1^2\bar{h}_1^{11} + 616h_1^5\bar{h}_1^{11} \\
& + 618h_1^8\bar{h}_1^{11} + 80h_1^{11}\bar{h}_1^{11} + 3\bar{h}_1^{12} + 54h_1^3\bar{h}_1^{12} + 155h_1^6\bar{h}_1^{12} \\
& + 84h_1^9\bar{h}_1^{12} + 6h_1^{12}\bar{h}_1^{12} \tag{B.3.2n} \\
z_{((11111)-)^2} & = 6h_1^3 + 95h_1^6 + 96h_1^9 + 9h_1^{12} - 2h_1\bar{h}_1 + 42h_1^4\bar{h}_1 + 454h_1^7\bar{h}_1 \\
& + 194h_1^{10}\bar{h}_1 - 36h_1^2\bar{h}_1^2 + 124h_1^5\bar{h}_1^2 + 1061h_1^8\bar{h}_1^2 + 194h_1^{11}\bar{h}_1^2 \\
& + 6\bar{h}_1^3 - 342h_1^3\bar{h}_1^3 + 156h_1^6\bar{h}_1^3 + 1460h_1^9\bar{h}_1^3 + 96h_1^{12}\bar{h}_1^3 \\
& + 42h_1\bar{h}_1^4 - 1300h_1^4\bar{h}_1^4 + 176h_1^7\bar{h}_1^4 + 1061h_1^{10}\bar{h}_1^4 + 124h_1^2\bar{h}_1^5 \\
& - 2856h_1^5\bar{h}_1^5 + 176h_1^8\bar{h}_1^5 + 454h_1^{11}\bar{h}_1^5 + 95\bar{h}_1^6 + 156h_1^3\bar{h}_1^6 \\
& - 3864h_1^6\bar{h}_1^6 + 156h_1^9\bar{h}_1^6 + 95h_1^{12}\bar{h}_1^6 + 454h_1\bar{h}_1^7 + 176h_1^4\bar{h}_1^7 \\
& - 2856h_1^7\bar{h}_1^7 + 124h_1^{10}\bar{h}_1^7 + 1061h_1^2\bar{h}_1^8 + 176h_1^5\bar{h}_1^8 \\
& - 1300h_1^8\bar{h}_1^8 + 42h_1^{11}\bar{h}_1^8 + 96\bar{h}_1^9 + 1460h_1^3\bar{h}_1^9 + 156h_1^6\bar{h}_1^9 \\
& - 342h_1^9\bar{h}_1^9 + 6h_1^{12}\bar{h}_1^9 + 194h_1\bar{h}_1^{10} + 1061h_1^4\bar{h}_1^{10} \\
& + 124h_1^7\bar{h}_1^{10} - 36h_1^{10}\bar{h}_1^{10} + 194h_1^2\bar{h}_1^{11} + 454h_1^5\bar{h}_1^{11} + 42h_1^8\bar{h}_1^{11} \\
& - 2h_1^{11}\bar{h}_1^{11} + 9\bar{h}_1^{12} + 96h_1^3\bar{h}_1^{12} + 95h_1^6\bar{h}_1^{12} + 6h_1^9\bar{h}_1^{12} \tag{B.3.2o}
\end{aligned}$$

$$\begin{aligned}
z_{(2121)+} &= 21h_1^3 + 70h_1^6 + 21h_1^9 + 8h_1\bar{h}_1 + 237h_1^4\bar{h}_1 + 344h_1^7\bar{h}_1 \\
&\quad + 34h_1^{10}\bar{h}_1 + 144h_1^2\bar{h}_1^2 + 1340h_1^5\bar{h}_1^2 + 886h_1^8\bar{h}_1^2 + 34h_1^{11}\bar{h}_1^2 \\
&\quad + 21\bar{h}_1^3 + 1368h_1^3\bar{h}_1^3 + 4596h_1^6\bar{h}_1^3 + 1360h_1^9\bar{h}_1^3 + 21h_1^{12}\bar{h}_1^3 \\
&\quad + 237h_1\bar{h}_1^4 + 5200h_1^4\bar{h}_1^4 + 7666h_1^7\bar{h}_1^4 + 886h_1^{10}\bar{h}_1^4 \\
&\quad + 1340h_1^2\bar{h}_1^5 + 11424h_1^5\bar{h}_1^5 + 7666h_1^8\bar{h}_1^5 + 344h_1^{11}\bar{h}_1^5 + 70\bar{h}_1^6 \\
&\quad + 4596h_1^3\bar{h}_1^6 + 15456h_1^6\bar{h}_1^6 + 4596h_1^9\bar{h}_1^6 + 70h_1^{12}\bar{h}_1^6 \\
&\quad + 344h_1\bar{h}_1^7 + 7666h_1^4\bar{h}_1^7 + 11424h_1^7\bar{h}_1^7 + 1340h_1^{10}\bar{h}_1^7 \\
&\quad + 886h_1^2\bar{h}_1^8 + 7666h_1^5\bar{h}_1^8 + 5200h_1^8\bar{h}_1^8 + 237h_1^{11}\bar{h}_1^8 + 21\bar{h}_1^9 \\
&\quad + 1360h_1^3\bar{h}_1^9 + 4596h_1^6\bar{h}_1^9 + 1368h_1^9\bar{h}_1^9 + 21h_1^{12}\bar{h}_1^9 + 34h_1\bar{h}_1^{10} \\
&\quad + 886h_1^4\bar{h}_1^{10} + 1340h_1^7\bar{h}_1^{10} + 144h_1^{10}\bar{h}_1^{10} + 34h_1^2\bar{h}_1^{11} + 344h_1^5\bar{h}_1^{11} \\
&\quad + 237h_1^8\bar{h}_1^{11} + 8h_1^{11}\bar{h}_1^{11} + 21h_1^3\bar{h}_1^{12} + 70h_1^6\bar{h}_1^{12} + 21h_1^9\bar{h}_1^{12} \quad (\text{B.3.2p})
\end{aligned}$$

$$\begin{aligned}
z_{(1111)+} &= 15h_1^3 + 75h_1^6 + 45h_1^9 + 3h_1^{12} + 8h_1\bar{h}_1 + 225h_1^4\bar{h}_1 + 480h_1^7\bar{h}_1 \\
&\quad + 110h_1^{10}\bar{h}_1 + 136h_1^2\bar{h}_1^2 + 1428h_1^5\bar{h}_1^2 + 1425h_1^8\bar{h}_1^2 + 130h_1^{11}\bar{h}_1^2 \\
&\quad + 15\bar{h}_1^3 + 1224h_1^3\bar{h}_1^3 + 5220h_1^6\bar{h}_1^3 + 2400h_1^9\bar{h}_1^3 + 75h_1^{12}\bar{h}_1^3 \\
&\quad + 225h_1\bar{h}_1^4 + 5302h_1^4\bar{h}_1^4 + 10230h_1^7\bar{h}_1^4 + 1995h_1^{10}\bar{h}_1^4 \\
&\quad + 1428h_1^2\bar{h}_1^5 + 13280h_1^5\bar{h}_1^5 + 12090h_1^8\bar{h}_1^5 + 960h_1^{11}\bar{h}_1^5 + 75\bar{h}_1^6 \\
&\quad + 5220h_1^3\bar{h}_1^6 + 20496h_1^6\bar{h}_1^6 + 8700h_1^9\bar{h}_1^6 + 225h_1^{12}\bar{h}_1^6 + 480h_1\bar{h}_1^7 \\
&\quad + 10230h_1^4\bar{h}_1^7 + 18592h_1^7\bar{h}_1^7 + 3468h_1^{10}\bar{h}_1^7 + 1425h_1^2\bar{h}_1^8 \\
&\quad + 12090h_1^5\bar{h}_1^8 + 10604h_1^8\bar{h}_1^8 + 855h_1^{11}\bar{h}_1^8 + 45\bar{h}_1^9 + 2400h_1^3\bar{h}_1^9 \\
&\quad + 8700h_1^6\bar{h}_1^9 + 3672h_1^9\bar{h}_1^9 + 105h_1^{12}\bar{h}_1^9 + 110h_1\bar{h}_1^{10} \\
&\quad + 1995h_1^4\bar{h}_1^{10} + 3468h_1^7\bar{h}_1^{10} + 680h_1^{10}\bar{h}_1^{10} + 130h_1^2\bar{h}_1^{11} \\
&\quad + 960h_1^5\bar{h}_1^{11} + 855h_1^8\bar{h}_1^{11} + 88h_1^{11}\bar{h}_1^{11} + 3\bar{h}_1^{12} + 75h_1^3\bar{h}_1^{12} \\
&\quad + 225h_1^6\bar{h}_1^{12} + 105h_1^9\bar{h}_1^{12} + 6h_1^{12}\bar{h}_1^{12} \quad (\text{B.3.2q})
\end{aligned}$$

B.4 List of Integrals over Polyakov Loops

This chapter contains a list of integrals over Polyakov loops, used in chapter 3.2.2. Appendix A.3 shows the process of their calculation.

$$\begin{aligned}
\int dU L^3 &= 1 \\
\int dU L^6 &= 5 \\
\int dU L^9 &= 42 \\
\int dU (L^\dagger)^3 &= 1 \\
\int dU (L^\dagger)^6 &= 5 \\
\int dU (L^\dagger)^9 &= 42
\end{aligned}$$

$$\begin{aligned}\int dUL(L^\dagger) &= 1 \\ \int dUL^2(L^\dagger)^2 &= 2 \\ \int dUL^3(L^\dagger)^3 &= 6 \\ \int dUL^4(L^\dagger)^4 &= 23 \\ \int dUL^5(L^\dagger)^5 &= 103 \\ \int dUL(L^\dagger)^4 &= 3 \\ \int dUL(L^\dagger)^7 &= 21 \\ \int dUL^2(L^\dagger)^5 &= 11 \\ \int dUL^2(L^\dagger)^8 &= 98 \\ \int dUL^3(L^\dagger)^6 &= 47 \\ \int dUL^4(L^\dagger) &= 3 \\ \int dUL^5(L^\dagger)^2 &= 11 \\ \int dUL^6(L^\dagger)^3 &= 47 \\ \int dUL^7(L^\dagger) &= 21 \\ \int dUL^8(L^\dagger)^2 &= 98\end{aligned}\tag{B.4.1}$$

Bibliography

- [1] Tillmann Boeckel and Jurgen Schaffner-Bielich. A little inflation at the cosmological QCD phase transition. *Phys. Rev.*, D85:103506, 2012. [arXiv:1105.0832](#), [doi:10.1103/PhysRevD.85.103506](#).
- [2] Y. Aoki, G. Endrodi, Z. Fodor, S. D. Katz, and K. K. Szabo. The Order of the quantum chromodynamics transition predicted by the standard model of particle physics. *Nature*, 443:675–678, 2006. [arXiv:hep-lat/0611014](#), [doi:10.1038/nature05120](#).
- [3] C. Gattringer and C. Lang. *Quantum Chromodynamics on the Lattice: An Introductory Presentation*. Lecture Notes in Physics. Springer Berlin Heidelberg, 2009.
- [4] I. Montvay and G. Münster. *Quantum Fields on a Lattice*. Cambridge Monographs on Mathematical Physics. Cambridge University Press, 1997.
- [5] M. Neuman. *Effective theory for heavy quark QCD at finite temperature and density with stochastic quantization*. PhD thesis, Goethe University Frankfurt, 2015.
- [6] Jens Langelage, Mathias Neuman, and Owe Philipsen. Heavy dense QCD and nuclear matter from an effective lattice theory. *JHEP*, 09:131, 2014. [arXiv:1403.4162](#), [doi:10.1007/JHEP09\(2014\)131](#).
- [7] J. Glesaaen. *Heavy Quark QCD at Finite Temperature and Density Using an Effective Theory*. PhD thesis, Goethe University Frankfurt, 2016.
- [8] Jens Langelage, Stefano Lottini, and Owe Philipsen. Centre symmetric 3d effective actions for thermal SU(N) Yang-Mills from strong coupling series. *JHEP*, 02:057, 2011. [Erratum: *JHEP*07,014(2011)]. [arXiv:1010.0951](#), [doi:10.1007/JHEP07\(2011\)014](#), [doi:10.1007/JHEP02\(2011\)057](#).
- [9] Alexander S. Christensen, Joyce C. Myers, and Peter D. Pedersen. Large N lattice QCD and its extended strong-weak connection to the hypersphere. *JHEP*, 02:028, 2014. [arXiv:1312.3519](#), [doi:10.1007/JHEP02\(2014\)028](#).
- [10] M. Creutz. On Invariant Integration Over SU(N). *J. Math. Phys.*, 19:2043, 1978. [doi:10.1063/1.523581](#).

- [11] Michael Fromm, Jens Langelage, Stefano Lottini, and Owe Philipsen. The QCD deconfinement transition for heavy quarks and all baryon chemical potentials. *JHEP*, 01:042, 2012. [arXiv:1111.4953](#), [doi:10.1007/JHEP01\(2012\)042](#).
- [12] Michael Fromm, Jens Langelage, Stefano Lottini, Mathias Neuman, and Owe Philipsen. Phase transitions in heavy-quark QCD from an effective theory. 2012. [*J. Phys. Conf. Ser.*432,012033(2013)]. [arXiv:1210.7994](#), [doi:10.1088/1742-6596/432/1/012033](#).
- [13] M. Wortis. Linked Cluster Expansion. In C. Domb and M. S. Green, editors, *Phase Transitions and Critical Phenomena*, volume 3, pages 113–180. London, England: Academic Press 694p, 1974.
- [14] T. Reisz. Advanced linked cluster expansion. Scalar fields at finite temperature. *Nucl. Phys.*, B450:569–602, 1995. [arXiv:hep-lat/9505023](#), [doi:10.1016/0550-3213\(95\)00370-8](#).
- [15] Jonas Glesaaen, Mathias Neuman, and Owe Philipsen. Equation of state for cold and dense heavy QCD. *JHEP*, 03:100, 2016. [arXiv:1512.05195](#), [doi:10.1007/JHEP03\(2016\)100](#).
- [16] Jonas Glesaaen, Mathias Neuman, and Owe Philipsen. Heavy dense QCD from a 3d effective lattice theory. *PoS, LATTICE2015*:173, 2016. [arXiv:1511.00967](#).
- [17] F. Englert. Linked Cluster Expansions in the Statistical Theory of Ferromagnetism. *Physical Review*, 129:567–577, January 1963. [doi:10.1103/PhysRev.129.567](#).
- [18] Ronaldo Rodrigues Silva. The trace formulas yield the inverse metric formula. *Journal of Mathematical Physics*, 39(11):6206–6213, 1998. [arXiv:http://dx.doi.org/10.1063/1.532624](#), [doi:10.1063/1.532624](#).
- [19] J. Langelage. *Phase transitions in finite temperature lattice QCD from strong coupling expansions*. PhD thesis, University of Muenster, 2009.
- [20] G. Münster. High Temperature Expansions for the Free Energy of Vortices, Respectively the String Tension in Lattice Gauge Theories. *Nucl. Phys.*, B180:23–60, 1981. [doi:10.1016/0550-3213\(81\)90153-X](#).
- [21] G. S. Rushbrooke, P. J. Wood, and G. A. Baker. HEISENBERG MODEL. In *12th School of Modern Physics on Phase Transitions and Critical Phenomena Ladek Zdroj, Poland, June 21-24, 2001*, pages 245–356, 1980.
- [22] Mark Gross, John Bartholomew, and David Hochberg. SU(N) DECONFINEMENT TRANSITION AND THE N STATE CLOCK MODEL. 1983.

Erklärung nach § 30 (12) Ordnung für den Bachelor- und dem Masterstudiengang

Hiermit erkläre ich, dass ich die Arbeit selbstständig und ohne Benutzung anderer als der angegebenen Quellen und Hilfsmittel verfasst habe. Alle Stellen der Arbeit, die wörtlich oder sinngemäß aus Veröffentlichungen oder aus anderen fremden Texten entnommen wurden, sind von mir als solche kenntlich gemacht worden. Ferner erkläre ich, dass die Arbeit nicht - auch nicht auszugsweise - für eine andere Prüfung verwendet wurde.

Frankfurt, den